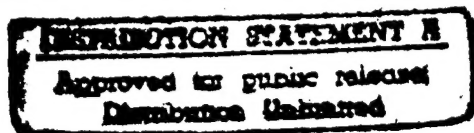LOCAL EFFECTS OF SOLID ROCKET MOTOR
EXHAUST ON STRATOSPHERIC OZONE
CONCENTRATIONS

THESIS

Brian K. George, Captain, USAF

AFIT/GEE/ENV/96D-04

DEPARTMENT OF THE AIR FORCE

AIR UNIVERSITY

AIR FORCE INSTITUTE OF TECHNOLOGY

Wright-Patterson Air Force Base, Ohio

LOCAL EFFECTS OF SOLID ROCKET MOTOR
EXHAUST ON STRATOSPHERIC OZONE
CONCENTRATIONS

THESIS

Brian K. George, Captain, USAF

AFIT/GEE/ENV/96D-04

19970328 032

Approved for public release; distribution unlimited

Disclaimer

The views expressed in this thesis are those of the author and do not reflect the official policy or position of the Department of Defense or the U. S. Government.

LOCAL EFFECTS OF SOLID ROCKET MOTOR EXHAUST ON

STRATOSPHERIC OZONE CONCENTRATIONS

THESIS

Brian K. George, Captain, USAF

Presented to the Faculty of the Graduate School of Engineering
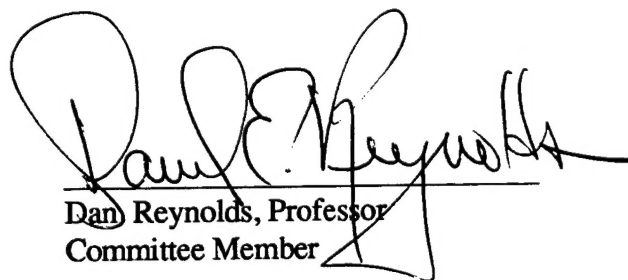
of the Air Force Institute of Technology

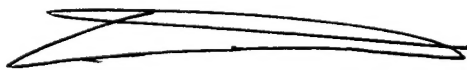In Partial Fulfillment of the

Requirements for the Degree of

Master of Science in Engineering and Environmental Management

Charles A. Bleckmann, Professor
Committee Chairman

Dan Reynolds, Professor
Committee Member

Glen Perram, Maj, USAF
Committee Member

AFIT/GEE/ENV/96D-04

Local Effects Of Solid Rocket Motor Exhaust On Stratospheric

Ozone Concentrations

THESIS

Presented to the Faculty of the School of Engineering

of the Air Force Institute of Technology

Air Education and Training Command

In Partial Fulfillment of the Requirements for the Degree of

Master of Science in Engineering and Environmental

Management

Brian K. George

Captain, United States Air Force

December 1996

ACKNOWLEDGMENTS

I would first like to thank my thesis advisor and committee chairman, Dr. Charles Bleckmann, for his enthusiasm, guidance, instruction and support during this thesis effort, and for keeping me from blasting off into an ozone hole of my own. I would also like to extend a thank-you to my other committee members and technical experts, Major Glen Perram and "Thunder Dan" Reynolds. I'll never look at statistics the same again.

And most of all, I am deeply indebted to my family, who were beside me when I needed the help and behind me when I needed the push to keep on going. To my father, Harold Eugene George, you may never have finished school, but you are the wisest man I've ever known. And Mom, thanks for letting Dad and I have so much time to play. To my sons, Halden, Brandon and Matty, thanks for being so patient and giving me an excuse to take a break and go play ball. And finally, Olga, you are truly a gift from God. Thank you for your patience with me, your intelligence, and your uncanny common sense approach to things. And thanks for reminding me, "Hey, there's only so much roofing one can do!"

TABLE OF CONTENTS

LIST OF FIGURES

LIST OF TABLES

AFIT/GEE/ENV/96D-04

ABSTRACT

Solid Rocket Motors (SRMs) power the initial flight of the Space Shuttle and Titan IV rocket. During those first two minutes after liftoff, the exhaust plumes from these motors emit large quantities of chlorine compounds and alumina particles into the atmosphere. For years scientists have argued that such a large chlorine input, injected directly into the stratosphere, would photochemically react with the surrounding air to cause significant ozone depletion over areas of tens of kilometers, for several hours after a launch. Though most of these theories have never been proven, they have caused the Air Force to consider further studies into the effects of solid rocket motor exhaust upon stratospheric ozone.

To answer the question of whether SRM exhaust causes a significant ozone depletion, Version 7 data from the Total Ozone Mapping Spectrometer (TOMS) instrument, flown aboard the Nimbus-7 satellite from October 1978 to May 1993, was used to study total column ozone levels over the launch sites of Cape Canaveral AFS, FL, and Vandenberg AFB, CA. Overpass data, which are measurements of total column ozone directly over each launch site, and Gridded Daily Field of View data, which are 50 km x 50 km pixel areas of ozone, were used in this study. Both TOMS data sets were analyzed for the 30 days prior to a launch to determine any trends and natural ozone variability, and a linear regression analysis was run to calculate a 95% Prediction Interval for the expected ozone range on the day of launch. If the prediction interval encompassed the actual post-launch ozone measurement, than it could be suggested with

95% confidence that there was no significant change in the stratospheric ozone process following the launch.

For the study, 23 Overpass data sets were analyzed, along with 14 Field of View data sets. Of the Overpass sets, 18 launches were space shuttle missions from the East Coast, while the remaining five were Titan III and IV launches from the West Coast. Gridded Daily Field of View data sets included 13 East Coast space shuttle launches and one West Coast Titan IV launch, with the specific 50 km x 50 km grid location based upon the expected plume drift due to predominant stratospheric wind conditions.

Of the 37 data sets analyzed, all of the TOMS post-launch total column ozone measurements were found to lie either within or higher than the 95% Prediction Interval range. Two Overpass post-launch ozone levels and one Field of View ozone measurement after liftoff were higher than the upper bounds predicted by the linear regression model, but in no case was the post-launch stratospheric ozone level below the predicted lower bound.

Thus, this analysis of the TOMS data indicated no significant reductions in the total column ozone process following a space shuttle or Titan rocket launch, either from Cape Canaveral AFS or Vandenberg AFB. Within the framework of this study, the answer to the SRM vs. ozone depletion question is that the exhaust from solid rocket motors does not appear to significantly reduce stratospheric ozone levels.

INTRODUCTION

OVERVIEW:

In the early 1970s, the impact of man's aerospace activities upon the earth's stratospheric ozone layer was first postulated based upon chemical reaction theories of exhaust plume constituents and the atmospheric chemical composition. This hypothesis led to the 1975 Climatic Impact Assessment Program, which studied the potential effects of supersonic aircraft and solid rocket motors on the ozone layer. In this study, the exhaust plume byproducts of the solid rocket motors used on NASA's Space Shuttle and the Air Force's Titan IV rocket were cited as potentially damaging to stratospheric ozone (4:18,583). Follow-up research by Michael Prather and others resulted in the World Meteorological Organization's Scientific Assessment of Stratospheric Ozone: 1989 findings that the exhaust plume from a space shuttle launch had the potential to deplete ozone by <0 .1% (1:10.1-10.12), which in turn sprouted other reports further implicating solid rocket motor exhaust gasses as a potential mechanism for ozone depletion (9). With such concerns being directed at the United States' Space program, this thesis will look at the inorganic compound called ozone, its cycles of creation and destruction, and the overall problem between solid rocket motor exhaust and ozone. Included will be an outline of the research approach that will be used to establish the results, conclusions and recommendations in this arena.

OZONE:

Ozone is a molecular compound that consists of three elemental oxygen atoms bonded together. This compound is gaseous in form, and is exceedingly rare in the

atmosphere. For every ten million molecules of air (10,000,000), only about three (3) are ozone. In contrast, about two million of those ten million molecules will be oxygen (O_2). Ozone is found mostly within two regions of the earth's atmosphere--the stratosphere and the troposphere. About 90% lies within 10 - 50 km (6-30 miles) above the earth's surface, in the region known as the stratosphere, where it forms the protective ozone layer. The remaining 10% can be found in the troposphere, which extends from the earth's surface to 10 km in altitude. The stratospheric ozone layer protects the earth by absorbing harmful ultraviolet radiation from the sun, more commonly called UV-B, allowing only small portions to reach the earth's surface. This absorption of ultraviolet radiation also forms a source of heat within the stratosphere, which in turn dictates the temperature structure of the atmosphere and affects the temperature profile of the earth (2). In the troposphere, ozone is considered a hindrance rather than a benefit, as it has been related to adverse health effects in humans, as well as damaging to plants, animals, and materials on the earth's surface.

OZONE PRODUCTION AND DESTRUCTION:

Ozone, or O_3, is produced by the combination of an oxygen molecule with an oxygen atom radical created when an O_2 molecule is separated into two O - O atoms by the absorption of ultraviolet light. The ozone production cycle therefore looks like this:

$$O_2 + hv \rightarrow O + O$$

$$O + O_2 + M \rightarrow O_3 + M$$
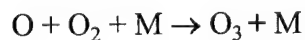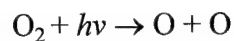
where M is a third body required for energy transfer in the reaction.

The exact concentration of ozone in the stratosphere varies naturally with seasons, latitudes, and sunspot activities that increase the amount of UV radiation released by the sun. Ozone itself is a very unstable molecule that absorbs light and quickly breaks back down into molecular and elemental oxygen in the reaction:

$$O_3 + hv \rightarrow O_2 + O$$
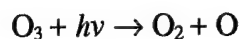
This natural ozone production and destruction process is continuous, occurring throughout the daytime in the presence of light. However, that cycle can be altered by the presence of chemicals capable of reacting with any of the constituents or intermediate species of the natural process, thus creating a net change in the final constituent concentrations. Both natural and manmade pollutants such as the halogens (F, Cl, Br, I), hydrogen, or nitrogen are capable of disrupting the ozone cycle, by reacting with and removing intermediate species of the natural chain of reactions and resulting in a net loss in the natural cycle balance. Such removal reactions are led primarily by manmade chlorofluorocarbons (CFCs). CFCs are the single largest anthropogenic source of ozone depleting chemicals. Their interaction within the ozone cycle will be depicted in more detail in the Background portion to provide a more thorough explanation of the impact anthropogenic sources can contribute to ozone destruction and ozone depletion.

PROBLEM STATEMENT:

Both the Space Shuttle and the Titan IV rocket are powered by solid rocket motors during initial flight. The exhaust streams of these SRMs deposit chlorine compounds directly into the stratosphere up to an altitude of approximately 45 km, where chlorine can play a pivotal role in stratospheric chemistry (3:144). The Space Shuttle solid

rocket motors release a total of 70 to 80 tons of chlorine combined in various chemical compounds between the altitudes of 15 and 45 km, whereas the Titian IV solid motors release approximately half as much chlorinated exhaust over a similar altitude range (10:7-8). The United States Air Force is faced with the task of answering the question, "Does the solid rocket motor exhaust from the Space Shuttle and/or the Titan IV rocket cause severe damage to the stratospheric ozone layer?" Since chlorine compounds can be particularly harmful to the ozone layer, the Aerospace Corporation attempted to model the effects of this direct Cl deposition in a November, 1994 report titled "Local Effects of Solid Rocket Motor Exhaust on Stratospheric Ozone" (3) This study by Martin Ross looked at both the homogeneous and heterogeneous chemistry between the exhaust plume and the atmosphere, and concluded that the SRMs used by the Titan IV and Space Shuttle may have the potential to cause nearly complete ozone loss in regions of up to several tens of kilometers in radius, depending upon the altitude, for several hours after a launch (3). The 1989 WMO Stratospheric Ozone Assessment report estimated that at nine space shuttle and six Titan IV launches per year, the total global stratospheric ozone level would see a .0072 to .024 percent depletion (1:10.8), while the Ross models predicted up to approximately 100% ozone depletion within the exhaust plume due to hot gas chemistry reactions for "several seconds" (3).

PRACTICAL PROBLEM:

There are many people who believe that the United States should do everything possible to protect the stratospheric ozone layer. Overall, natural sources of stratospheric chlorine contribute anywhere from ten to one hundred times less chlorine than

manufactured organic chlorine compound sources (9:21). Since solid rocket motors can contribute over 800 tons of chlorine and 1000 tons of alumina particles to the stratosphere annually, these high numbers make regulation of SRMs appear advantageous. However, this chlorine level is only a small percentage, about .25 %, of the total inorganic chlorine produced in the stratosphere which meets with ozone (9:26). In comparison, the backlog of accumulated CFCs, with an estimated atmospheric lifetime of 50-100 years, is expected to contribute close to 300,000 tons of inorganic chlorine well into the next century (9:21). Still, the WMO report, quoting several modeling studies with values of <0.1 percent total column ozone depletion in some cases, and a range of .0072 to .024 percent in other cases, has triggered some alarming comments. In a 1994 _Nature_ article by Ko, Sze and Prather, it was strongly suggested that rocket launches would be considered in future legislation relating to stratospheric ozone depletion (15). In their research, Ko, Sze and Prather concluded that the equivalent ozone depletion potential appropriate for the inorganic chlorine released from rocket exhaust, while very controversial, is about 1.3, which means that the solid rocket motor is approximately 1.3 times as harmful to ozone as CFC-113 (9:19). The Aerospace Corporation followed by conducting modeling studies to attempt to assign a more accurate ozone depletion potential to solid rocket motors (3,9,10), which in turn has led to the development of new technologies for measuring the constituents and chemical reactions between the solid rocket motor exhaust and the atmosphere. The Aerospace Corporation is developing the High Resolution Ozone Imager (HIROIG) satellite measuring device, which is capable of measure the exhaust/atmospheric chemical reactions within an exhaust plume immediately after a

launch (23). In light of these reports and technological developments, this thesis will look at 1) do solid rocket motor exhaust gasses markedly deplete stratospheric ozone, and 2) for how long after a launch are these affects felt? Preliminary studies have been conducted in the past by NASA/Goddard Space Flight Center using satellite column ozone measurement data, but this thesis effort will expand on those works in an attempt to provide a more accurate answer based upon the latest version of the satellite data and information we now have available.

RESEARCH OBJECTIVES:

There are several objectives to this research project. The first objective is to look at the state of the science of stratospheric ozone depletion, and determine if any significant evidence has been found linking solid rocket motor exhaust to stratospheric ozone depletion. The current scientific articles regarding this subject will be synthesized into a basic overview of what scientists feel are the pertinent facts surrounding SRMs and ozone depletion. Along with this synthesis will be a study to determine if Space Shuttle and Titan IV rocket launches directly affect local, regional, or column stratospheric ozone levels, and if so, to what extent. This will be accomplished by the statistical analysis of the latest release, Version 7, of the Total Ozone Mapping Spectrometer (TOMS) data received from the Nimbus-7 satellite by the NASA/Goddard Space Flight Center (28). The research will determine if the TOMS data reveals any significant changes in the stratospheric ozone levels following a shuttle or rocket launch, which in turn can be used as a baseline to see if further studies are warranted or if improvements to past studies can be accomplished with the latest version of the TOMS satellite data.

APPROACH:

This work will use a three step methodology. The first phase will be a thorough literary search of past and present research in order to determine the state of the science of ozone depletion and the relationship between solid rocket motors and stratospheric ozone levels after a launch. This will be followed by a compilation of the latest version, Version 7, of the data from the NASA TOMS instrument flown on board the NIMBUS-7 satellite, taken over the lifetime of the equipment, along with the dates and times of all Space Shuttle and Titan III, Titan 34D, and Titan IV rockets launched over that same period. These space launch vehicles all used similar solid rocket motors during their initial flight. Finally, as detailed statistical analysis of the satellite data will be conducted for a variety of locations, wind conditions and data regions in order to determine pre-launch and post-launch stratospheric ozone levels, and whether or not there is, in fact, any correlation between space shuttle/rocket launches and stratospheric ozone depletion, as measured by the TOMS satellite instrument.

In conducting the literature review and synthesis of the state of the science of ozone depletion and rocket launches, several sources will be used. These sources will include trade journals, peer-reviewed scientific journals, industry studies and experimental efforts, and interviews with experts in the field of ozone depletion and interpretation of the satellite data relating to such work. Major providers of work in this arena are the World Meteorological Organization, *Science*, *The Journal of Geophysical Research*, The Aerospace Corporation, and NASA / Goddard Space Flight Center. The WMO performs periodic Scientific Assessments of Ozone Depletion, and typically uses over 200 scientists

world-wide in their efforts to obtain the latest information on current research, experiments, findings, and trends in the fields of stratospheric and tropospheric ozone. Peer-reviewed journals contain much of the specific works of the scientists who contribute to the WMO reports, or research efforts by those scientists who are recognized as experts in the field of ozone depletion and/or space launch chemistry. The Aerospace Corporation has conducted several studies regarding space shuttle and rocket launches, exhaust gas chemistry and stratospheric ozone levels, and their scientists are actively working on new technologies to answer many of the open questions posed by the WMO research. Finally, the NASA/Goddard Space Flight Center is the home of the TOMS satellite data, along with scientists responsible for reviewing and updating the data to ensure its accuracy and accessibility for the scientific community. Many of the NASA/Goddard SFC personnel are also published in the field of stratospheric ozone depletion based upon TOMS data, and are recognized as experts and an excellent source of knowledge and information in the arena of stratospheric ozone.

Through the NASA/Goddard Space Flight Center, this research effort will use the entire data set of the TOMS instrument spanning the entire lifetime of the NIMBUS-7 satellite, which orbited the earth from 31 October 1978 to 6 May 1993. Along with the latest version of the data, NASA/Goddard SFC provided a detailed users guide outlining all instrument and data error analyses, and a customized software package designed to read column ozone data for various latitudes, longitudes, specific locations and regions, which enabled the performance of a variety of statistical analyses over a range of locations, regions and time sequences. Along with the TOMS data, work by the

Aerospace Corporation was used to estimate stratospheric wind conditions and map exhaust plume footprints at various locations and times after launch.

Finally, this data was used to perform descriptive statistical analyses of total column stratospheric ozone levels over specific locations at times directly related to Space Shuttle and Titan rocket launches. A localized study of the column ozone levels before and after a launch was performed using the TOMS 50 km by 50 km grid data at specific latitude/longitude locations corresponding to predicted exhaust plume paths at specified pre-launch and post-launch times. This provided insight into natural background column ozone variability and post-launch ozone changes as related directly to a launch. In addition to these localized analyses, a study of ozone levels directly over the launch sites both before after launches was completed, again based upon TOMS data. Finally, a brief error analysis was conducted on both of the TOMS data statistical analyses. This established sensitivity of the results, and better delineated errors associated with the instrument or the analysis from those changes in total column ozone that can be attributed to natural variability in the ozone levels over the region of interest.

OUTLINE:

Work performed in this thesis effort followed a standard graduate work format. The introduction is followed by a background section designed to present the results of the literature review and give the synthesis of the general state of the science of stratospheric ozone depletion, as it is related to space shuttle and rocket launches. The approach and methodology used to conduct the descriptive statistical analyses of the TOMS satellite data is next presented, depicting a detailed description of what statistical

analysis work will be performed, and how that work will be accomplished. This is followed by the results section, covering the numerical findings of the stratospheric ozone levels and error analysis associated with each section. Finally, the conclusions and recommendations that can be drawn from these results are discussed. Here, just what the numbers mean will be presented, as well as how these facts can be used by the Air Force in future decisions/discussions of solid rocket motor effects upon stratospheric ozone levels. Any recommendations on improving the work performed within this thesis or suggestions for follow-on study will be included at this time.

BACKGROUND

OVERVIEW:

Ever since the Climatic Impact Assessment Program cited the potential for damage

to the ozone layer by the space shuttle's solid rocket motors, the study of the relationship

between SRMs and ozone depletion has been controversial. Our understanding of

stratospheric chemistry has improved greatly since the 1975 report (4:18,583), but the fact

remains that there has been only one reported in-situ measurement of ozone depletion

following a launch. And that study was conducted over twenty years ago. In 1973, a U2

aircraft conducted a sampling flight through the SRM exhaust plume of a Titan III rocket

at an altitude of 18 km thirteen minutes after launch. The measurement did not provide

the scale of the ozone depletion, but a drop in ozone intensity by 40% was reported

(9:16). Although the accuracy of this measurement has been questioned in other studies

(5,6), the report is still used as the basis of proof that there is a definite correlation

between solid rocket motor exhaust and ozone depletion. Couple this with the possibility

that solid rocket motors may soon be regulated as ozone depleting mechanisms and it

becomes quickly evident why this topic is of such great concern to the Air Force. This

section will present a background of the stratospheric ozone layer, ozone depletion, and

the relationship to space shuttle and rocket launches, through a comprehensive look at the

complex chemistry of the stratospheric ozone cycles, as well as the ozone destruction

cycles of hydrogen, nitrogen, chlorine, and other halogen compounds. In addition, this

section will detail the chemical constituents of the primary solid rocket motor propellant

used by both the space shuttle and Titan IV rocket, along with its exhaust gas products

that can interact with the surrounding atmosphere. Following that will be an introduction to the latest scientific areas of investigation between SRM exhaust and ozone depletion, known as "hot gas chemistry", which includes both homogeneous and heterogeneous chemical reaction theories between the exhaust plume and the stratosphere. This section will conclude with a detailed description of the NASA Total Ozone Mapping Spectrometer , used extensively for this thesis effort as well as other analyses in this arena. Along with the instrument's flight and measurement history, we will look at how this data was used by the NASA/Goddard Space Flight Center to analyze column ozone depletion following a series of space shuttle launches.

THE STRATOSPHERIC OZONE LAYER:

The Earth's ozone layer protects all forms of life from harmful radiation emitted from the sun. In order to "safeguard" the ozone layer, the United States, in cooperation with over 140 other countries, has agreed to phase out the production of its ozone depleting substances through such agreements as the Montreal Protocol and the Copenhagen Amendments. This concern for the ozone layer is primarily because of the scarcity of ozone in the atmosphere. Ozone is a rare compound, averaging only around three molecules of O_3 for every ten million molecules of air. In comparison, two million of those air molecules are O_2 or "normal" oxygen molecules (2:19). Composed of three oxygen atoms bonded together, ozone is blue in color, has a strong odor, and is very unstable. It is found mainly within two regions of the atmosphere--the troposphere and the stratosphere. Extending from the earth's surface to an altitude of 10 km, the troposphere contains virtually all human activities (22). For reference, the tallest mountain

on earth, Mount Everest, is only 9 km high. This region contains approximately 10% of the atmospheric ozone concentration. Just above the troposphere is the stratosphere, extending from 10 to 50 km altitude. Again for reference, most commercial airline traffic occurs in the lower portion of the stratosphere. However, some 90% of the atmospheric ozone is located between 10 and 50 km, with the majority found between the altitudes of 15 and 30 km (2:19).

Ozone is both harmful and beneficial, depending upon its location. At the planet's surface, ozone can come in direct contact with life-forms, and because it reacts strongly with other molecules, ozone can be toxic to living systems. At high concentration levels, ozone can severely damage the tissues of plants and animals (2:19). However, in the upper troposphere and stratosphere, ozone plays a beneficial role by absorbing most of the biologically damaging ultraviolet sunlight known as UV-B. This absorption of radiation causes the temperature profile of the stratosphere to increase with height, creating a very stable region of the atmosphere that directly affects the temperature profile at the earth's surface. In addition to these climatic effects, there are also biological benefits from the UV absorption. Many experimental studies of plants and animals, and clinical studies of humans, have shown the harmful effects of excessive exposure to UV-B radiation, including the potential for severe tissue damage and skin cancer. These two opposing aspects of ozone have created two separate environmental issues. In the troposphere, there is concern about increases in the ozone concentration, while the widespread scientific and public interest is in the ozone concentrations in the stratosphere, where the concern is about ozone losses. Lower altitude ozone is a key component of smog, a

problem associated with larger cities worldwide. But even in the smoggiest cities, the lower altitude ozone concentration levels are very much smaller than the concentrations routinely found in the stratosphere (2).

STRATOSPHERIC OZONE CYCLES:

While the stratospheric concentration of ozone averages only three molecules for every ten million molecules of air, there are constant natural ozone creation and destruction cycles continuing throughout the day and night, which can vary the ozone concentration at specific locations. In addition, latitude, season and solar sunspot activity can also create changes in ozone concentrations within a specific region. Here, we will look at the many cycles of ozone, as well as some of the stratospheric chemistry that directly affects stratospheric ozone concentrations.

Ozone is produced when a normal or molecular oxygen atom (O_2) absorbs solar ultraviolet energy and breaks down into two elemental oxygen atoms, which in turn can combine with another normal oxygen molecule in a three-body reaction to form O_3. Molecular oxygen photodissociates at all wavelengths greater than 240 nm to produce either ground state atomic oxygen $O(^3P)$ or an excited state oxygen atom, $O(^1D)$. The chemical reaction equations appear as follows:

$$O_2 + h\nu \rightarrow 2O\ (^3P) \qquad\qquad \lambda < 240\ nm$$

$$O_2 + h\nu \rightarrow O\ (^3P) + O\ (^1D) \qquad\qquad \lambda < 195\ nm$$

$$O\ (^1D) + O_2 + M \rightarrow O_3 + M$$
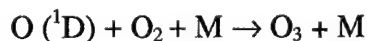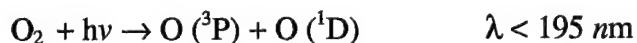
$O\ (^1D)$ is rapidly relaxed collisionally, with M, the third body, required to remove excess internal energy in the ozone molecule formation (17).

Ozone itself is very unstable, and is primarily destroyed photochemically during its natural absorption of sunlight at all wavelengths less than 1180 nm. Ozone absorbs most strongly at the near UV-region below 350 nm, in the reaction:

$$O_3 + h\nu \rightarrow O + O_2 \qquad\qquad \lambda < 1180 \, nm$$

with ozone effectively blocking all UV radiation in the 240 - 290 nm range (17). A complete ozone production / destruction model was developed and termed the "Chapman Cycle" in order to describe the stratospheric ozone chemistry, and contains the following series of reactions depicting the life of an ozone molecule:

$$O_2 + h\nu \rightarrow O + O$$

$$O + O_2 + M \rightarrow O_3 + M$$

$$O_3 + h\nu \rightarrow O + O_2$$

$$O_3 + O \rightarrow O_2 + O_2$$
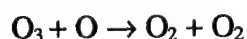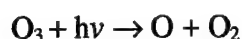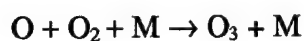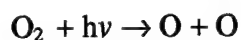
where M is a third body required to remove excess energy in the reaction. However, the Chapman cycle alone overestimates the ozone concentration by a factor of five (17). Thus, there must be additional loss mechanisms going on within the stratosphere. These loss mechanisms can be described by a simple "catalytic cycle" series of reactions that can be depicted:

$$X + O_3 \rightarrow XO + O_2$$

$$XO + O \rightarrow X + O_2$$
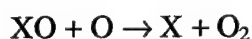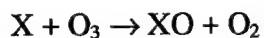
which results in a net effect of removing two odd oxygen species and producing two even oxygen species.

Above 50 km, the dominant X in the catalytic cycle is OH and H* radicals that are created during the natural "hydrogen cycle." The hydrogen cycle includes the following series of reactions (19):

$$H + O_3 \rightarrow OH + O_2$$

$$OH + O \rightarrow H + O_2$$

$$OH + O_3 \rightarrow HO_2 + O_2$$

$$HO_2 + O \rightarrow HO + O_2$$
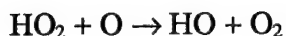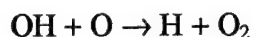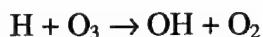
At altitudes of 40 - 45 km, the dominant catalyst is NO, which is produced in the "nitrogen cycle." This cycle is as follows (19):

$$NO + O_3 \rightarrow NO_2 + O_2$$

$$NO_2 + O \rightarrow NO + O_2$$

$$NO_2 + h\nu \rightarrow NO + O$$
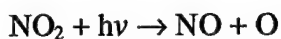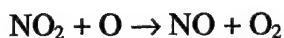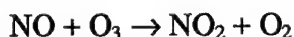
This nitrogen cycle is the primary ozone destroying cycle throughout the stratosphere, with the majority of these reactive nitrogen compounds derived from the decomposition of nitrous oxide(2). This predominance is due to the fact that, although the nitrogen cycle is slower in reaction time than other cycles and nitrous oxide is increasing at a slower rate than CFCs, nitrogen is still many times more abundant than hydrogen or chlorine compounds (2). Chlorine still remains the primary focus of most scientific research, though, and includes a complex array of possible chemical reactions than can deplete stratospheric ozone levels.

CHLORINE DESTRUCTION OF OZONE:

At altitudes above 30 km, the catalytic cycle above is dominated by both chlorine and bromine, in what is termed the "halogen cycle." It has been postulated by the scientific community that the majority of chlorine in the stratosphere comes from the photodissociation of chlorofluorocarbons that were released in the troposphere. These CFCs are very stable compounds that are slowly transported from the troposphere to the stratosphere through atmospheric winds. While most compounds are either washed out by rain in the troposphere, chemically reacted with other atmospheric constituents, or dissociated by photolysis reactions, CFCs are insoluble in water and do not react quickly with other gasses in the atmosphere. Those wavelengths of light that do pass down to the troposphere are not strong enough to photodissociate CFCs, so their lifespan at lower altitudes is quite long. Even in the stratosphere they are very stable, with the primary source of breakdown coming from somewhat rapid photodissociation by shorter wavelength UV radiation that is found mainly above the ozone layer (17).

The chlorine contribution from solid rocket motors comes primarily in the form of hydrogen chloride (hydrochloric acid). HCl is the major exhaust product of solid rocket motors, and is injected directly into the stratosphere during initial launch. Much like CFCs, hydrogen chloride is inert with respect to ozone, and would take a great deal of time to be converted into a catalytically active form of chlorine, either Cl or ClO (5).

In comparison to the amount of chlorine emitted by solid rocket motors, the industrial contribution of Cl to the stratosphere was approximately 300,000 tons in 1990 (4). Of this Cl, the vast majority was in the form of CFCs (CFC-11, CFC-12, and CFC-

13) and CCl$_4$, comprising some 70% of all anthropogenic chlorine loading. These compounds are mainly used in refrigeration, as foam blowing agents, and as solvents. Within the stratosphere, they are broken down into Cl radicals by photodissociation, from which they can begin a number of chlorine reaction cycles. The primary chlorine cycle of ozone destruction is:

$$Cl + O_3 \rightarrow ClO + O_2$$

$$ClO + O \rightarrow Cl + O_2$$
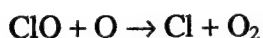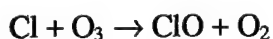
The net result is the destruction of one ozone molecule and the removal of an intermediate atomic oxygen atom from the reaction cycle, while the chlorine radical is returned where it can repeat the reaction/destruction process again.

Another somewhat lengthy chain of reactions known as the "alternative chlorine cycle" is another potential mechanism for ozone destruction. Here, the series of reactions includes:

$$Cl + O_3 \rightarrow ClO + O_2$$

$$Cl + O_3 \rightarrow ClO + O_2$$

$$ClO + ClO + M \rightarrow Cl_2O_2 + M$$

$$Cl_2O_2 + h\nu \rightarrow Cl + ClO_2$$

$$ClO_2 + M \rightarrow Cl + O_2 + M$$
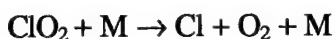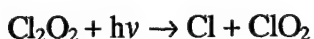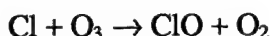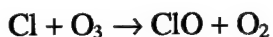
where M is a third body required to remove excess energy in the reaction.

The net result is the conversion of two O$_3$ molecules into three O$_2$ molecules.

As is evident, all of these reactions can remove both ozone molecules and intermediate ozone cycle constituents, resulting in a net loss in the overall balance of the

ozone cycle. It has been estimated that this chlorine catalytic cycle can repeat some 100,000 times before the chlorine is finally returned to the troposphere (21). Thus, whenever chlorine radicals are present in the stratosphere, they have the potential to do a great deal of harm to the level of ozone within that region. This has brought even more attention to solid rocket motor propellants, as they inject HCl directly into the stratosphere, where it is feared the Cl can become active and begin this catalytic process very quickly. A brief overview of the propellants and their composition will demonstrate why they are being considered for regulation in light of the chlorine destruction cycles above.

PROPELLANTS:

From what is currently known, there are no rocket propellants, including the liquid oxygen / liquid hydrogen family of propellant systems, which are completely benign to the environment (27:21). Thus, the total elimination of the current solid rocket motors would only lead to the use of another environmentally damaging replacement. The key is to compute the potential effects the current system can have upon the environment and determine if that is acceptable. In the hazardous waste arena, one study found that the rocket industry as a whole contributes only one tenth of one percent of hazardous waste in the United States (27:21). This number is relatively minor, so it is more likely that the potential for ozone depletion is what makes solid rocket motor propellants come under such heavy public scrutiny.

The most common solid rocket motor propellant is ammonium perchlorate, or AP (27:28). This propellant consists of ammonium perchlorate as the solid particle oxidizer,

aluminum powder as the solid particulate fuel, and a hydroxy-terminated polybutadiene cured elastomer to bind the mix together (27:29). During ignition, the solid rocket motor exhaust contains large quantities of gasses and particulates that can potentially perturb stratospheric ozone (1). The gasses include HCl, NOx compounds, and hydrogen compounds (H_2 and H_2O). These compounds are suspected to take place in the homogeneous chemistry between the exhaust plume and surrounding atmosphere. Additionally, the SRM exhaust plume also contains the particulate matter aluminum oxide, or Al_2O_3, which has also been postulated as a potential ozone depleter, either by direct reaction with ozone or by providing a surface area for heterogeneous chemical reactions to occur (27:29).

Prather et al. concluded that, based upon the current understanding of stratospheric chemistry, of the species emitted during rocket motor operations, chlorine appears to be the most significant contributor to ozone removal on a global scale, although the contribution is extremely small (4). In his study of the homogeneous chemistry, Prather assumed that the HCl released during flight became a Cl radical, but other studies have concluded that the HCl is not reactive, and would quickly wash out of the atmosphere (10). Instead of direct HCl reactions, the phenomenon of "hot gas chemistry" was introduced in an attempt to explain the potential ozone depletion reactions that have been hypothesized to occur within the exhaust plume. In addition, a great deal of current study is being conducted in the area of heterogeneous chemistry, in an effort to implicate the aluminum oxide particles as major players in the ozone depletion equation.

Each of these types of chemical reactions will be studied in detail, along with the current state of the science of both.

HOMOGENEOUS CHEMISTRY:

Homogeneous chemistry, as it pertains to solid rocket motors, is simply the direct chemical reactions between exhaust gasses and atmospheric gasses. In the highly reduced environment at the SRM nozzle exit plane, nearly all chlorine exiting the nozzle is in the form of HCl, along with large mole fractions of H_2 and CO (10:9). Chlorine that emerges from the exhaust plume as HCl has little immediate impact on ozone, since HCl does not react directly with ozone, and photolyzes and reacts very slowly with ambient species (10:9). However, it is believed that the high temperatures within the exhaust plume and the high levels of H_2 and CO present are capable of supporting vigorous "afterburning" upon downstream mixing with the ambient atmosphere. As ambient oxygen is mixed into the plume exhaust gasses, the H_2 and CO form high local concentrations of OH radicals and O and H atoms. The high temperatures and high density of reactive radicals created by this afterburning provide an environment for the reaction of HCl and the release of chlorine atoms (10:10). The reactions below occur very rapidly at exhaust plume temperatures:

$$OH + HCl \rightarrow Cl + H_2O$$

$$O + HCl \rightarrow Cl + OH$$

$$H + HCl \rightarrow Cl + H_2$$
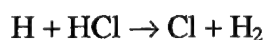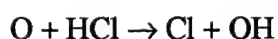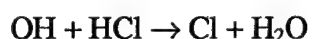
In addition, small fractions of ClO, HOCl, and ClOO are also present, but close to zero. The Cl will combine to form Cl_2 in the cooler post-afterburning region of the immediate

plume, but sunlight will quickly photodissociate the Cl_2 back into two Cl atoms (10:10-17). The Aerospace Corporation modeled the chemical identity of chlorine in a Titan IV SRM exhaust plume as well as the far-field chemical identity of chlorine as a function of altitude in Figure 2-1 and Figure 2-2 below (10:13).
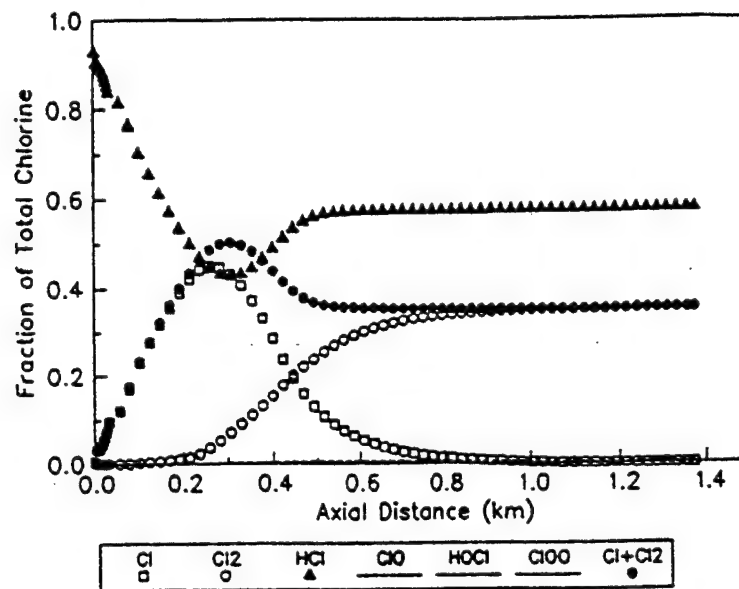
Figure 2-1. Chemical identity of chlorine in plume @ 20 km (10:13)
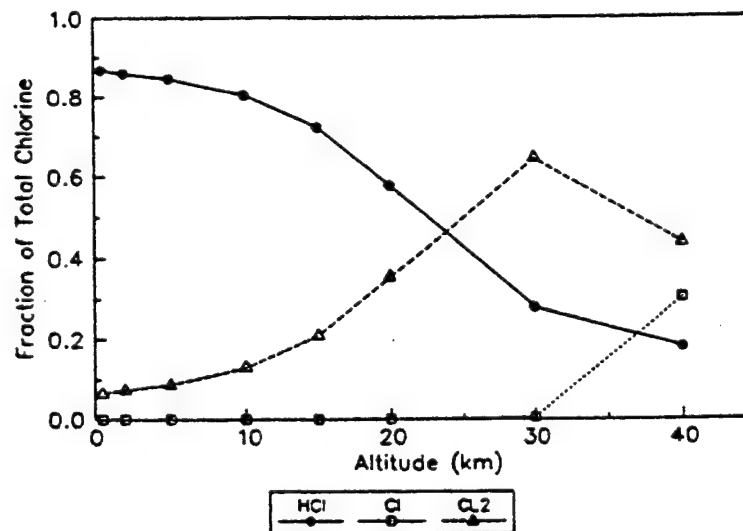
Figure 2-2. Far-field chemical identity of chlorine as a function of altitude (10:13)

In addition, the chemical distribution of chlorine in the far field of the plume, and the

minimum, nominal, and maximum fractions of total exhaust chlorine deposited in the far

field of the plume as free chlorine, according to three chemical rate constants used in the

model, are shown in Table 2-1 and Figure 2-3 as a function of altitude (10:14).

Motor Altitude (km)	Percent of Total Chlorine [b]					
	Cl	Cl_2	HCl	ClO	HOCl	ClOO
15	0.01	21.0	72.2	0.2	2×10^{-8}	1×10^{-3}
20	0.1	35.3	57.6	0.4	8×10^{-9}	2×10^{-3}
30	0.4	64.5	27.7	0.8	7×10^{-8}	1×10^{-3}
40	30.8	43.4	17.7	1.5	4×10^{-6}	2×10^{-3}

[a] Determined at downstream (axial) distances of 1.1, 1.4, 5.5, and 6.9 km for motor altitudes of 15, 20, 30, and 40 km, respectively.

[b] Note that 6.6% of total chlorine is in Fe and Al compounds.

Table 2-1. Chemical Distribution of Chlorine in Far Field of Plume (10:14)
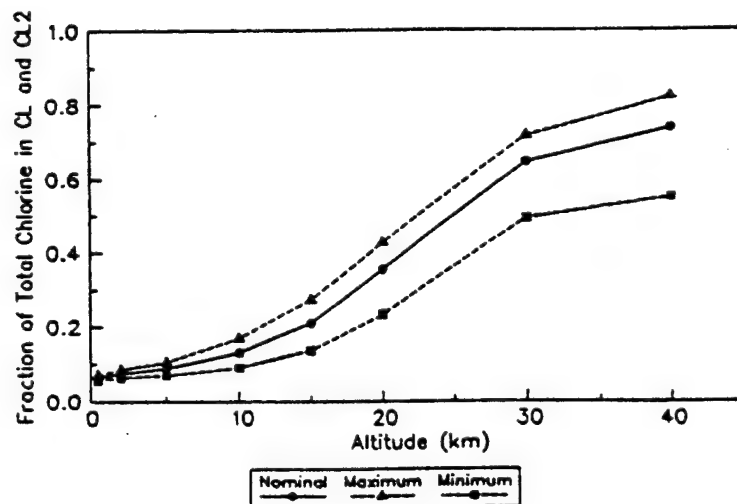
Figure 2-3. Effects of chemical rate constant variations on Cl and Cl_2 Production (10:14)

The fraction of the total chlorine exhaust deposited in the stratosphere as free chlorine (Cl and Cl_2) therefore is predicted to range from approximately 20% at an altitude of 15 km to approximately 70% at an altitude of 40 km.

The relevant reactions of this free chlorine that take place within the exhaust plume can be broken down into two phases. The first phase entails the exhaust gasses expanding to a diameter of a few kilometers, at which time it should encounter the amount of ozone equivalent to the free chlorine residue predicted. The time scale for the first phase of expansion and chlorine/ozone chemistry is estimated to be on the order of one hour (10:21). Phase two involves the expansion of the exhaust gasses from the diameter of a few kilometers around the vehicle track to larger, but still relatively local, dimensions (10:19). Phase one reactions includes the afterburning reactions previously stated, along with the following chlorine reactions:

$$Cl_2 + h\nu \rightarrow 2\ Cl$$

$$Cl + O_3 \rightarrow ClO + O_2$$

$$Cl + CH_4 \rightarrow HCl + CH_3$$
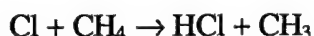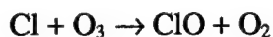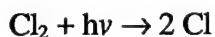
HCl reactions in the far field are also limited to the hot gas chemistry equations above, in addition to possible photodissociation.

$$HCl + h\nu \rightarrow H + Cl$$

$$HCl + OH \rightarrow Cl + H_2O$$
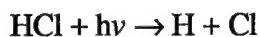
Following the initial expansion of the exhaust gases and the complete consumption of Cl and Cl_2 by ozone, the dynamics and kinetics of the problem become more complex.

The ClO molecule generated above does not react rapidly with ozone, if at all. Instead, it is more likely to participate in one of the following reactions:

$$ClO + h\nu \rightarrow Cl + O$$

$$ClO + NO \rightarrow Cl + NO_2$$

$$ClO + O \rightarrow Cl + O_2$$
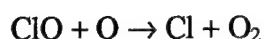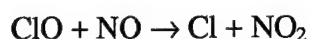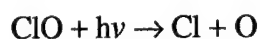
However, at the beginning of Phase Two of the expansion the major chlorine-containing compound is, in fact, the ClO (10:19). The complex reactions of the second phase have yet to be modeled correctly, thus it is still unclear whether the second phase of the plume gas expansion is characterized by a slow, continuing depletion of O_3 due to photodissociation of ClO and ClO chemistry, or by a cessation of ozone destruction and a refilling of the initial hole by mixing of ozone-containing surrounding air (10:20).

These Aerospace studies have predicted that the results of such homogeneous chemistry would be anywhere from 1) nearly complete depletion of ozone over a region 1-2 km in diameter along the vehicle track at 15-20 km or approximately 4-5 km in diameter at an altitude of 40 km (10:21), to 2) an ozone "hole" with a diameter of tens of kilometers at an altitude of 30 km, depending on the rate of dispersion of the plume (9:16). A third Aerospace modeling study of the local effects of solid rocket motor exhaust on stratospheric ozone presented a simulation of SRM exhaust mixing and chemistry that predicts the three-dimensional structure of the prompt local ozone loss during the eight hours following a Titan IV launch. Model maps of the total column ozone abundance show that the maximum loss of about 30% occurs about one hour after

launch. At four hours after launch, the area of column ozone loss exceeding 8% covers up to 2000 km^2 (3).

Although the current scientific thinking is leaning towards a direct correlation between solid rocket motor exhaust and stratospheric ozone depletion, the fact of the matter is that scientists to date have no definitive proof of these theories. The same Aerospace study above predicting 30% and 8% column ozone loss also freely admits that, "the afterburning of HCl in SRM plumes has not been proven to occur" (3:144). In addition, the NASA/Goddard Space Flight Center conducted a study of ozone depletion following a rocket launch, which will be discussed later, that found no evidence of such ozone depletion following a space shuttle launch. There is some dispute over whether the TOMS instrument can detect the ozone depletion discussed in the Aerospace reports due to the instrument's 50 km x 50 km spatial resolution, but given the predicted areas of ozone depletion and the extent of ozone depletion depicted in the above reports, the TOMS resolution should reveal this flux in column ozone.

Another common theme of the reports is that the effects of the aluminum oxide particles are largely unknown, but that it is expected these particulates provide a surface area for heterogeneous chemical reactions to occur (3,9,10). We'll next look into the latest studies in this arena.

HETEROGENEOUS CHEMISTRY:

Heterogeneous chemical reactions are those reactions occurring between compounds or matter in different states or phases (27:30). Heterogeneous chemistry has become an important area of study in the field of stratospheric ozone depletion, as

scientific experiments have shown that the gas hydrogen chloride can react with solid ice crystals at stratospheric temperatures and liberate radical chlorine molecules. In the study of solid rocket motor exhaust reactions, the concern is for the interaction of the aluminum oxide particles released during flight with the exhaust and/or atmospheric gasses also present within the exhaust plume. Such heterogeneous chemistry has been hypothesized as providing another mechanism for stratospheric ozone depletion (1,3,9,10), with the belief that these particles act much the same way as polar stratospheric clouds do in enhancing ozone depletion. While there has been little scientific evidence that this type of heterogeneous chemistry actually occurs, Gary Lund completed a Master's Degree thesis on this very subject (27).

In his literature research, Lund found that the impact of heterogeneous chemistry from solid rocket motor exhaust particles was believed to be relatively insignificant by many experts (27:30). In addition, the 1991 WMO assessment concluded that the long term global effects of Al_2O_3 is likely to be negligible (1).

Just as interesting as his literature findings were the actual results of Lund's thesis experiment. In attempting to model the heterogeneous reactions of HCl and aluminum oxide particles to see if a chlorine radical was, in fact, liberated, Lund found that CFC-12 did chemisorb onto the alumina particles, but that the energy required to desorb the chlorine off of the particle was too great for the stratospheric energy levels available to overcome. Thus, the Al_2O_3 particles actually formed a chlorine sink rather than a mechanism for ozone depletion (27:99-100).

Further studies are being conducted around the scientific community, but as yet none are able to prove that the aluminum oxide particulate matter released during the initial flight of either the space shuttle or Titan IV rocket are contributing to ozone depletion through the mechanism of heterogeneous chemistry.

Thus, the primary reactions of concern remain those homogeneous chemical reactions between the exhaust gasses and the atmosphere. While the scientific community struggles to accurately model the effects of this type of ozone depletion reaction, stratospheric column ozone data from the TOMS instrument has been in use for years to study actual atmospheric conditions, and provide and interesting comparison to computer model predictions. To better understand the column ozone studies performed by NASA/GSFC, it is important to know the details of instrument used to gather the data, and the manner in which this data was used to reach the reported conclusions.

INSTRUMENT DESCRIPTION:

NASA's Total Ozone Mapping Spectrometer (TOMS) instrument was launched aboard the polar-orbiting, sun-synchronous Nimbus-7 satellite on October 24, 1978, and began sending measurements one week later. The data consists of daily high-resolution global maps of atmospheric column ozone levels, broken down by latitude/longitude grids from October 31, 1978 to May 6, 1993 (20:1).

TOMS measured the solar irradiance and the radiance backscattered by the atmosphere in six selected wavelength bands in the ultraviolet. The data was obtained via a six-channel Fastie-Ebert downward viewing spectrometer, at 312.5, 317.5, 331.2, 339.8, 360, and 380 nm (7:12,784). The instrument scanned in 3-degree steps to 51 degrees on

each side of the subsatellite point in a direction perpendicular to the orbit plane, and the six radiances measured at each of the 35 cross-track positions continuously covered the regions between the orbital paths. These consecutive cross-scans also overlapped, creating a contiguous mapping of ozone (7,20). The spatial resolution is 50 km x 50 km for the nadir view, and approximately 50 km x 200 km at the extreme cross-track scan positions, 1 and 35 (7:12,784). The extreme positions are used only in the equatorial and very high latitude polar regions to provide complete spatial coverage, since away from these locations there is enough overlap between adjacent orbits that the preferential central scans can be used. Because of the Nimbus-7's sun-synchronous orbit, full global coverage is obtained on a daily basis.

At least once per day, the TOMS instrument measures the solar irradiance at each wavelength channel. Then, for each wavelength, the radiance-irradiance ratio is formed, termed the directional albedo, which is used to eliminate dependence on day-to-day changes in the spectrometer's sensitivity (7). Ratios of albedos from pairs of wavelengths are combined to minimize uncertainties in the wavelength independent portions of the diffuser plate reflectivity, the lower boundary reflectivity, and possible background aerosol effects. After the conversion of the measured albedo ratios from each scan position into ozone values via precomputed table lookup, the ozone data is stored scan-by-scan, in a 1 degree latitude by 1.25 degree longitude gridded format (7:12,784).

A comprehensive study of the instrument properties and their variations with time has been made by NASA/Goddard SFC, producing a more accurate derivation of radiances from the raw instrument counts. Improvements have also been made to the

input physical data, the treatment of physical processes, and the parameterizations of atmospheric conditions used in the radiative transfer calculations that are part of the algorithm. In addition, the process of deriving ozone and reflectivity has also been modified to incorporate a linear correction for wavelength dependence in the reflectivity, other wavelength-dependent physical effects, or wavelength-dependent errors. The resultant version of TOMS data, Version 7, has a long-term two sigma calibration uncertainty of ± 1.5 percent in total ozone over 14.5 years (20:1). This data, and the ozone trends computed from it, compares favorably with those same trends calculated from the Stratospheric Aerosol and Gas Experiment (SAGE) instrument data (7:12,783).

Although our work will, in fact, be based upon this latest Version 7 of TOMS data, the earlier work by the NASA/Goddard SFC scientists did not have the advantage of such improved data. Their previous work is still useful as an indication of just what the TOMS data can show in the correlation of space shuttle or rocket launch activity to stratospheric ozone levels, as was performed in a 1991 report compiled by Dr. Richard McPeters (6). The details of this report will be discussed in the following section.

NASA/GSFC APPROACH:

In response to Prather's 1990 report on the potential global and regional impacts on stratospheric ozone produced by exhaust from the space shuttle and Titan rockets, Steven Aftergood commented in the *Journal of Geophysical Research* that he believed such releases of chlorinated compounds would create local ozone "holes" or at least "soft spots" for several hours after a launch directly above the launch site (5). Prather enlisted

the services of Dr. McPeters to see if the TOMS data indicated any such change in column

ozone around a launch site following a space shuttle or Titan rocket launch (6).

McPeters theorized that if the proposed rapid loss mechanism Aftergood proposed

was in fact having an impact on ozone large enough to be of real concern in terms of

enhanced ultraviolet sunlight at the ground, it should be visible in the TOMS ozone image

data. In his report, McPeters studied the ozone record data for evidence of rapid local

decreases in ozone following eight space shuttle launches (6:17,379). Each 50 km x 50

km TOMS field of view measurement, stored in latitude/longitude grids, was used to

produce a colored ozone image of the area above and around the Cape Canaveral, Fl,

launch site. Each grid was colored according to its Dobson-Unit (DU) ozone content,

with a fairly sensitive color scale used. For each change in the column ozone level of

12.5 Dobson Units, the color of the grid cell would change, becoming lighter at lesser

ozone amounts and darker at increased amounts. If ozone were depleted by 40% over an

area the size of 1/4 the TOMS field of view, i.e. 20 km x 20 km, a 120 DU reduction

would be measured as a 30-DU average change, which in turn would show up as a three

color step change on the color image map (6).

McPeters plotted the color grids from satellite passes immediately following the

eight launches, and found no such color change / ozone reduction. His results did not

support the existence of a measurable localized depletion of ozone following a space

shuttle launch, although he did allow that if the ozone depletion took place over a very

small area or for a very short duration, the TOMS instrument may not be able to detect it.

However, he also questioned whether a decrease so localized could even be considered significant (6).

This thesis effort will closely follow McPeters' work, using the Version 7 of the TOMS data. This version was not available to McPeters during his 1991 report, and should provide an improved depiction of column ozone levels immediately after space shuttle and Titan IV rocket launches. The methodology this new study will use will be presented in the next chapter.

SUMMARY:

Through a thorough analysis of the current state of the science of stratospheric ozone depletion, a great deal of background knowledge can be obtained. First, stratospheric ozone is, in fact, a rather rare commodity in the atmosphere. It is this scarcity of O_3 that makes any impact upon the ozone layer an important concern for mankind. Our understanding of the natural stratospheric ozone cycles, as well as the complex chemistry continuously going on within the stratosphere, has improved greatly in the last decade, and has led to many new theories on the relationship between solid rocket motor exhaust and stratospheric ozone depletion. The hydrogen, nitrogen, and chlorine destruction cycles, which can be accelerated by the introduction of higher atmospheric concentrations of these chemical compounds, are of primary concern to the both atmospheric scientists and the Air Force, as space launch vehicles have the potential to inject tons of these catalytic compounds directly into the atmosphere during initial flight. And although it has yet to be definitively proven, the theory of hot gas chemistry, incorporated into homogeneous and heterogeneous chemical reactions between the

exhaust gas plume and the surrounding atmosphere, has given rise to a great deal of concerns for the effects that solid rocket motors can have upon stratospheric ozone levels.

Despite the theories, the use of column ozone data from the TOMS instrument directly following a series of space shuttle launches does not support the scientific models or hypothetical conclusions that space shuttle and Titan IV rocket launches have any significant impact upon stratospheric ozone levels immediately after a launch. The experts at the NASA/Goddard Space Flight Center used 1991 TOMS data to refute these claims, and have since made further improved the TOMS measurements. This study will employ that latest version of data to follow up the NASA/GSFC results with a more detailed statistical analysis of stratospheric ozone levels following both space shuttle and Titan IV rocket launches.

APPROACH/METHODOLOGY

OVERVIEW:

To extend the research performed by McPeters and Ross (6,3), this thesis effort will consist primarily of a thorough descriptive statistical analysis of the TOMS satellite column ozone data. This analysis will be performed with the intent of 1) developing the background trends and variations in TOMS-measured column ozone data at specific sites before space shuttle and Titan IV rocket launches, and 2) compare this background ozone level and variation to the ozone level measured the same day after a launch to determine if there is any significant change in column ozone following a launch. To carry out the aforementioned work, this effort will focus on two areas of analysis. The first will be a study of the TOMS Overpass data for two specific sites, Cape Canaveral AFS, FL and Vandenberg AFB, CA. This will be in direct response to the questions posed by Aftergood (5) and answered by McPeters (6) as to whether or not there would be any significant depletion in column ozone directly over a launch site following a space shuttle or Titan rocket launch. The second area of study will be a statistical analyses of the TOMS 50 km x 50 km field of view (FOV) gridded daily ozone data, performed for column ozone level changes 30 days prior to and immediately after a launch. This analysis will focus on a more precise area where the SRM exhaust plume trail is expected to have transported.. The plume drift due to upper atmospheric winds will contain the most probable area of exhaust plume/atmospheric photochemistry and potential ozone depletion. This section will conclude with a description of the statistical analysis methods and software packages utilized in determining average column ozone levels,

background level changes, trends and variability, for pre- and post-launch total column ozone levels taken from the TOMS satellite data. A brief error analysis will then be performed to determine a measure of accuracy of these results, and identify other possible sources of either qualitative or quantitative error within the methodology.

SPECIFIC SITE OVERPASS DATA ANALYSIS:

In his 1991 comment in *Journal of Geophysical Research* regarding Prather's "The Space Shuttle's Impact of the Stratosphere," Steven Aftergood proposed that it would seem possible that a local ozone hole of several tens of kilometers, or at least an ozone "soft spot", could occur directly over a launch site for several hours after launch (5). At Prather's request, McPeters responded with a color pixel analysis of TOMS Gridded Daily total column ozone levels captured immediately after eight separate space shuttle launches (6). This study of post-launch data only failed to detect any significant changes in total column ozone levels as measured by color step changes for varying total column ozone values. This thesis will further the work by McPeters by utilizing the latest version of the TOMS Overpass data, Version 7, to perform a pre-launch column ozone analysis, focused on determining background ozone trends, changes, and variability before each launch to compare and contrast with the total column ozone level measured by the TOMS instrument immediately following a launch.

Each TOMS Overpass data file contains daily total column ozone data for each of 371 individual ground locations. Each day the single TOMS field of view closest to the latitude/longitude of the site is selected as the "best match", and stored as the day, scan angle, universal time of the satellite pass over the site, the latitude and longitude of the

measurement, the total column ozone in Dobson Units, the reflectivity within the field of view, the TOMS solar zenith angle, the average terrain pressure within the FOV and any error flags on the data (24). Here we will study the TOMS Overpass data for locations 449 (Cape Canaveral AFS) and 494 (Vandenberg AFB) before and after 18 East coast space shuttle and Titan rocket launches and five West coast Titan rocket launches.

LOCAL TOMS FOV ANALYSIS:

The local TOMS Field Of View analysis will be performed according to where the solid rocket motor exhaust plume is most likely to have traveled, as well as an analysis of trends and variability in total column ozone directly before and after a launch. The local TOMS FOV is important because it provides the smallest area of total column ozone analysis, which should match up to the predicted area of plume expansion and ozone depletion as predicted by Ross, Prather and Aftergood (3,1,5). These 50 km by 50 km "pixels" are the most sensitive TOMS data likely to show any changes in total column ozone immediately after a launch.

Pixel regions selected for analysis will be based upon expected plume exhaust transport as modeled by Martin Ross in his work for the Aerospace Corporation (3). Ross modeled the SRM exhaust plume transport due to upper atmospheric winds for both East-coast and West-coast launches during the months of January and July. These two months experience upper atmospheric winds which are predominantly out of a direction and of a magnitude representative of either the winter or summer stratospheric climate conditions. This model and the predicted exhaust plume transport are based upon the daily mean windspeed and direction expected during winter or summer launch periods,

and are usable for the months of December through February in the winter and June through August in the summer. During the other months, the stratosphere is experiencing its seasonal shift in predominant wind direction, which actually occurs around each equinox. At these times, the standard deviation of the daily mean windspeed and direction is actually greater than the average windspeed and direction themselves, and predicting an average or predominant plume transport path would be highly inaccurate and virtually useless (24).

Given the timeframe limitations dictated by Ross' plume models, there are 13 East coast space shuttle and Titan rocket launches that can be analyzed, along with one West coast Titan rocket launch. Again, we will study the thirty days prior to each launch to determine a background trend and variability of zonal column ozone levels, then compare the post launch zonal column ozone value from the TOMS instrument to the pre-launch trends to determine if there are any significant changes occurring in the stratospheric ozone levels immediately after a launch.

Daily Gridded TOMS measurements have been averaged into grid cells covering 1° of latitude by 1.25° of longitude, providing a field of view for each grid of approximately 50 km by 50 km, depending upon the zenith angle of the satellite. TOMS collects 35 measurements every eight seconds as it scans from right to left, which is then averaged to obtain each grid's total column ozone value. Each pass' ozone measurement typically ranges between 100 and 650 Dobson Units.

DESCRIPTIVE STATISTICAL ANALYSIS METHODOLOGY:

As previously described, each area and each launch will be analyzed in a similar statistical method. First, the data from the 30 days prior to launch will be gathered, and a time series plot constructed in order to visually determine any trends in the data and the amount of natural variability of the total column ozone levels. This effort will specifically look for the amount of change in the mean and the amount of change in the variance over those 30 days. A typical Statistix time series plot will look like the following:
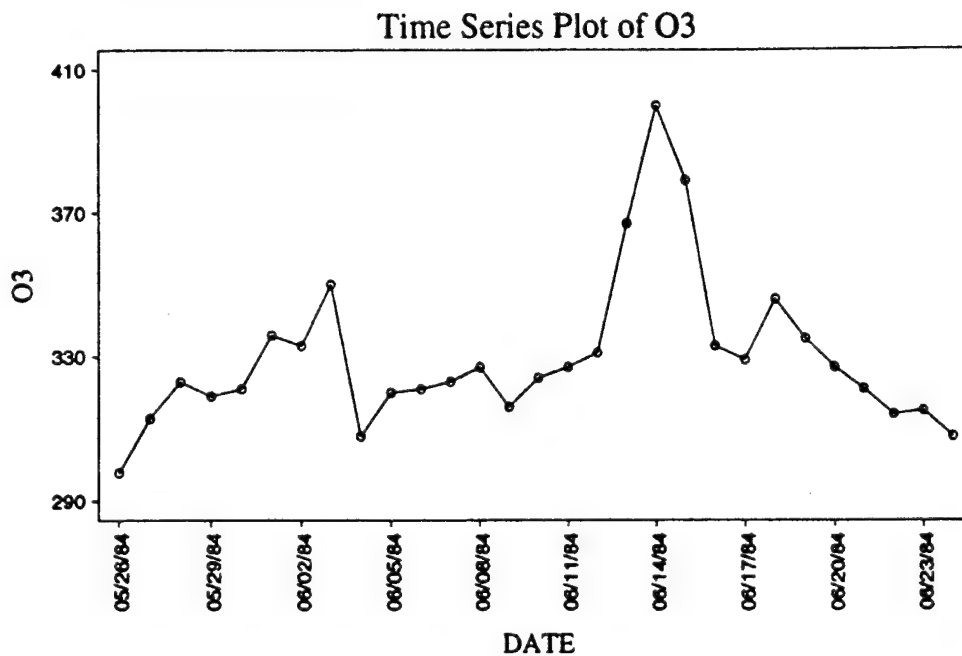
Figure 3-1. Time Series Plot of Prelaunch Column Ozone Levels (DU).

If the data appears to be "stable", that is, the mean is constant and there is constant variance, then the data can be used to create a prediction interval for a new independent observation--which in this thesis will be the total column ozone reading immediately

following a launch. As further support for the visual determination of trend, a regression curve fit will be run on each 30-day data set to support the claim of normality of the population, equality of variance, and determination of trend. The Statistix software package will be used for each of these tests. Where there is no trend, the mean of the total column ozone data will be calculated using the equation:

$$\bar{x} = \sum x_i/n \qquad \text{where } i = 1..n \text{ and } n = \text{the number of days analyzed (30)}$$

Statistix uses the Wilk-Shapiro/Rankit Plot procedure to examine whether a particular random sample of size n conforms to a normal distribution. A rankit plot of the variable is produced, and an approximate Wilk-Shapiro normality statistic, the Shapiro-Francia statistic, is calculated (26). If the Wilk-Shapiro statistic is approximately .90 or greater, then the variable may be considered normally distributed. The chart below is an example of a Statistix Wilk-Shapiro/Rankit Plot used for the normality test:
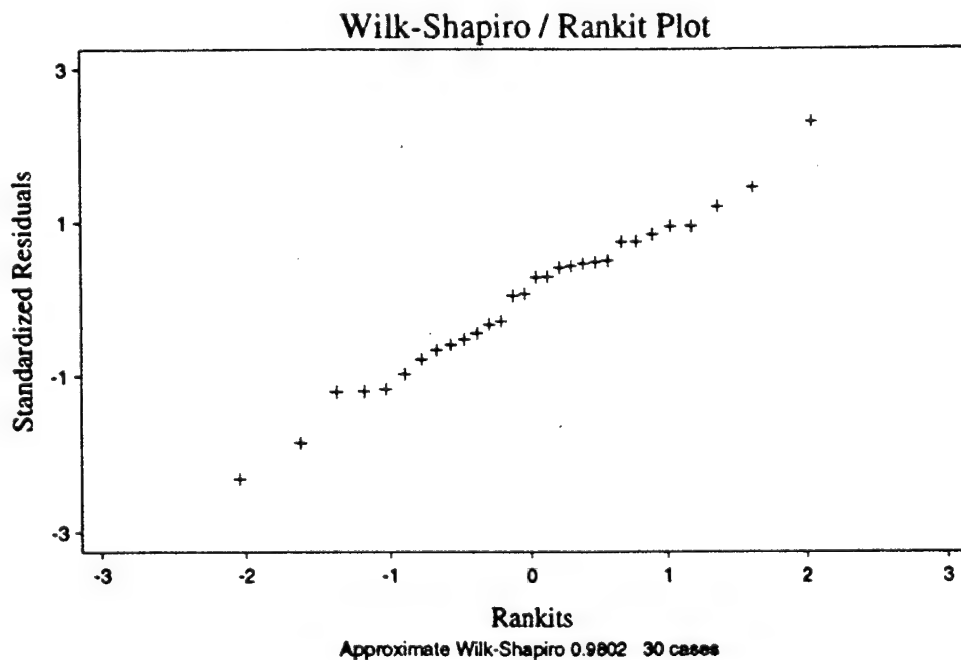
Figure 3-2. Statistix Wilk-Shapiro/Rankit Plot.

As a test of constancy or equality of variance, Statistix will be used to create a plot of residuals. If the residuals are evenly distributed about the zero line of the plot, then it can be said that there is equality of variance. If the residuals indicate a change or trend in the variance, another statistical approach must be used to analyze the data set. A sample regression plot is seen below:
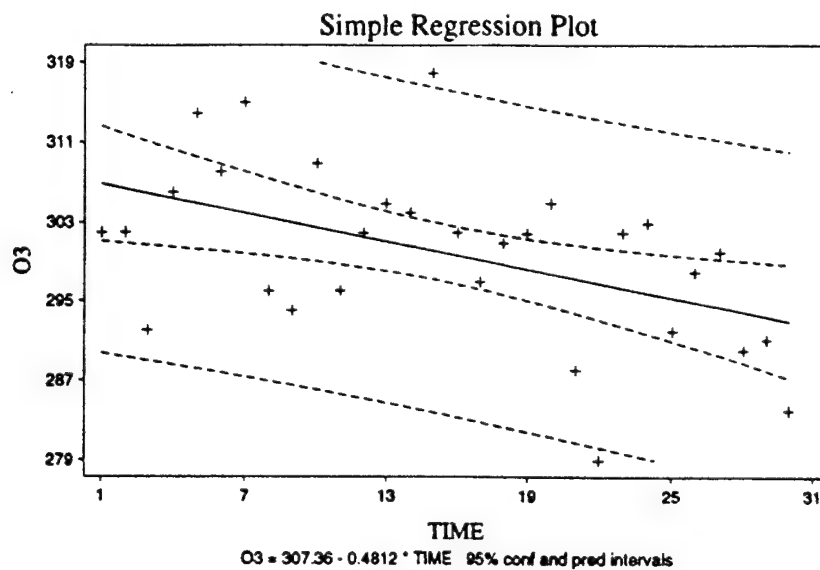
Figure 3-3. Statistix Regression Plot

Finally, Statistix also has the capability of evaluating the data for trends by utilizing the linear model section of the software. The linear model's linear regression procedure will calculate a slope coefficient and P-value for the data, which in turn is an indication of data trends. If the null hypothesis that the slope coefficient is approximately zero cannot be rejected, then one can suggest that there is no trend in the data. Below is a typical linear regression table from Statistix:

```
UNWEIGHTED LEAST SQUARES LINEAR REGRESSION OF O3
```

PREDICTOR VARIABLES	COEFFICIENT	STD ERROR	STUDENT'S T	P
CONSTANT	307.359	2.94884	104.23	0.0000
TIME	-0.48120	0.16610	-2.90	0.0072

R-SQUARED	0.2306	RESID. MEAN SQUARE (MSE)	62.0100
ADJUSTED R-SQUARED	0.2031	STANDARD DEVIATION	7.87464

SOURCE	DF	SS	MS	F	P
REGRESSION	1	520.419	520.419	8.39	0.0072
RESIDUAL	28	1736.28	62.0100		
TOTAL	29	2256.70			

```
CASES INCLUDED 30    MISSING CASES 0
```

Figure 3-4. Statistix Linear Regression Table

Once the data is determined normal, of constant variance, and no trend exists, a prediction interval can be calculated. The interval will be based upon a 95% confidence coefficient that the calculated prediction interval will "hook" an independent sample taken from the same population, if there is no change in the process. The 95% confidence coefficient is chosen based upon the $\pm 2\sigma$ level, which should capture 95% of the population under study. To obtain this prediction interval, the t-distribution prediction interval approach outlined in Devore's Probability and Statistics for Engineering and the Sciences will be used (25:296). The prediction interval is based upon the assumptions that 1) the population of interest is normally distributed, and 2) the mean, μ, and standard deviation, σ, are unknown. From these assumptions, the prediction interval (PI) for a

single observation to be selected from a normal population distribution with no trend would be:

$$PI = \bar{x} \pm t_{\alpha/2,\, n\text{-}1} \cdot s \sqrt{1 + 1/n}$$

The prediction level is thus $100(1 - \alpha)\%$ (25:296). At this level, the chance of making the error that an insignificant change in total column ozone is labeled significant will be 5%. Post-launch observations will then be compared to the prediction intervals in a test of significance. If the prediction interval includes or "hooks" the post-launch measurement, then it can be suggested with 95% confidence that the change in total column ozone following a launch is not significant. If the post launch measurement is not hooked by the predicted interval, then it can be said that the change in total column ozone is, in fact, significant, again with 95% confidence.

If the thirty days prior to launch does show correlation, i.e. there is some trend in the change of the mean and/or variance of total column ozone, then a different method of obtaining a prediction interval must be used. In this case, the data will be checked for normality and equality of variance as before, along with a simple linear regression analysis, but in this case a linear regression prediction interval will be obtained. This regression prediction interval will take into account any trends and variance changes of the 30 days preceding the launch, in order to more accurately predict a range of values that the independent launch day ozone level would normally fall within. Again, the 95% confidence coefficient will be established for the prediction interval of the post launch measurement to determine any significant changes in the total column ozone level. A linear regression prediction interval from Statistix will look like the following:

```
STUDENT EDITION OF STATISTIX 4.0

PREDICTED/FITTED VALUES OF O3

LOWER PREDICTED BOUND    275.22    LOWER FITTED BOUND     286.40
PREDICTED VALUE          292.44    FITTED VALUE           292.44
UPPER PREDICTED BOUND    309.67    UPPER FITTED BOUND     298.48
SE (PREDICTED VALUE)     8.4087    SE (FITTED VALUE)      2.9488

UNUSUALNESS (LEVERAGE)   0.1402
PERCENT COVERAGE           95.0
CORRESPONDING T            2.05

PREDICTOR VALUES: TIME = 31.000
```

Figure 3-5. Statistix Linear Regression Prediction Interval

Depending upon the results of the statistical analysis of each launch, a further

analysis on the number of significant changes in total column ozone following a launch

may be required. In this event, the number of significant changes in total column ozone

will be used to create a prediction statement as to what the probability would be that a

significant change in total column ozone will be observed following a space shuttle or

Titan rocket launch. This estimate will be another indication of the likelihood that there

is, in fact, a direct correlation between space vehicle launches, solid rocket motor exhaust

plumes, and stratospheric ozone levels.

ERROR ANALYSIS:

A brief error analysis will also be presented, using the variability of total column

ozone data and the TOMS measurement error calculated by the NASA/Goddard Space

Flight Center. This error analysis will be used to provide an estimate of the accuracy of

the predictions as to whether any of the changes noted in the descriptive statistical analyses are significant or not. In addition, a discussion of qualitative and quantitative errors arising from the methodology and the Ross exhaust plume transport model will be included, along with any other sources of error not easily quantifiable.

SUMMARY:

By utilizing Version 7 of the TOMS instrument data, the methodology proposed should improve the studies performed by McPeters, Prather, and Ross on the effects of solid rocket motor exhaust plumes to stratospheric ozone levels. Through analysis of the TOMS Overpass data, Aftergood's hypothesis that the total column ozone levels over a launch site would experience either a "hole" or a "soft spot" can be either proven or disproven. In addition, the use of the Gridded Daily TOMS FOV data can provide an indication of significant changes in total column ozone over specific locations where the solid rocket motor exhaust plume is most likely to have traveled when the Nimbus 7 satellite passes overhead. Through the descriptive statistical analysis methods posed, prediction intervals can be developed based upon prelaunch data, which will include any trends or natural variability in the total column ozone levels. This in turn will be used in a test of significance to answer the questions of whether the post-launch ozone measurements indicate any significant change from prelaunch levels. Ultimately, this should provide an answer to the specific problem statement of this thesis -- does the solid rocket motor exhaust of a space shuttle or Titan rocket launch have an affect upon stratospheric ozone levels?

RESULTS

OVERVIEW:

After retrieving the ozone data off of the two TOMS satellite ozone data compact discs provided by NASA/Goddard Space Flight Center, the analyses of the Overpass data and Gridded Daily Field of View data were performed as described previously in the methodology/approach section. For the Overpass data analysis, 18 space shuttle launches from Cape Canaveral AFS and five Titan III/IV launches from Vandenberg AFB were studied, while for the Gridded Daily Field of View pixel data analysis, 13 East coast space shuttle launches and one West coast Titan IV launch were targeted for ozone depletion analysis before and after each launch. Consideration for stratospheric winds and plume drift are also included in the Gridded Daily ozone data analysis. In each analysis, the thirty days prior to launch were used to study stratospheric ozone trends and create a 95% Prediction Interval for the ozone level on the day of the launch. This prediction interval was then compared to the actual launch day ozone level to determine if there was any significant change in total column ozone following the launch. Simply for comparison's sake, a brief analysis of ozone levels from the day before the launch and the day of the launch was conducted to illustrate the importance of considering the natural variation and pre-launch trends in the stratospheric ozone levels. Following the Overpass and Gridded Daily ozone analyses will be a brief error analysis, focusing on a qualitative discussion of potential sources of error in these studies.

OVERPASS DATA ANALYSIS RESULTS:

Results of the Overpass analysis are based upon the post-launch total column ozone and a 95% Prediction Interval of total column ozone, calculated through a statistical analysis of the 30 days prior to launch and compared with the satellite ozone measurement immediately after launch. Table 4-1 is a list of the launch dates and launch times for the 18 space shuttle launches from Cape Canaveral and five Vandenberg AFB Titan rocket launches, as well as the satellite overpass time after each launch. Launch and satellite overpass times are in Universal Time (UT).

LAUNCH DATE	LAUNCH TIME	OVERPASS TIME
Cape Canaveral AFS, FL		
27 Jun 82	1500	1637
18 Jun 83	1133	1647
30 Aug 83	0632	1636
03 Feb 84	1300	1607
30 Aug 84	1241	1733
17 Jun 85	1133	1617
27 Aug 85	1058	1708
12 Jan 86	1155	1555
28 Jan 86	1638	1719
02 Dec 88	1430	1634
08 Aug 89	1237	1544
09 Jan 90	1235	1522
05 Jun 91	1325	1609
02 Aug 91	1502	1605
22 Jan 92	1452	1530
31 Jul 91	1357	1451
02 Dec 92	1324	1506
13 Jan 93	1359	1523
Vandenberg AFB, CA		
18 Jun 80	1230	1917
20 Jun 83	1245	1910
25 Jun 84	1247	1958
04 Dec 84	1203	1911
28 Aug 85	1520	1913

Table 4.1 Satellite Overpass Data Launch Information

After performing the linear regression analysis of each launch's 30-day precedence, 9 of the 23 data sets showed definite linear trends in total column ozone, while the remaining 14 did not show a significant trend. For those nine showing a trend, the

Statistix software package calculated a prediction interval for the expected launch day

ozone level, accounting for that trend. Prediction intervals for the 14 data sets showing

no trend were calculated using the mean and standard deviation, t-distribution and the

Devore equation identified in the previous chapter. For comparison, pre-launch total

column ozone levels are compared with post-launch levels ignoring any trends or natural

variation. These results are tabulated in Table 4-2, with ozone measurements reported in

Dobson Units (DU).

LAUNCH DATE	PRE-LAUNCH O_3	POST-LAUNCH O_3
Cape Canaveral AFS, FL		
27 Jun 82	308	302
18 Jun 83	308	296
30 Aug 83	309	317
03 Feb 84	295	292
30 Aug 84	300	299
17 Jun 85	282	291
27 Aug 85	287	283
12 Jan 86	272	277
28 Jan 86	320	328
02 Dec 88	242	259
08 Aug 89	319	317
09 Jan 90	248	245
05 Jun 91	330	323
02 Aug 91	302	304
22 Jan 92	290	275
31 Jul 91	300	292
02 Dec 92	238	245
13 Jan 93	230	231
Vandenberg AFB, CA		
18 Jun 80	332	342
20 Jun 83	320	326
25 Jun 84	308	325
04 Dec 84	306	275
28 Aug 85	284	280

Table 4.2 Pre-launch and Post-launch Overpass Ozone Levels

As can be seen in Table 4-2, the post-launch ozone levels were higher than the pre-

launch level 11 times (47.8%), while the after-launch ozone was lower then the day prior

12 out of 23 times (52.2%). Again, this table ignores any trend in the data, and is

provided for comparison only.

The results of the trend statistical analyses are reported in Table 4-3. Actual prediction interval calculations can be seen in Appendix A. The launch day ozone levels are also presented in order to determine in there was a significant change in launch day total column ozone, based upon the calculated 95% Prediction Interval. Both the prediction intervals and post-launch ozone measurements are reported in Dobson Units.

LAUNCH DATE	PREDICTION INTERVAL	POST-LAUNCH O₃
Cape Canaveral AFS, FL		
27 Jun 82	277.66 - 324.88	302
18 Jun 83	283.24 - 340.56	296
30 Aug 83	289.14 - 316.40	317
03 Feb 84	246.19 - 327.55	292
30 Aug 84	287.68 - 319.28	299
17 Jun 85	251.90 - 328.15	291
27 Aug 85	275.62 - 302.85	283
12 Jan 86	238.85 - 294.35	277
28 Jan 86	268.34 - 321.10	328
02 Dec 88	225.56 - 260.37	259
08 Aug 89	302.10 - 323.84	317
09 Jan 90	229.53 - 290.33	245
05 Jun 91	292.25 - 348.15	323
02 Aug 91	294.23 - 322.25	304
22 Jan 92	230.12 - 309.08	275
31 Jul 91	286.09 - 310.31	292
02 Dec 92	220.48 - 268.26	245
13 Jan 93	228.24 - 281.98	231
Vandenberg AFB, CA		
18 Jun 80	266.12 - 359.69	342
20 Jun 83	294.41 - 362.59	326
25 Jun 84	284.93 - 374.65	325
04 Dec 84	242.45 - 312.29	275
28 Aug 85	275.22 - 309.67	280

Table 4.3 Overpass Data Statistical Analysis Results

From the statistical analysis it can be seen that, of the 23 launches, post-launch total column ozone was higher than the prediction interval on two occasions (8.7%), associated with the 30 August 1983 and 12 January 1986 launches. None of the post-launch ozone measurements fell below the interval predicted, while the remaining 21 ozone levels fell within the 95% Prediction Interval (91.3%). Thus, all of the post-launch

total column ozone levels were either within or higher than the predicted total column ozone levels, at the 95% level.

GRIDDED DAILY FOV ANALYSIS RESULTS:

Analysis of the Gridded Daily Field of View total column ozone data was performed for the 30 days prior to 13 space shuttle launches and one Titan IV rocket launch to create the statistical prediction intervals. After considering plume drift due to stratospheric winds, the launches analyzed and the latitude/longitude of the closest grid pixel, based upon satellite pass time after each launch, are presented in Table 4.4 below.

LAUNCH DATE	LATITUDE	LONGITUDE
Cape Canaveral AFS, FL		
27 Jun 82	28.5	-81.875
03 Feb 84	28.5	-78.125
12 Jan 86	28.5	-77.000
28 Jan 86	28.5	-80.625
02 Dec 88	28.5	-79.375
08 Aug 89	28.5	-83.125
09 Jan 90	28.5	-78.125
05 Jun 91	28.5	-83.125
02 Aug 91	28.5	-81.875
22 Jan 92	28.5	-80.625
31 Jul 91	28.5	-81.875
02 Dec 92	28.5	-79.375
13 Jan 93	28.5	-79.375
Vandenberg AFB, CA		
28 Aug 85	33.5	-121.875

Table 4.4 Satellite Field of View Launch Information

For the Field of View linear regression analysis of the 30 pre-launch days, results indicated a trend in five of the 14 data sets, whereas nine data sets showed no significant trend in total column ozone levels. Table 4-5, which compares the total column ozone level on the day prior to launch and the post-launch ozone level, indicates that in six of the 14 cases observed, the post-launch total column ozone was higher than the pre-launch level. There were also six cases in which the post-launch ozone was lower than the

previous day's measurement. In the remaining two cases, the pre-launch and post-launch

ozone levels were the same.

LAUNCH DATE	PRE-LAUNCH O$_3$	POST-LAUNCH O$_3$
Cape Canaveral AFS, FL		
27 Jun 82	306	298
03 Feb 84	298	298
12 Jan 86	270	275
28 Jan 86	318	324
02 Dec 88	244	259
08 Aug 89	321	315
09 Jan 90	248	242
05 Jun 91	321	325
02 Aug 91	304	304
22 Jan 92	288	277
31 Jul 91	301	301
02 Dec 92	238	247
13 Jan 93	228	233
Vandenberg AFB, CA		
28 Aug 85	283	278

Table 4.5 Pre-launch and Post-launch FOV Ozone Levels

Analysis calculation results are in Table 4.6 and Appendix B.

LAUNCH DATE	PREDICTION INTERVAL	POST-LAUNCH O$_3$
Cape Canaveral AFS, FL		
27 Jun 82	280.93 - 320.72	303
03 Feb 84	242.16 - 324.18	298
12 Jan 86	249.09 - 292.29	277
28 Jan 86	268.74 - 320.04	324
02 Dec 88	228.74 - 258.47	259
08 Aug 89	297.36 - 324.98	315
09 Jan 90	230.28 - 284.98	242
05 Jun 91	292.52 - 344.62	325
02 Aug 91	296.82 - 327.86	304
22 Jan 92	231.65 - 308.15	277
31 Jul 91	284.97 - 310.29	301
02 Dec 92	223.62 - 266.64	247
13 Jan 93	223.40 - 269.08	233
Vandenberg AFB, CA		
28 Aug 85	272.71 - 304.12	278

Table 4.6 Field Of View Data Statistical Analysis Results

From the statistical analysis of the Field of View ozone data, it can be seen that

post-launch total column ozone was higher than the prediction interval two times (14.3%),

while the ozone level was never lower than the interval predicted. The remaining 12 post-

launch ozone levels fell within the 95% Prediction Interval calculated (85.7%). Thus, again, 100% of the post-launch total column ozone measurements were either within or higher than the predicted total.

ERROR ANALYSIS:

Each area of analysis has its own sources of potential error, which can have either little or no affect upon the results, or could possibly change the results entirely. For the Overpass ozone data analysis, the potential sources of error include the TOMS instrument measurement error, the defined 5% Prediction Interval error, and errors associated with the use of the linear regression model to fit the data and calculate the 95% Prediction Interval. Measurement error from the TOMS instrument is calculated by NASA/Goddard SFC as $\pm 1.5\%$, which would not change the calculated results appreciably, and is smaller than the 5% error accepted in the 95% Prediction Interval. The largest probable error source is in the linear regression model used to fit the data and determine trends. Visually, some data sets indicated linear trends, but the time series plots in Appendix A also indicate that there are probably more trigonometric trends, such as sine and cosine waves in the data sets. Fitting this type of curve to the data would probably reduce the residuals and provide a tighter, more accurate prediction interval to estimate the post-launch ozone range. This tighter curve fit could alter the results significantly, as a smaller range would greatly improve the accuracy of the comparison of pre-launch and post-launch stratospheric ozone conditions.

Error sources associated with the Gridded Daily total column ozone analysis are more prevalent. As with the Overpass data analysis, there is the 1.5% instrument

measurement error, the defined 5% Prediction Interval error, and the errors associated with the linear regression model used to analyze the data for trends and prediction intervals. However, the largest source of error with the Daily Field of View data analysis could be in estimating the actual plume drift and pixel area to analyze at the precise time that the satellite passes over the solid rocket motor exhaust area. Here error can come from modeled plume transport locations, which are based upon estimates of the prevailing stratospheric wind conditions for the time period of the launch, and not from actual post-launch wind magnitudes and directions. This data could place the SRM exhaust plume in an entirely different location than the pixel grid analyzed, which would require a new analysis. There is also a small source of human error in the plume location analysis, coming from errors projecting the modeled area and location onto a gridded map correctly.

SUMMARY:

Through the statistical analysis of the 30 days prior to each launch, the 95% Prediction Interval was calculated for each Overpass and Field Of View data set, within which should fall the total column ozone measurement the next day if all conditions of the ozone creation/destruction process continue unchanged. For the Overpass data sets, 100% of the cases saw the post-launch ozone level either hooked by or higher than the calculated prediction interval. Only one of the 14 Field Of View post-launch ozone levels fell outside of the 95% Prediction Interval, but it, too, was higher than the predicted range.

Potential error sources in the data include the ± 1.5% measurement error of the TOMS instrument, the 5% Prediction Interval error, and the errors associated with fitting the ozone data with a linear regression model. In the Field of View analysis, another large potential source of error can be found in modeling the location and shape of the exhaust plume at the time the satellite passes over the SRM exhaust plume after launch.

Ultimately these results and the limitations posed by the methodology and approach will be used for the basis of the conclusions and recommendations formed in the next section of this thesis effort.

CONCLUSIONS AND RECOMMENDATIONS

OVERVIEW:

This thesis effort was undertaken to answer the question of whether the solid

rocket motor exhaust plume from a space vehicle launch had any affect upon stratospheric

ozone. Prather hypothesized that the local-plume ozone reductions decrease to near zero

over the course of a day, but that due to the path of a space shuttle flight path, the

corridor of exhaust gasses is spread over a lateral extent of more than 1000 km (1:10.11,

4:18,589). Still, Aftergood felt that there would be enough ozone depletion over a launch

site following a shuttle launch due to exhaust gas chemistry that it would leave a

noticeable ozone hole for several hours after a launch (5:17,377). From an analysis of the

TOMS total column ozone measurements for both Overpass data and Gridded Daily Field

of View data, these questions can be answered, within the framework and limitations of

this thesis methodology and approach. There is also further work that can be performed

to improve the findings of this report, or to expand this effort to the analysis of newer,

similar TOMS data.

OVERPASS DATA ANALYSIS CONCLUSIONS:

Based upon the results of the Overpass data analysis, the work performed by

McPeters is strongly supported. His answer to Aftergood's question on the existence of

an ozone hole or "soft spot" over a launch site following a space shuttle or Titan rocket

launch is also well founded.

McPeters took a post-launch "snapshot" of the total column ozone condition with

a Gridded Daily Ozone measurement analysis using color-coded pixels to represent each

grid. The pixel colors were shaded in steps according to Dobson Unit measurements. This work showed no holes or areas of significantly reduced total column ozone anywhere around the launch site following a launch (6). Since McPeters performed a post-launch analysis only, this thesis improved that effort by analyzing the 30 days prior to a launch to determine natural trends and variability in stratospheric ozone over each launch site before each launch. This, in turn, provided a better answer to the question of whether the solid rocket motors had a significant affect upon the ozone levels over each site.

Using the 95% Prediction Interval approach, in all 23 cases studied the total column ozone measured by the TOMS instrument immediately after a space vehicle launch was within the predicted range. If Aftergood was correct, given the range and extent of ozone depletion he hypothesized, there should have been a significant change in post-launch total column ozone as measured by the TOMS instrument. This was not found in any of the analyses. Thus, there was no evidence that any significant reductions in total column ozone occurred following a launch. In fact, in two cases the post-launch ozone was actually higher than the predicted upper bounds, further supporting the position that solid rocket motor exhaust is not a significant contributor to stratospheric ozone depletion, nor does it cause a significant "hole" in the ozone layer over a launch site.

GRIDDED DAILY FOV ANALYSIS CONCLUSIONS:

To further improve the work by McPeters and account for the plume drift modeled by Ross (3), the Gridded Daily Field of View analysis was conducted in a similar manner to the Overpass data analysis. Taking into account the time after launch that the Nimbus-7 satellite passed over the launch trajectory area, and the spread and location of the solid

rocket motor exhaust plume at this same time, specific TOMS 50 km x 50 km data grids were selected and analyzed for the 30 days prior to 14 space shuttle and Titan rocket launches.

Again, in every case, the 95% Prediction Interval captured the measured post-launch total column ozone measurement recorded by the TOMS instrument. While the actual plume configuration and location are subject to the limitations of the Ross model, the analysis performed showed no significant changes in the natural stratospheric ozone processes after the launch of a space vehicle.

SUMMARY:

Several of the articles reviewed during the literature search for this thesis posed the question of whether or not the exhaust plume of a space shuttle or Titan rocket launch would significantly reduce stratospheric ozone. The problem statement of this work asked, "Does the solid rocket motor exhaust from the Space Shuttle and/or Titan IV rocket cause severe damage to the stratospheric ozone layer?" Based upon the findings here, the answer to that question is no. After the analysis of 23 Overpass data sets over Cape Canaveral AFS and Vandenberg AFB, and 14 Gridded Daily Field of View data sets that accounted for plume drift due to stratospheric winds, not one case of significant ozone depletion was found after a space vehicle launch.

Another consideration regarding the accuracy of the prediction intervals calculated is the "Unusualness Factor" reported by the Statistix software whenever a prediction interval was calculated for a data set showing trend. If the Unusualness Factor is greater than one, than the prediction interval specified by Statistix is highly suspect. In all cases

where Statistix calculated a 95% Prediction Interval, the Unusualness Factor was around 0.14 (See Appendix A and B). Thus, the Statistix prediction intervals for both the Overpass analysis and the Gridded Daily data analysis were well within acceptable probability and statistics limits.

Finally, an argument posed by Ross and the WMO (4,1) was that the TOMS instrument could not detect such ozone depletion because of the large field of view each measurement encompassed, as opposed to the small area of the solid rocket motor exhaust plume where there was expected to be 100% ozone depletion. However, given the areas of plume spread modeled by Ross, and the fact that 100% ozone depletion is theorized to occur within those confinements, such a significant reduction should be noticeable. And again, no significant changes in total column ozone, other than significant increases, were detected.

The fact that there was not one case of a significant drop in total column ozone is, itself, important to consider. If significant ozone depletion is occurring, and harmful UV-B radiation is, in fact, finding its way to the earth's surface, then the Air Force has a definite problem. But for the hypotheses of SRM exhaust photochemistry leading to an increase in UV-B radiation at the earth's surface to be true, one would have to construct a mental picture or how the UV-B could get from the upper stratosphere to the earth via the SRM exhaust plume ozone hole. Assuming that there was, in fact, 100% ozone depletion within the exhaust plume does occur, the TOMS instrument would act similarly to UV-B radiation as the satellite passed by to record a post-launch ozone measurement. The TOMS instrument sends specific wavelength pairs down through the stratosphere, and

through a reading of those wavelengths reflected back, the instrument determines the total column ozone by the absorption of the wavelength, either from ozone or and any other particle/chemical capable of absorbing the radiation. Now consider a UV-B photon from the sun similarly trying to reach the earth. Just like the TOMS wavelength, the UV-B photon can be absorbed as it travels towards the earth's surface, either by ozone or some other constituent of the stratosphere. In order to for the UV-B radiation to reach the earth's surface due to the solid rocket motor photochemistry and associated local ozone depletion, the photons would have to travel down the same path as the exhaust plume. This is an extremely unlikely occurrence. The photon would more likely travel the same path as the TOMS instrument emission, and thus experience the same conditions measured by the satellite. This photon can be absorbed by ozone either above or below the localized SRM exhaust plume, even if that plume area contains zero ozone. This thesis studied that hypothesis, and found that a UV-B photon would, in fact, encounter the same stratospheric conditions after a space shuttle or Titan rocket launch as it would have on the day before the launch.

RECOMMENDATIONS:

Based upon this thesis effort, there seems to be little support for spending a great deal of time and money in further examining the effects of solid rocket motors upon stratospheric ozone levels. There appears to be no significant decrease in total column ozone after a space vehicle launch, if the methodology and approach of this work is accepted. Despite the findings of this thesis effort, however, there are areas in which this work could either be improved or expanded. Improvements could be made in the area of

curve fitting of the TOMS data, while the work could be expanded to include measurements by the new TOMS instrument launched by NASA.

As mentioned in the error analysis of the Results section, one of the greatest potential sources of error in creating the 95% Prediction Intervals can come from the linear regression curve fit of the TOMS data. Using the linear regression model assumed that the data is, in fact, linear, but a visual examination of time series plots of each data set lends credibility to the belief that the data is more varied than that. Some trigonometric curve fitting could reduce the residuals found during the linear regression, and thus improve the accuracy of the prediction intervals. This, in turn, would provide greater fidelity into the significance of post-launch total column ozone changes as measured by the TOMS instrument.

To expand this work, a similar study of TOMS data from the new TOMS instrument launched in 1995 by NASA could be performed. This instrument has a much smaller field of view, 20km x 20km, and would by even more sensitive to smaller regions of ozone depletion, as in that within a solid rocket motor exhaust plume if it is occurring. In addition, both NASA and the Aerospace corporation are planning to fly aircraft through the solid rocket motor exhaust plume of a Titan IV rocket in December of 1996. Aerospace will fly a B-57 through the plume to measure ozone depletion levels and SRM/atmospheric photochemistry, while NASA will send an ER-2 through the same plume to look at ozone depletion. Comparing these results with the new TOMS satellite data, which should pass over the plume at the same time as the aircraft will fly through,

would provide further support for the accuracy of this thesis effort and the TOMS data in general.

REFERENCES

[1] Harwood, R. S. and others. In <u>Scientific Assessment of Ozone Depletion: World Meteorological Association Global Ozone Research and Monitoring Project</u>, *Report No. 25*, Chapter 10. World Meteorological Association, Geneva, Switzerland, (1991)

[2] WMO. <u>Scientific Assessment of Ozone Depletion: 1994 World Meteorological Association Global Ozone Research and Monitoring Project</u>, *Report No. 37*, Executive Summary. World Meteorological Association, Geneva, Switzerland, (1994)

[3] Ross, Martin. "Local Effects of Solid Rocket Motor Exhaust on Stratospheric Ozone," <u>Journal of Spacecraft and Rockets, Vol 33, No. 1, January-February</u>, p. 144 (1996)

[4] Prather, Michael J., and others. "The Space Shuttle's Impact on the Stratosphere," <u>Journal of Geophysical Research, Vol 95, No. D11</u>, p. 18,583 (1990)

[5] Aftergood, Steven. "Comment on "The Space Shuttle's Impact on the Stratosphere" by Michael J. Prather et al," <u>Journal of Geophysical Research, Vol 96, No. D9</u>, p. 17,377 (1991)

[6] McPeters, R., M. Prather, S. Doiron. "Reply to Aftergood's "Comment on "The Space Shuttle's Impact on the Stratosphere" by Michael J. Prather et al"," <u>Journal of Geophysical Research, Vol 96, No. D9</u>, p. 17,379-17,381 (1991)

[7] Herman, J. R., R. McPeters, D. Larko. "Ozone Depletion at Northern and Southern Latitudes Derived From January 1979 to December 1991 Total Ozone Mapping Spectrometer Data," <u>Journal of Geophysical Research, Vol 98, No. D7</u>, p. 12,783-12,793 (1993)

[8] Gleason, J. F. and others. "Record Low Global Ozone in 1992," <u>Science Vol 260</u>, p. 523-526 (1993)

[9] Brady, B. B., E. W. Fournier, L. R. Martin, R. B. Cohen. <u>Stratospheric Ozone Reactive Chemicals Generated by Space Launches Worldwide</u>, *Report No. TR-94(4231)-6*. The Aerospace Corporation, Los Angeles AFB, CA, USA (1994)

[10] Zittel, P. F. <u>Computer Model Predictions of the Local Effects of Large, Solid-Fuel Rocket Motors on Stratospheric Ozone</u>, *Report No. TR-94(4231)-9*. The Aerospace Corporation, Los Angeles AFB, CA, USA (1994)

[11] Strand, A., O. Hov. "The Impact of Man-Made and Natural NOx Emissions on Upper Tropospheric Ozone: A Two-Dimensional Model Study," <u>Atmospheric Environment, Vol 30 No. 8</u>, p 1291-1303 (1996)

[12] Montzka, S. A. and others. "Decline in Tropospheric Abundance of Halogen from Halocarbons: Implications for Stratospheric Ozone Depletion," <u>Science Vol 272</u>, p. 1318 (1996)

[13] Chipperfield, Martyn. "Satellite Maps Ozone Destroyer," <u>Nature Vol 362</u>, p. 592 (1993)

[14] Fahey, D. W. and others. "*In Situ* Measurements Constraining the Role of Sulphate Aerosols in Mid-latitude Ozone Depletion," <u>Nature Vol 363</u>, p. 509 (1993)

[15] Ko, M., N. Sze, M. Prather. "Better Protection of the Ozone Layer," <u>Nature Vol 367</u>, p. 505 (1994)

[16] Hilsenrath, E. and others. "Ozone Depletion in the Upper Stratosphere Estimated From Satellite and Space Shuttle Data," Nature Vol 358, p. 131 (1992)

[17] McCoustra, M., A. Horn. "Towards a Laboratory Strategy for the Study of Heterogeneous Catalysis in Stratospheric Ozone Depletion," Chemical Society Reviews, p. 195 (1994)

[18] Schwartz, S.E., M. Andreae. "Uncertainty in Climate Change Caused by Aerosols," Science Vol 272, p. 1121 (1996)

[19] Toumi, R., S. Bekkl, K. S. Law. "Indirect Influence of Ozone Depletion on Climate Forcing by Clouds," Nature Vol 372, p. 348 (1994)

[20] McPeters, R. D. and others. Nimbus-7 Total Ozone Mapping Spectrometer Data Products User's Guide, *NASA Reference Publication 1384*, NASA Goddard Space Flight Center, Greenbelt, Maryland, USA (1996)

[21] Stolarski, R. S., and others. "Total Ozone Trends Deduced from Nimbus 7 TOMS Data," Geophysical Research Letters Vol 18 No. 6, p. 1015-1018 (1991)

[22] US EPA, Stratospheric Protection Division, Ozone Depletion Science, EPA Ozone Depletion Home Page, United States Environmental Protection Agency, USA (1996)

[23] HQ SMC/PA. HIROIG High Resolution Ozone Imager Profile, USAF Space and Missile Systems Center, El Segundo, CA, USA (1996)

[24] Ross, Martin. Teleconference on Upcoming Aerospace Stratospheric Ozone Research Projects. Conversation held 2 October 1996, Air Force Institute of Technology, Wright-Patterson AFB, OH

[25] Devore, Jay L. Probability and Statistics for Engineering and the Sciences. California: Wadsworth Publishing, Inc., 1995

[26] Statistix, Users Manual, Version 4.1, New York: 1995

[27] Lund, Gary L. Model of Chlorocarbon (CFC-12) Chemisorption on Solid Rocket Motor Alumina Exhaust Particles, Air Force Institute of Technology, Wright-Patterson AFB, OH (1995)

[28] McPeters, R. and E. Beach. TOMS Version 7 O3 Gridded Data: 1978-1993, NASA Goddard Space Flight Center, Ref. No. USA_NASA_916_OPT_004A and _004B, NASA/GSFC, Greenbelt, MD, January 1996

APPENDIX A

VIEW DATA

CASE	DATE	O3
1	05/28/82	338.00
2	05/29/82	330.00
3	05/30/82	317.00
4	05/31/82	311.00
5	06/01/82	312.00
6	06/02/82	303.00
7	06/03/82	303.00
8	06/04/82	300.00
9	06/05/82	300.00
10	06/06/82	301.00
11	06/07/82	310.00
12	06/08/82	306.00
13	06/09/82	319.00
14	06/10/82	314.00
15	06/11/82	314.00
16	06/12/82	331.00
17	06/13/82	323.00
18	06/14/82	313.00
19	06/15/82	320.00
20	06/16/82	304.00
21	06/17/82	290.00
22	06/18/82	295.00
23	06/19/82	316.00
24	06/20/82	308.00
25	06/21/82	298.00
26	06/22/82	291.00
27	06/23/82	295.00
28	06/24/82	308.00
29	06/25/82	308.00
30	06/26/82	308.00

27 Jun 82 Wilk-Shapiro / Rankit Plot

Standardized Residuals
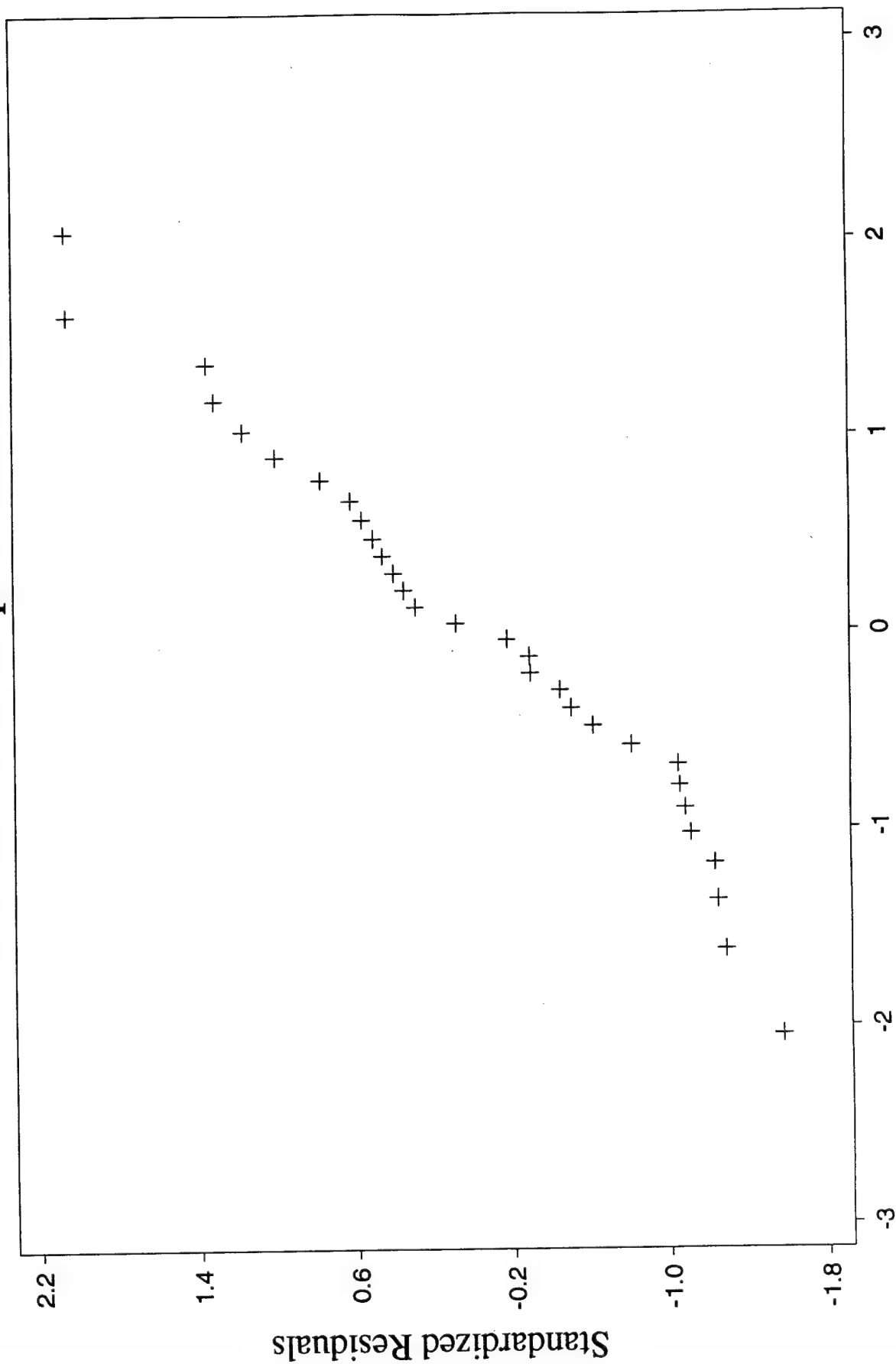
Rankits

Approximate Wilk-Shapiro 0.9640   30 cases

A-3

27 Jun 82 Simple Regression Plot
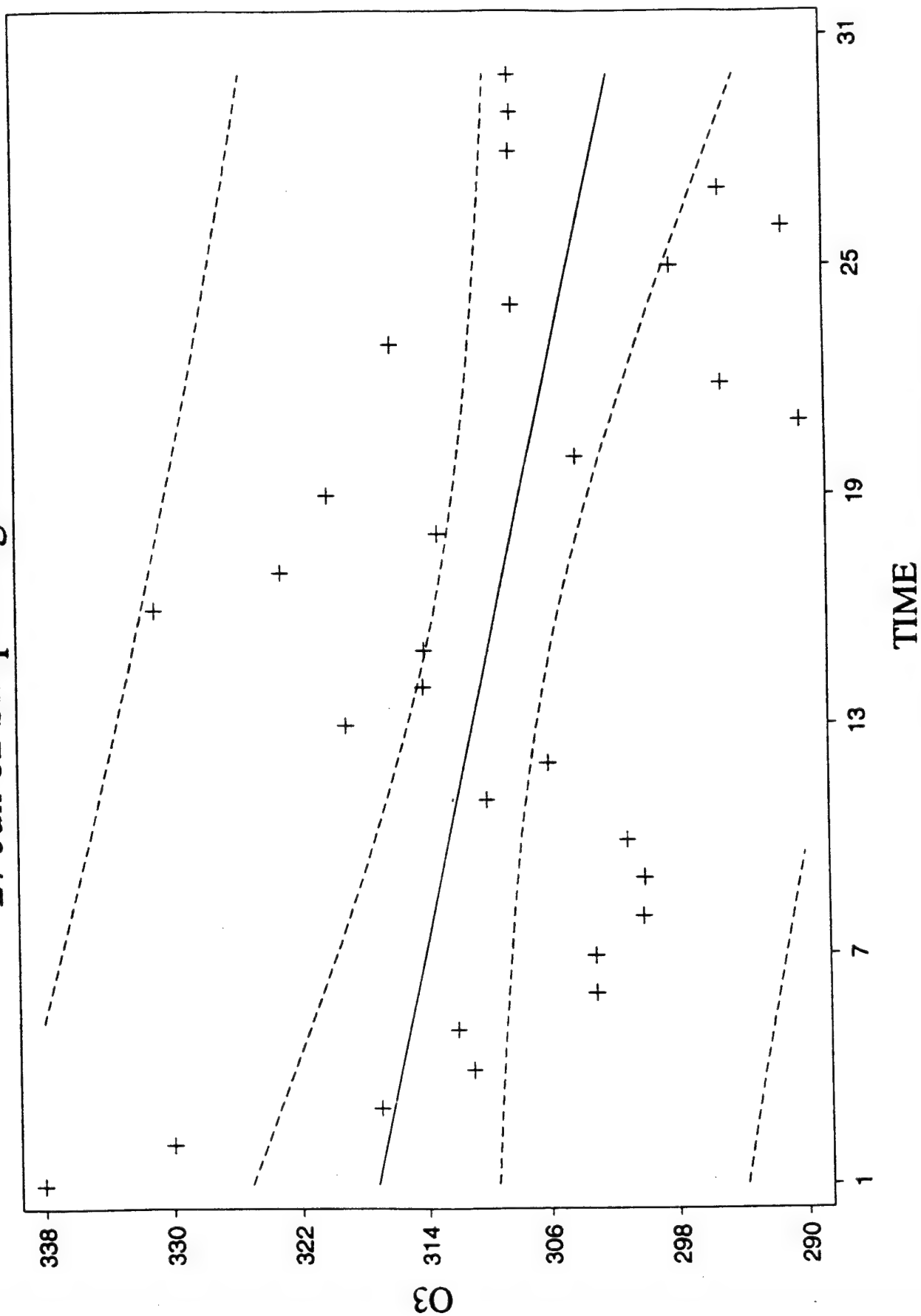
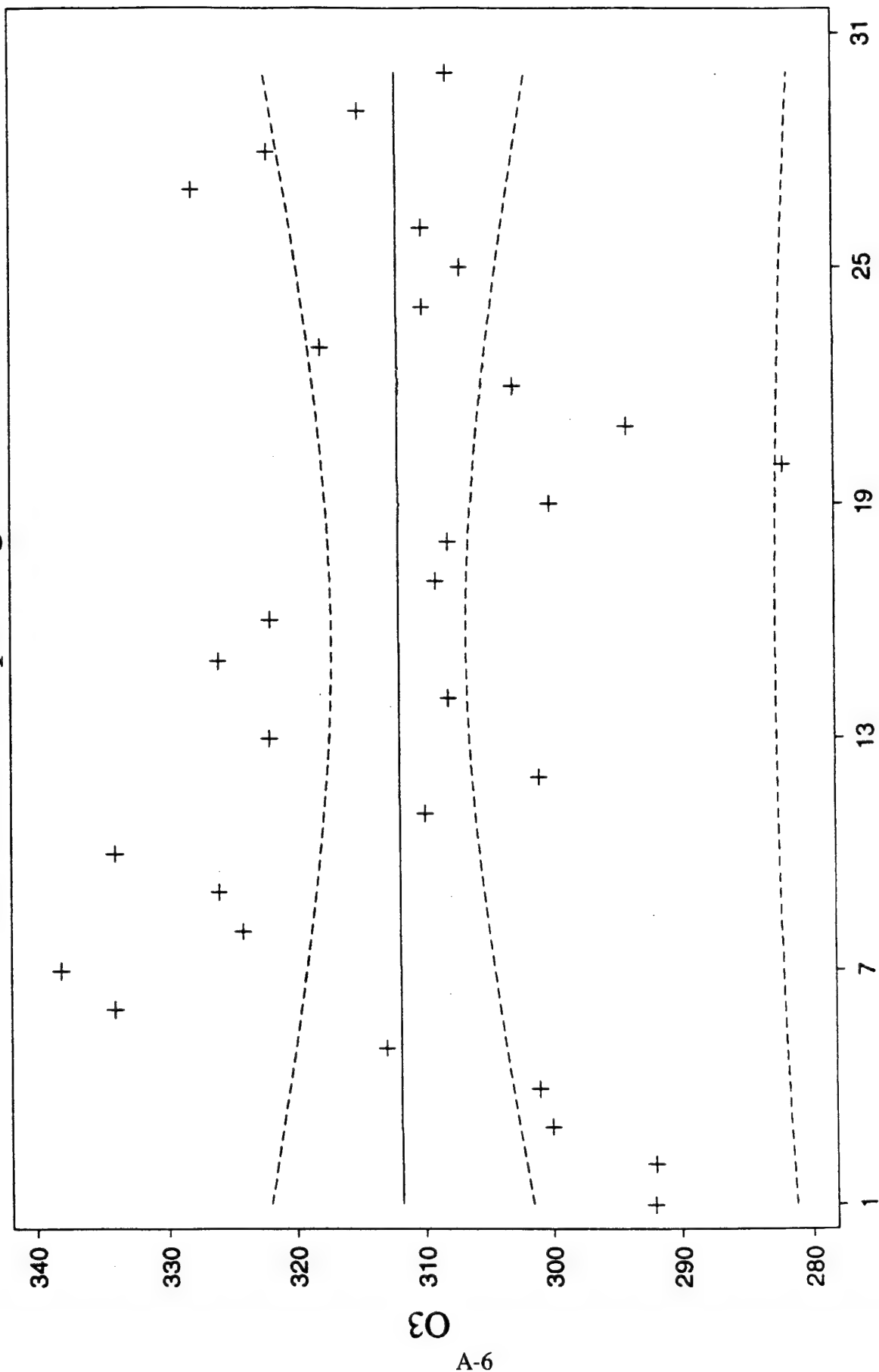
O3 = 317.80 - 0.5330 * TIME   95% conf and pred intervals

A-4

PREDICTED/FITTED VALUES OF O3

LOWER PREDICTED BOUND	277.66	LOWER FITTED BOUND	292.99
PREDICTED VALUE	301.27	FITTED VALUE	301.27
UPPER PREDICTED BOUND	324.88	UPPER FITTED BOUND	309.55
SE (PREDICTED VALUE)	11.527	SE (FITTED VALUE)	4.0424

UNUSUALNESS (LEVERAGE)	0.1402
PERCENT COVERAGE	95.0
CORRESPONDING T	2.05

PREDICTOR VALUES: TIME = 31.000

18 Jun 83 Simple Regression Plot

O3 = 311.74 + 0.0100 * TIME   95% conf and pred intervals

TIME

O3

DESCRIPTIVE STATISTICS

VARIABLE	N	MEAN	SD	MINIMUM	MAXIMUM
O3	30	311.90	13.785	282.00	338.00

$$PI = 311.9 \pm 2.045 \cdot 13.785 \sqrt{1 + 1/30}$$

$$PI = (283.24, \ 340.56)$$

30 Aug 83 Simple Regression Plot
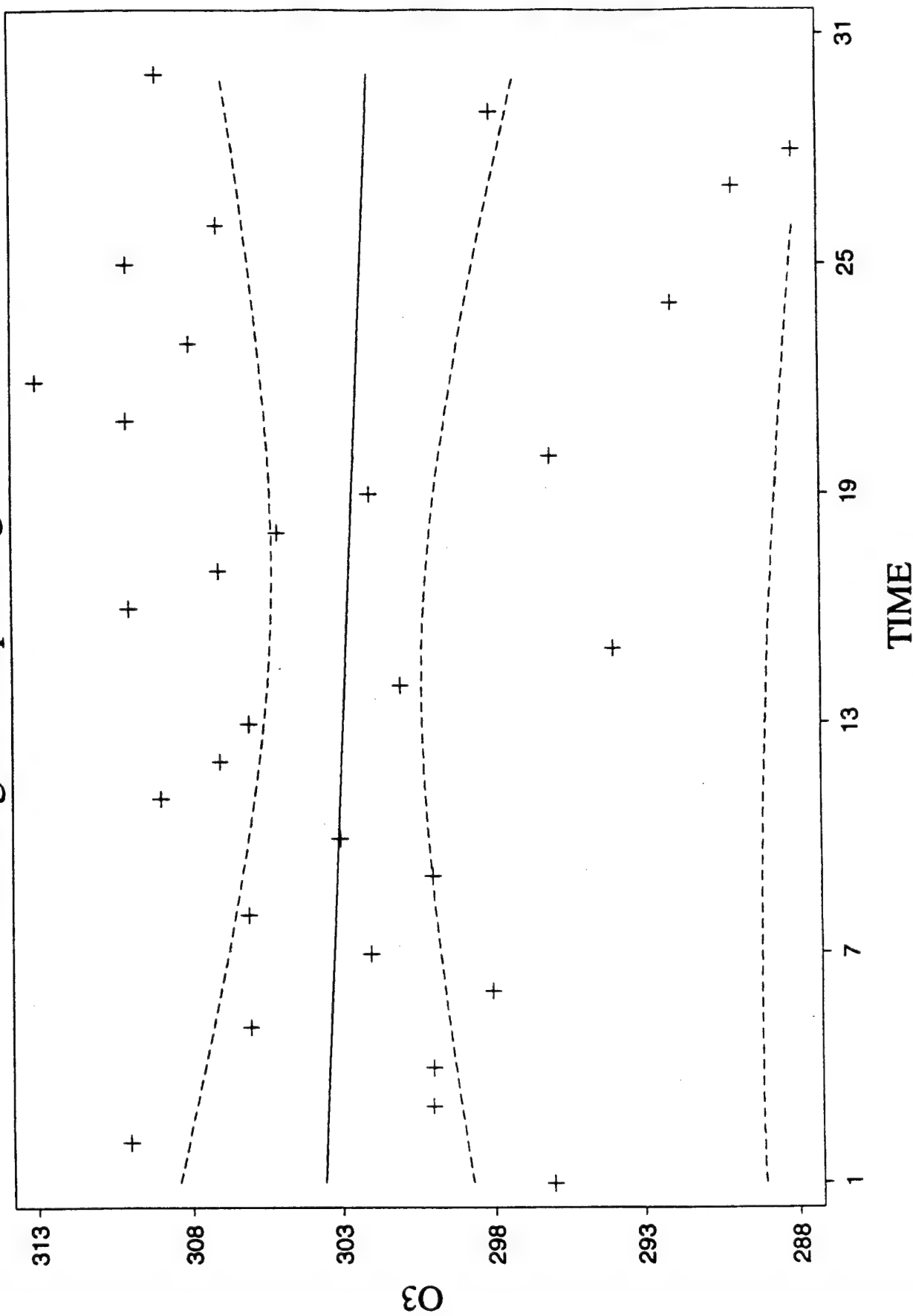
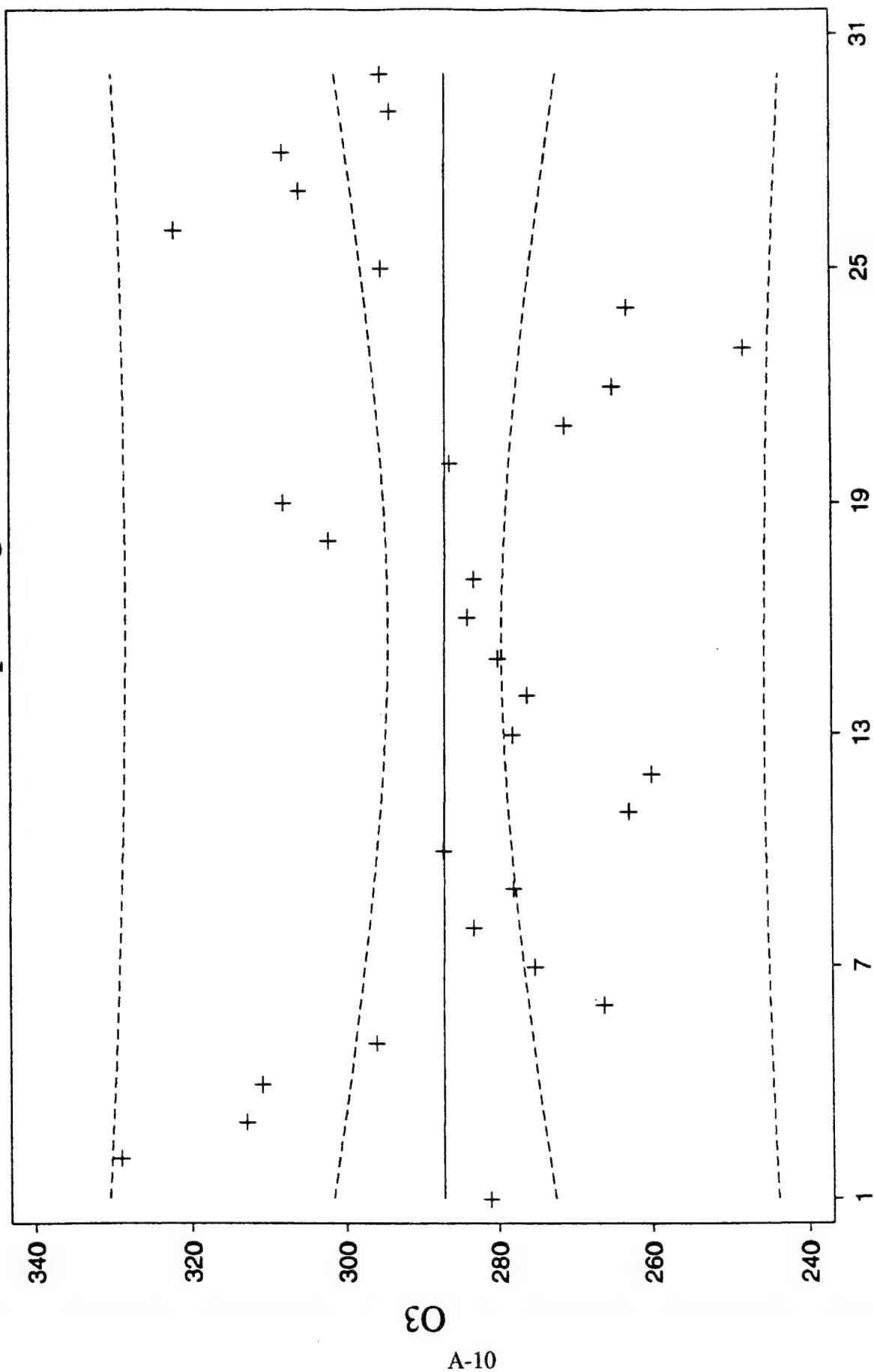O3 = 303.61 - 0.0545 * TIME   95% conf and pred intervals

A-8

DESCRIPTIVE STATISTICS

VARIABLE	N	MEAN	SD	MINIMUM	MAXIMUM
O3	30	302.77	6.5584	288.00	313.00

$$PI = 302.77 \pm 2.045 \cdot 6.5584 \sqrt{1 + 1/30}$$

$$PI = (289.14, \ 316.4)$$

3 Feb 84 Simple Regression Plot

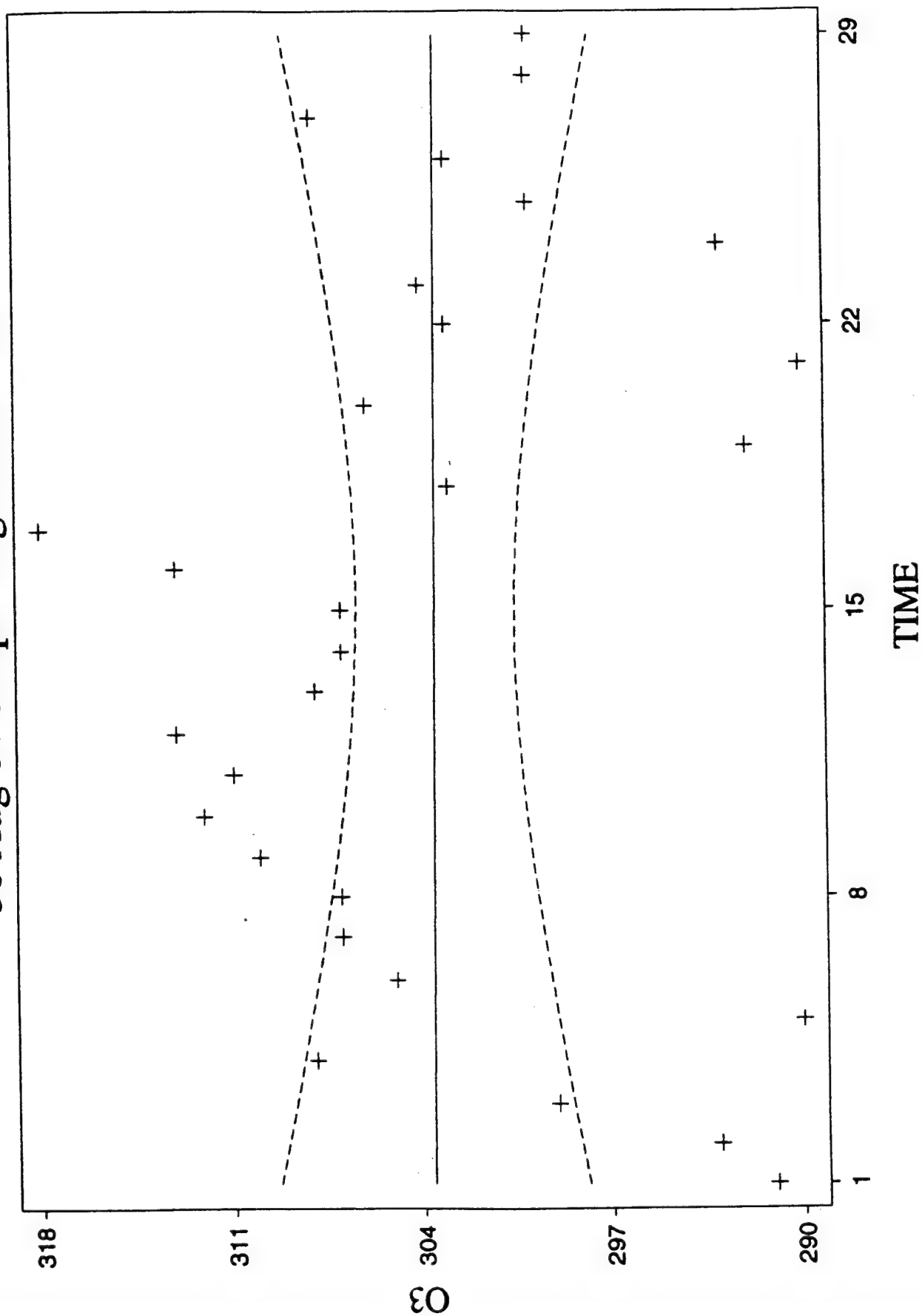

O3 = 287.10 - 0.0151 * TIME   95% conf and pred intervals

A-10

DESCRIPTIVE STATISTICS

VARIABLE	N	MEAN	SD	MINIMUM	MAXIMUM
O3	30	286.87	19.567	248.00	329.00

$$PI = 286.87 \pm 2.045 \cdot 19.567 \sqrt{1 + 1/30}$$

$$PI = (246.19, \; 327.55)$$

30 Aug 84 Simple Regression Plot
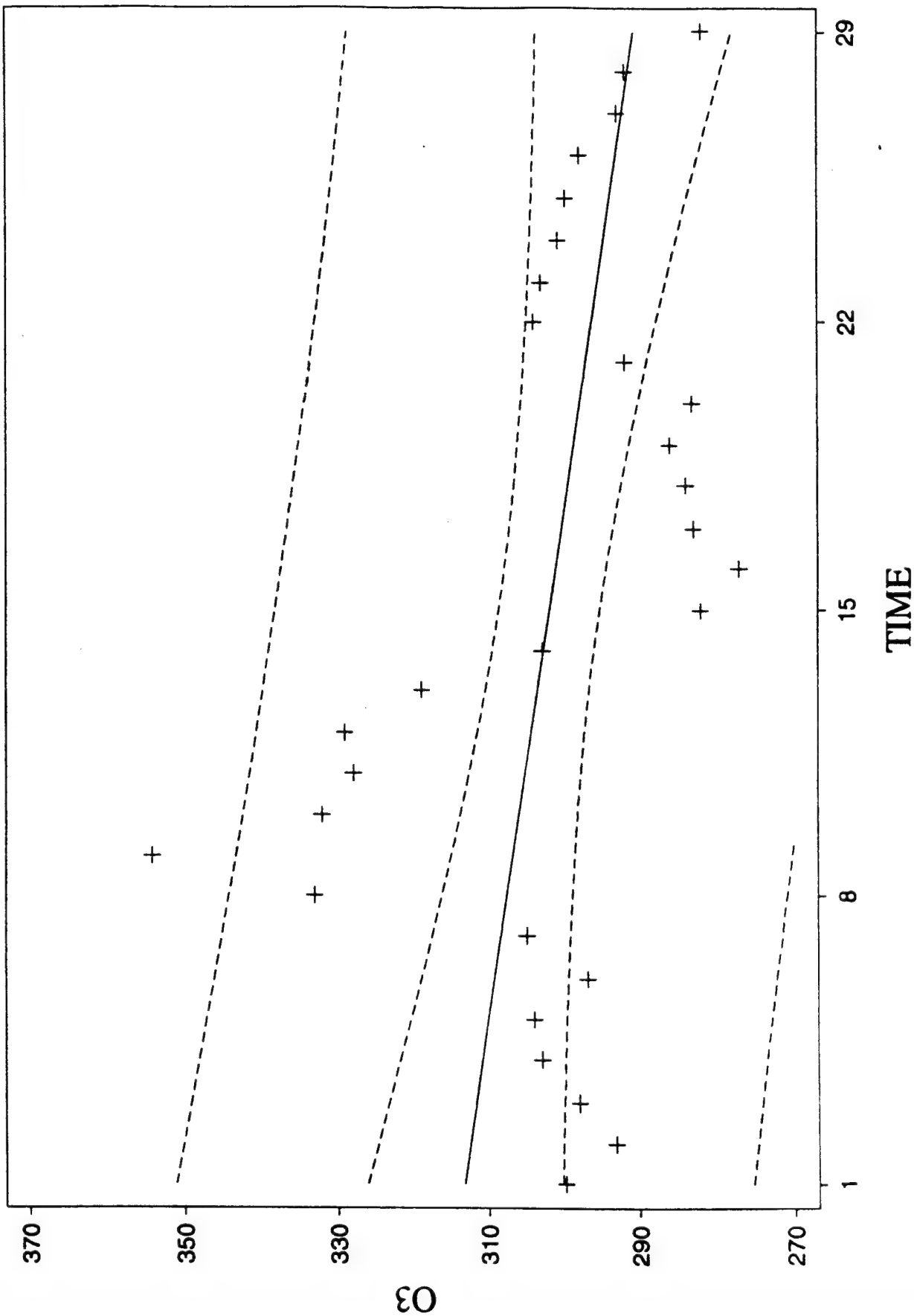
O3 = 303.63 - 9.85E-03 * TIME   95% conf and pred intervals

DESCRIPTIVE STATISTICS

VARIABLE	N	MEAN	SD	MINIMUM	MAXIMUM
O3	29	303.48	7.5858	290.00	318.00

$$PI = 303.48 \pm 2.048 \cdot 7.5858 \sqrt{1 + 1/29}$$

$$PI = (287.68, 319.28)$$

17 Jun 85 Simple Regression Plot

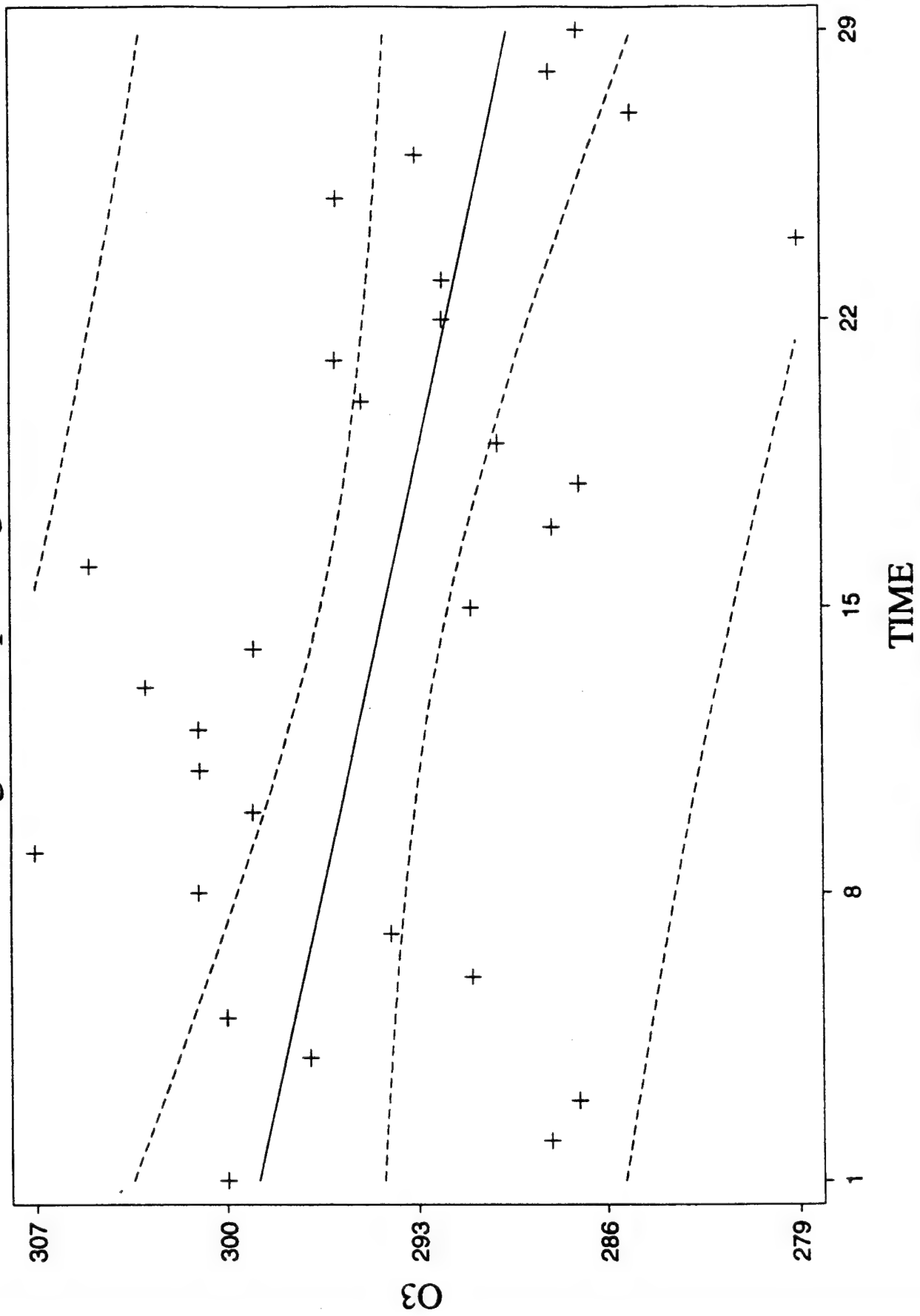O3 = 313.98 - 0.7985 * TIME   95% conf and pred intervals

PREDICTED/FITTED VALUES OF O3

LOWER PREDICTED BOUND	251.90	LOWER FITTED BOUND	276.44
PREDICTED VALUE	290.02	FITTED VALUE	290.02
UPPER PREDICTED BOUND	328.15	UPPER FITTED BOUND	303.60
SE (PREDICTED VALUE)	18.582	SE (FITTED VALUE)	6.6188

UNUSUALNESS (LEVERAGE)	0.1453
PERCENT COVERAGE	95.0
CORRESPONDING T	2.05

PREDICTOR VALUES: TIME = 30.000

27 Aug 85 Simple Regression Plot

O3 = 299.18 - 0.3315 * TIME   95% conf and pred intervals

A-16

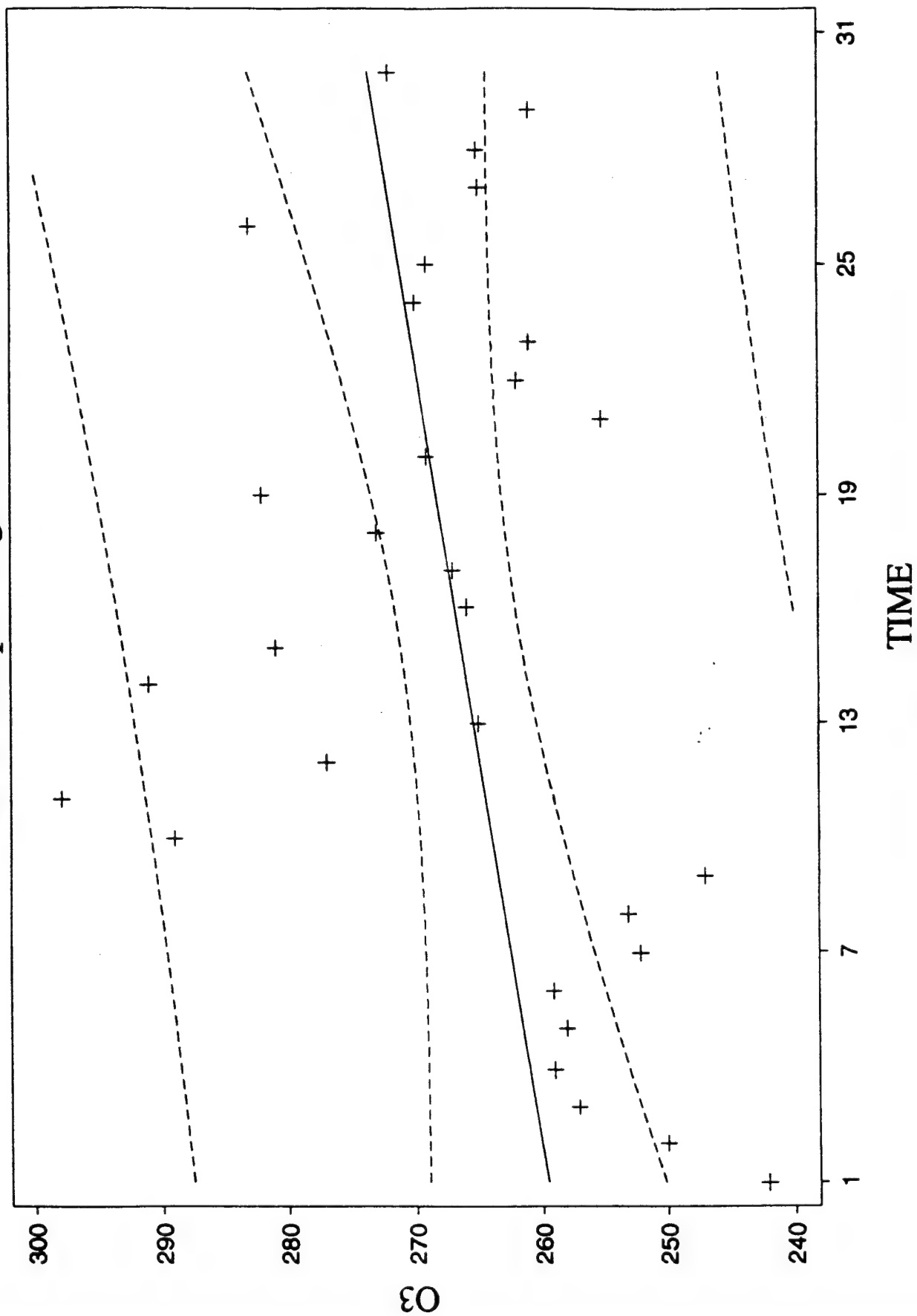PREDICTED/FITTED VALUES OF O3

LOWER PREDICTED BOUND	275.62	LOWER FITTED BOUND	284.39
PREDICTED VALUE	289.23	FITTED VALUE	289.23
UPPER PREDICTED BOUND	302.85	UPPER FITTED BOUND	294.08
SE (PREDICTED VALUE)	6.6345	SE (FITTED VALUE)	2.3632

UNUSUALNESS (LEVERAGE)	0.1453
PERCENT COVERAGE	95.0
CORRESPONDING T	2.05

PREDICTOR VALUES: TIME = 30.000

12 Jan 86 Simple Regression Plot

O3 = 259.03 + 0.4881 * TIME   95% conf and pred intervals

DESCRIPTIVE STATISTICS
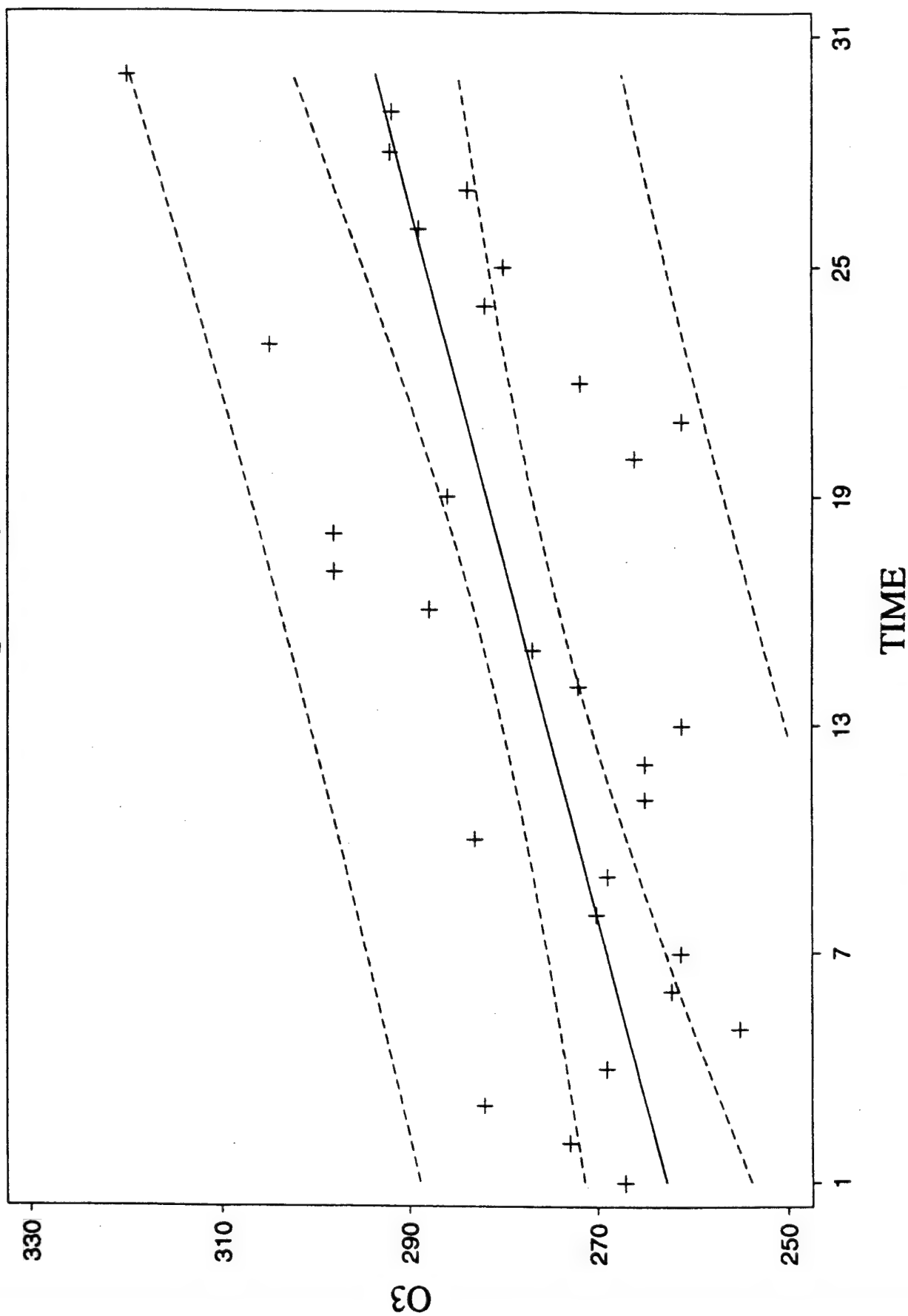
VARIABLE	N	MEAN	SD	MINIMUM	MAXIMUM
O3	30	266.60	13.351	242.00	298.00

$$PI = 266.60 \pm 2.045 \cdot 13.351 \sqrt{1 + 1/30}$$

$$PI = (238.85, 294.35)$$

28 Jan 86 Simple Regression Plot

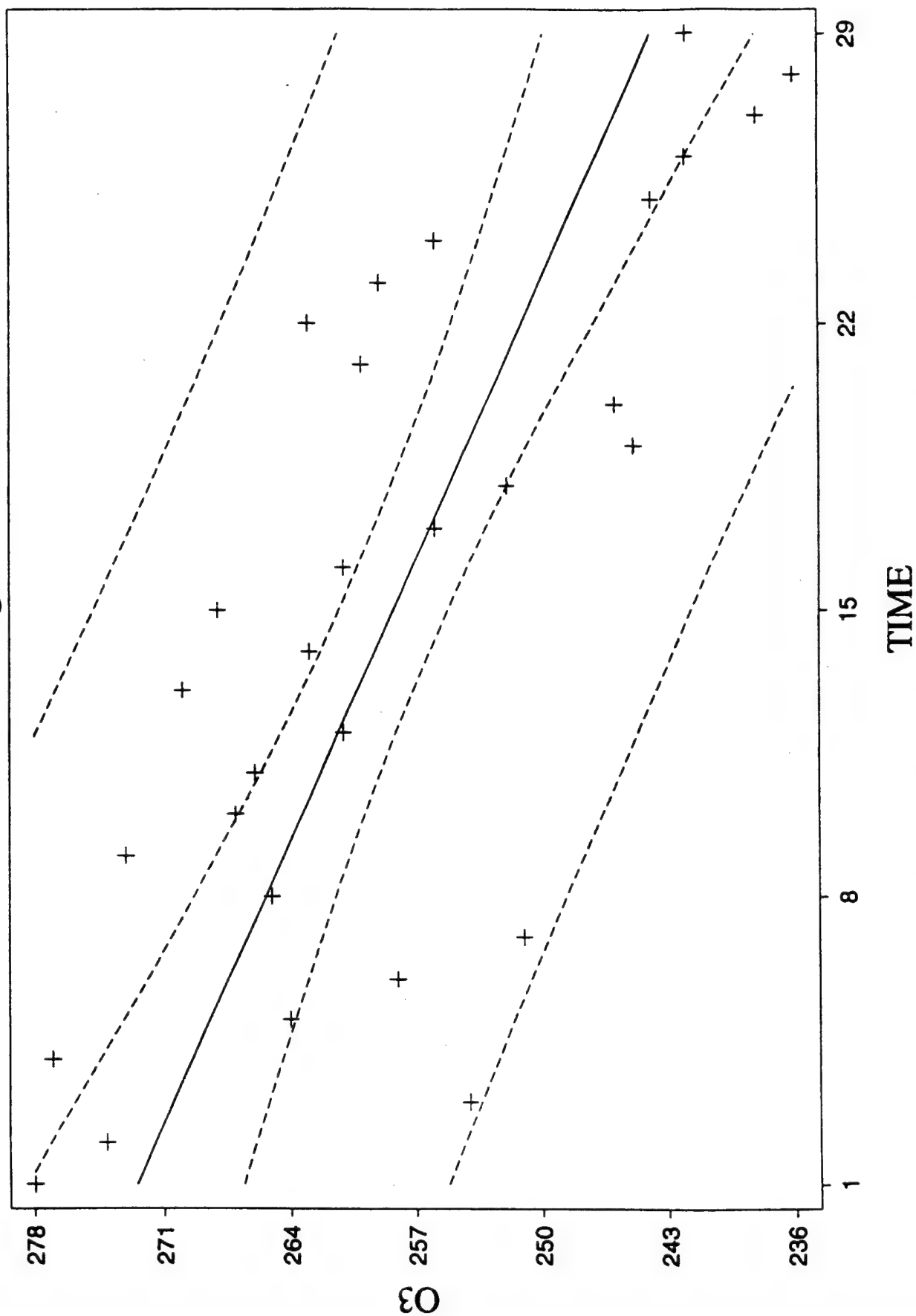
O3 = 261.55 + 1.0701 * TIME   95% conf and pred intervals

PREDICTED/FITTED VALUES OF O3

LOWER PREDICTED BOUND	268.34	LOWER FITTED BOUND	285.47
PREDICTED VALUE	294.72	FITTED VALUE	294.72
UPPER PREDICTED BOUND	321.10	UPPER FITTED BOUND	303.97
SE (PREDICTED VALUE)	12.877	SE (FITTED VALUE)	4.5159

UNUSUALNESS (LEVERAGE)	0.1402
PERCENT COVERAGE	95.0
CORRESPONDING T	2.05

PREDICTOR VALUES: TIME = 31.000

2 Dec 88 Regression Plot
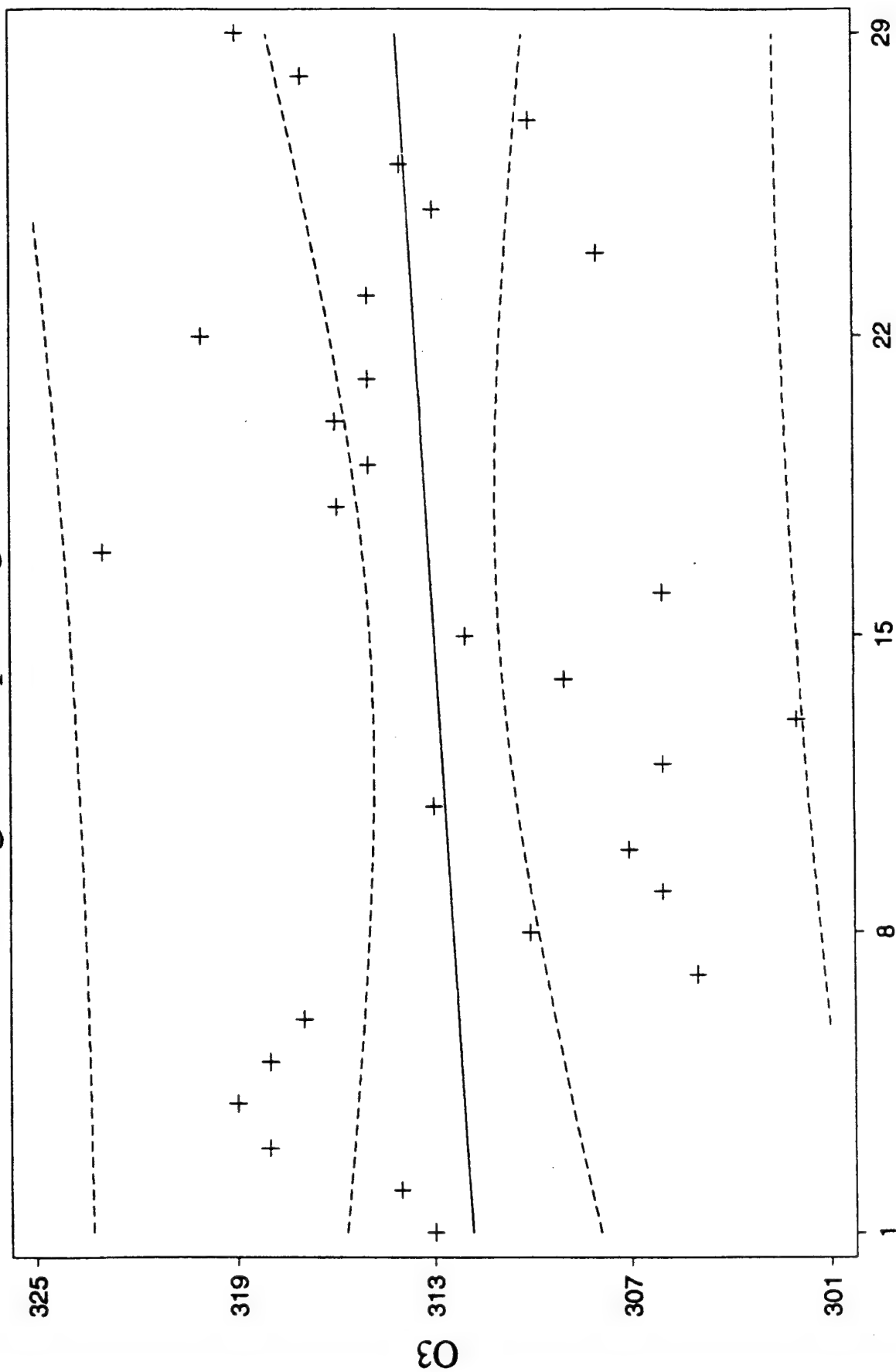
O3 = 273.51 - 1.0182 * TIME   95% conf and pred intervals

TIME

O3

A-22

PREDICTED/FITTED VALUES OF O3

LOWER PREDICTED BOUND	225.56	LOWER FITTED BOUND	236.77
PREDICTED VALUE	242.97	FITTED VALUE	242.97
UPPER PREDICTED BOUND	260.37	UPPER FITTED BOUND	249.17
SE (PREDICTED VALUE)	8.4835	SE (FITTED VALUE)	3.0219

UNUSUALNESS (LEVERAGE)	0.1453
PERCENT COVERAGE	95.0
CORRESPONDING T	2.05

PREDICTOR VALUES: TIME = 30.000

8 Aug 89 Simple Regression Plot

O3 = 311.73 + 0.0823 * TIME   95% conf and pred intervals

A-24

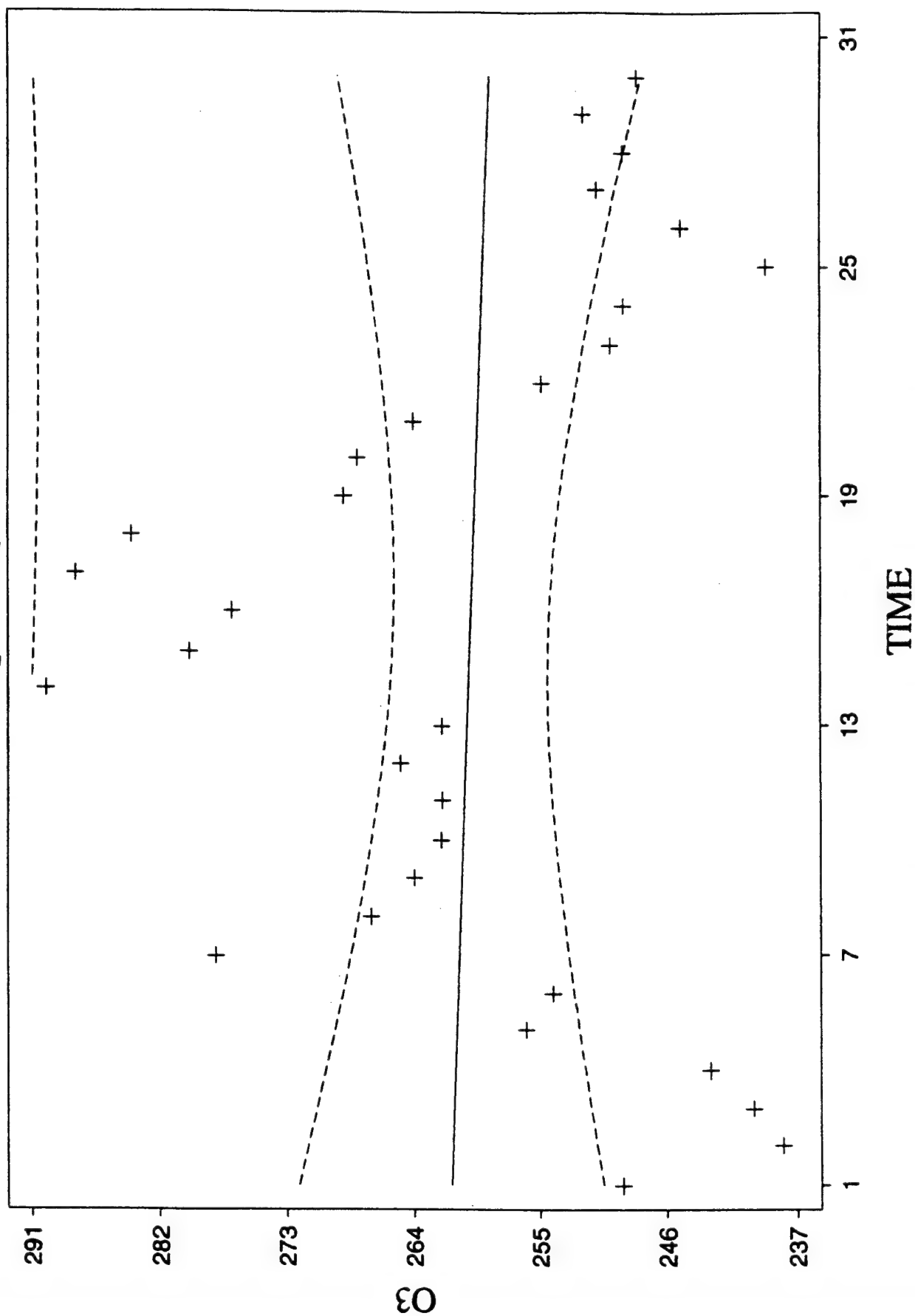DESCRIPTIVE STATISTICS

VARIABLE	N	MEAN	SD	MINIMUM	MAXIMUM
O3	29	312.97	5.2200	302.00	323.00

$$PI = 312.97 \pm 2.048 \cdot 5.22 \sqrt{1 + 1/29}$$

$$PI = (302.1, 323.84)$$

9 Jan 90 Simple Regression Plot
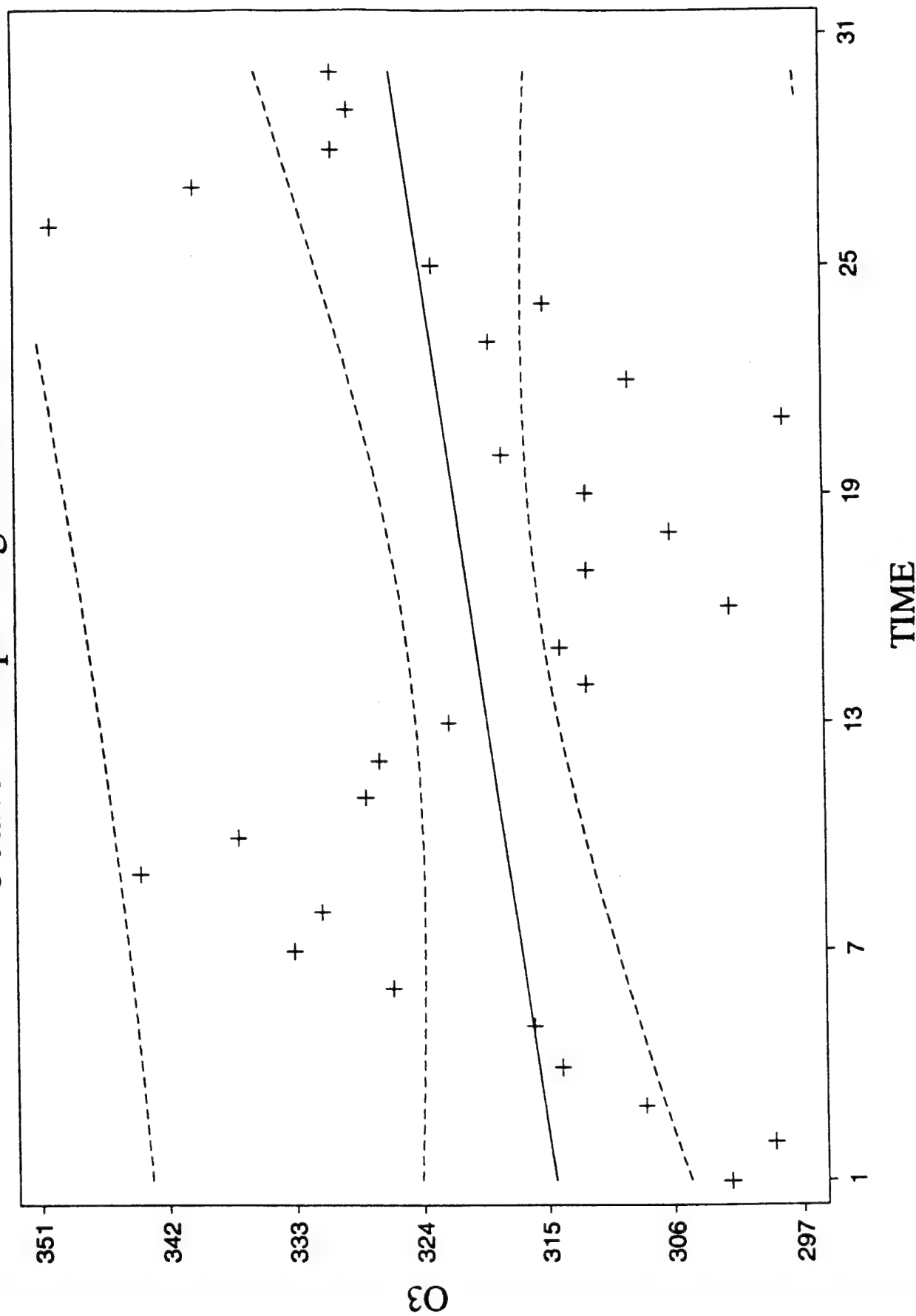
O3 = 261.37 - 0.0930 * TIME   95% conf and pred intervals

TIME

O3

DESCRIPTIVE STATISTICS

VARIABLE	N	MEAN	SD	MINIMUM	MAXIMUM
O3	30	259.93	14.626	238.00	290.00

$$PI = 259.93 \pm 2.045 \cdot 14.626 \sqrt{1 + 1/30}$$

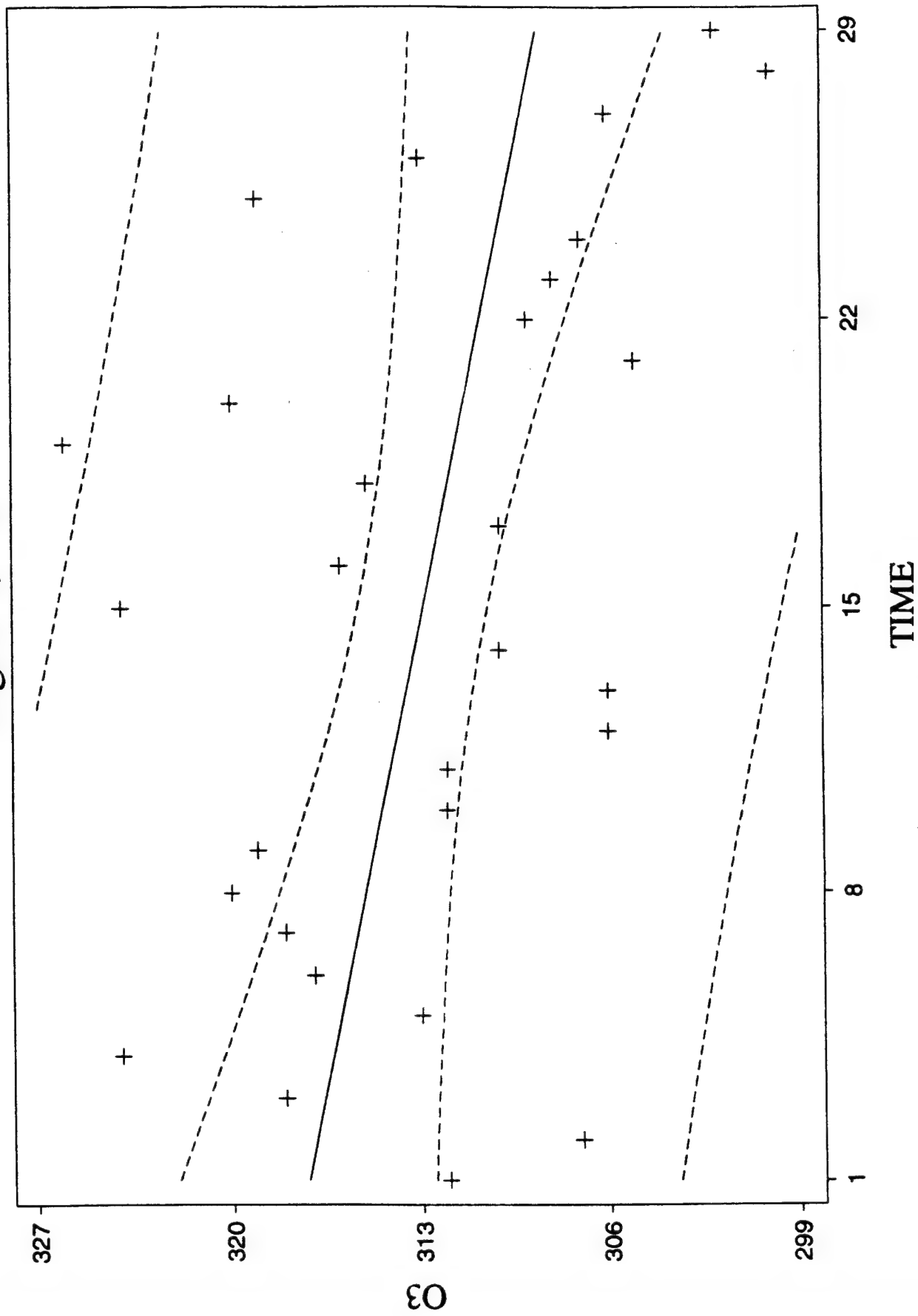$$PI = (229.53, 290.33)$$

5 Jan 91 Simple Regression Plot

O3 = 314.10 + 0.3938 * TIME   95% conf and pred intervals

A-28

DESCRIPTIVE STATISTICS

VARIABLE	N	MEAN	SD	MINIMUM	MAXIMUM
O3	30	320.20	13.443	298.00	350.00

$$PI = 320.2 \pm 2.045 \cdot 13.443 \sqrt{1 + \frac{1}{30}}$$

$$PI = (292.25, 348.15)$$

August 2, 1991

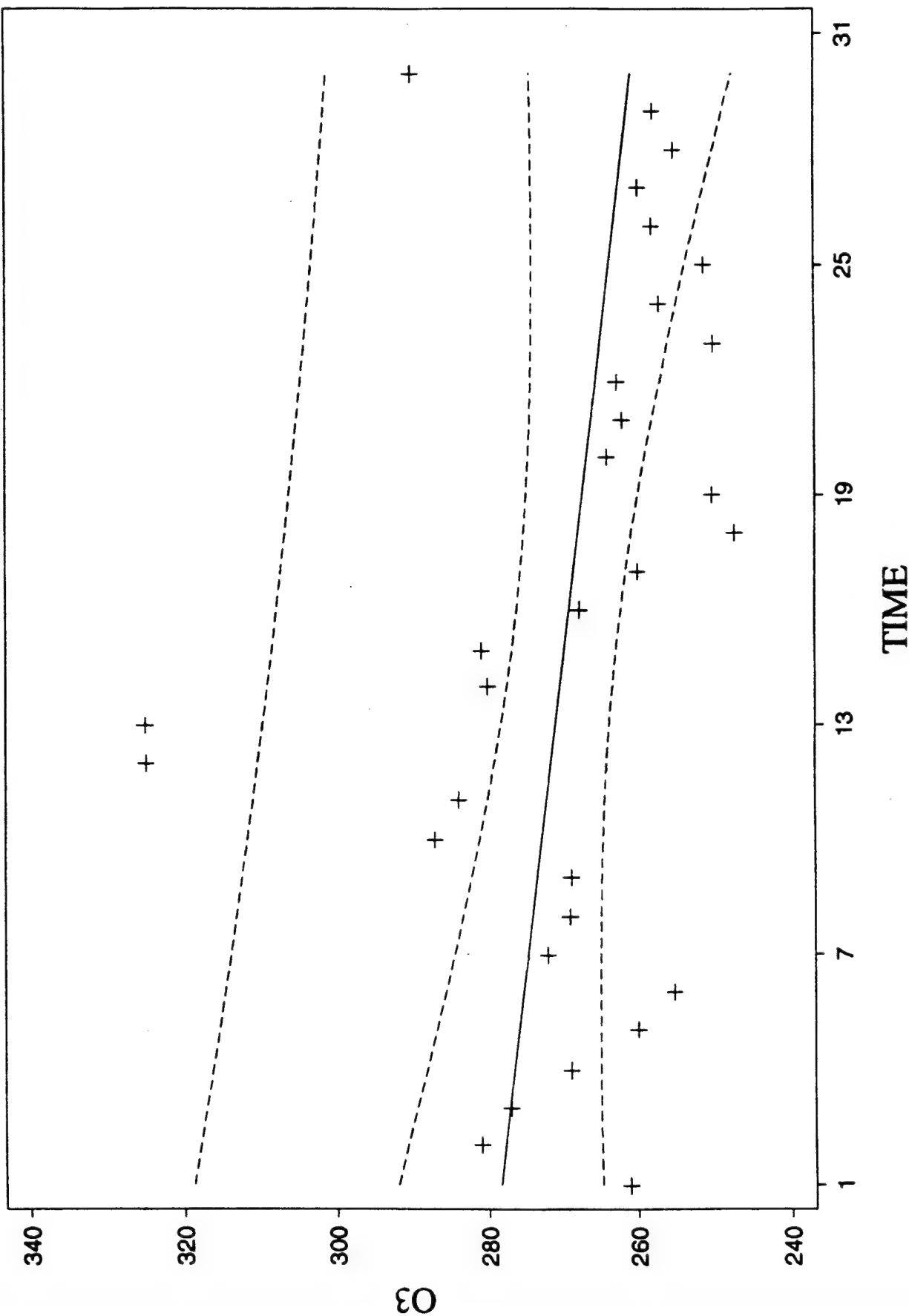O3 = 317.55 - 0.3103 * TIME   95% conf and pred intervals

TIME

O3

PREDICTED/FITTED VALUES OF O3

LOWER PREDICTED BOUND	294.23	LOWER FITTED BOUND	303.25
PREDICTED VALUE	308.24	FITTED VALUE	308.24
UPPER PREDICTED BOUND	322.25	UPPER FITTED BOUND	313.23
SE (PREDICTED VALUE)	6.8283	SE (FITTED VALUE)	2.4323

UNUSUALNESS (LEVERAGE)	0.1453
PERCENT COVERAGE	95.0
CORRESPONDING T	2.05

PREDICTOR VALUES: TIME = 30.000

22 Jan 92 Simple Regression Plot
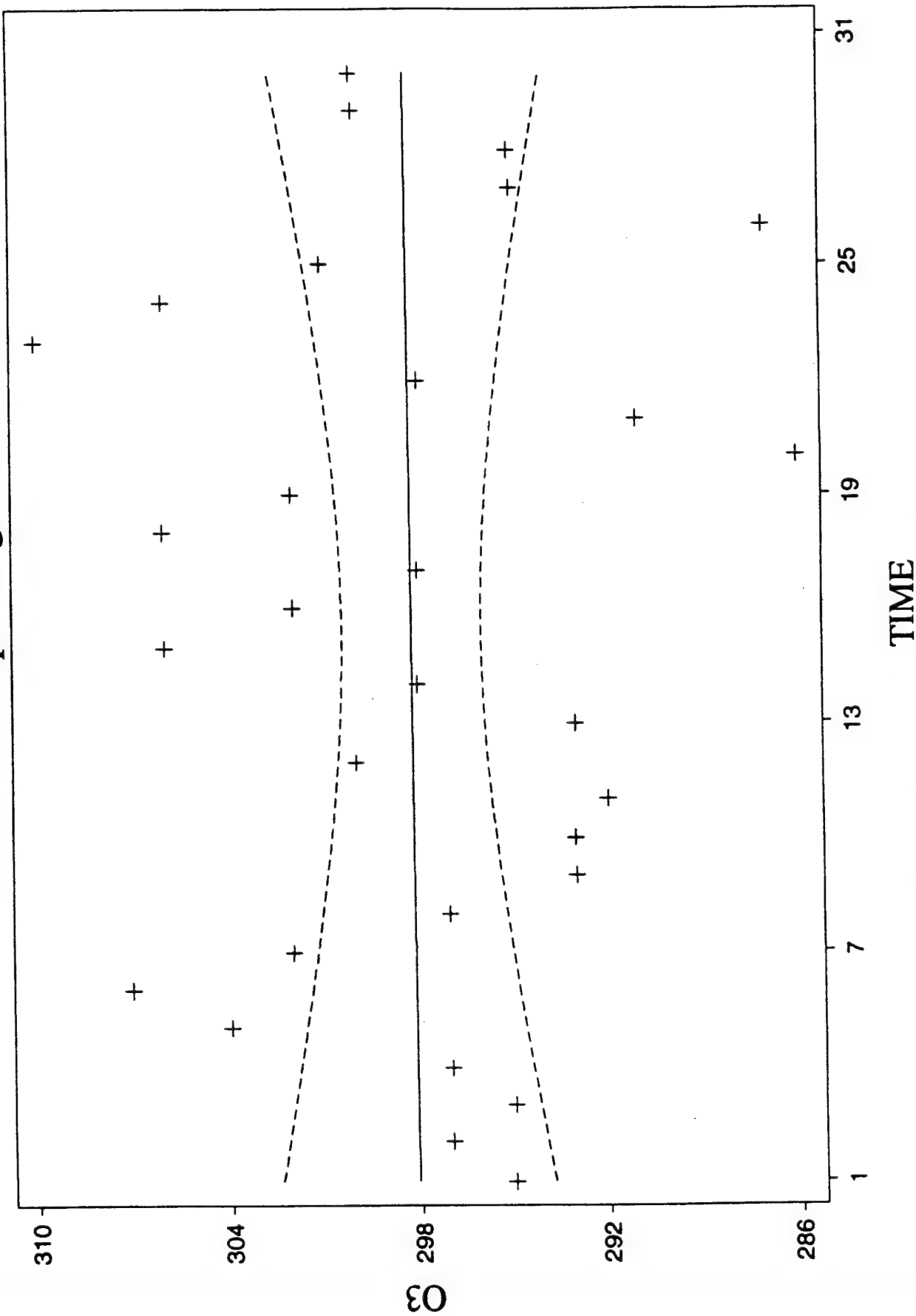
O3 = 278.97 - 0.6042 * TIME   95% conf and pred intervals

DESCRIPTIVE STATISTICS

VARIABLE	N	MEAN	SD	MINIMUM	MAXIMUM
O3	30	269.60	18.991	247.00	325.00

$$PI = 269.6 \pm 2.045 \cdot 18.991 \sqrt{1 + 1/30}$$

$$PI = (230.12, 309.08)$$

31 Jul 92 Simple Regression Plot

TIME

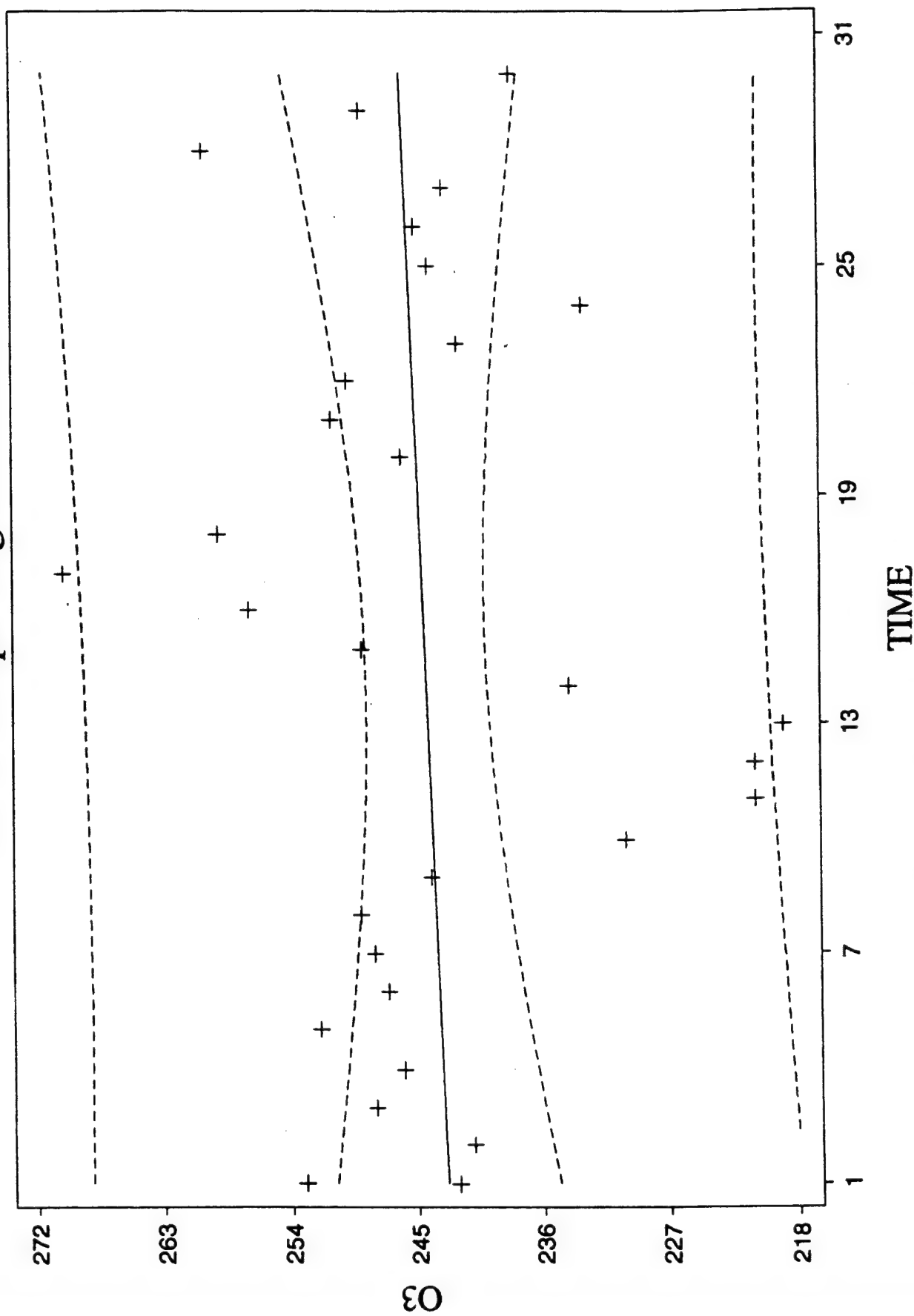O3 = 298.08 + 8.01E-03 * TIME   95% conf and pred intervals

O3

A-34

DESCRIPTIVE STATISTICS

VARIABLE	N	MEAN	SD	MINIMUM	MAXIMUM
O3	30	298.20	5.8274	286.00	310.00

$$PI = 298.2 \pm 2.045 \cdot 5.8274 \sqrt{1 + 1/30}$$

$$PI = (286.09, 310.31)$$

2 Dec 92 Simple Regression Plot

O3 = 242.74 + 0.1089 * TIME   95% conf and pred intervals

PREDICTED/FITTED VALUES OF O3

LOWER PREDICTED BOUND	228.24	LOWER FITTED BOUND	245.54
PREDICTED VALUE	255.11	FITTED VALUE	255.11
UPPER PREDICTED BOUND	281.98	UPPER FITTED BOUND	264.68
SE (PREDICTED VALUE)	13.096	SE (FITTED VALUE)	4.6649

UNUSUALNESS (LEVERAGE)   0.1453
PERCENT COVERAGE   95.0
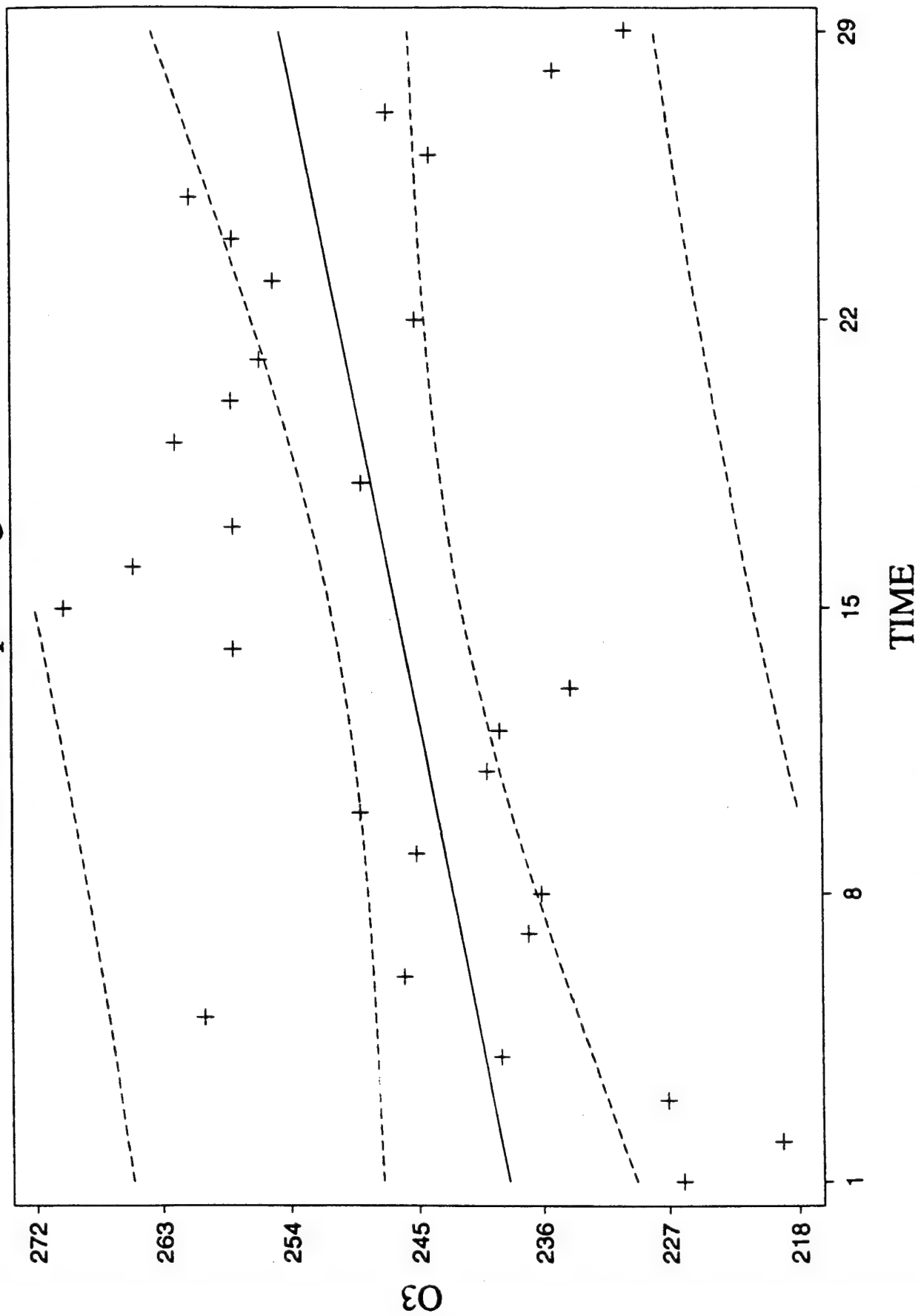CORRESPONDING T   2.05

PREDICTOR VALUES: TIME = 30.000

DESCRIPTIVE STATISTICS

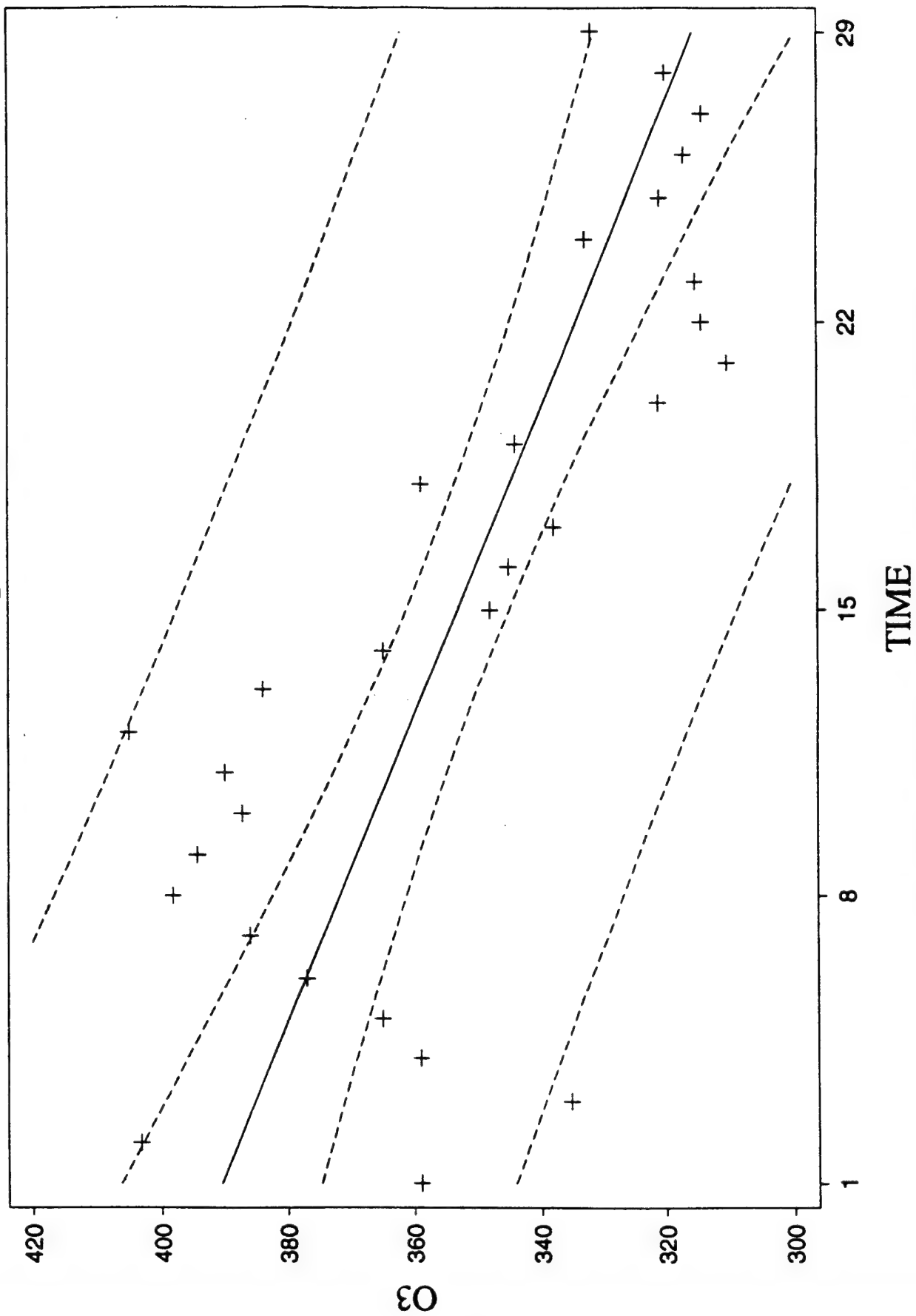| VARIABLE	N	MEAN	SD	MINIMUM	MAXIMUM
O3	30	244.37	11.494	219.00	270.00

$$PI = 244.37 \pm 2.045 \cdot 11.494 \sqrt{1 + 1/30}$$

$$PI = (220.48, 268.26)$$

13 Jan 93 Simple Regression Plot

TIME

O3 = 237.85 + 0.5754 * TIME   95% conf and pred intervals

18 Jun 80 WTR Simple Regression Plot

O3 = 393.17 - 2.6754 * TIME   95% conf and pred intervals

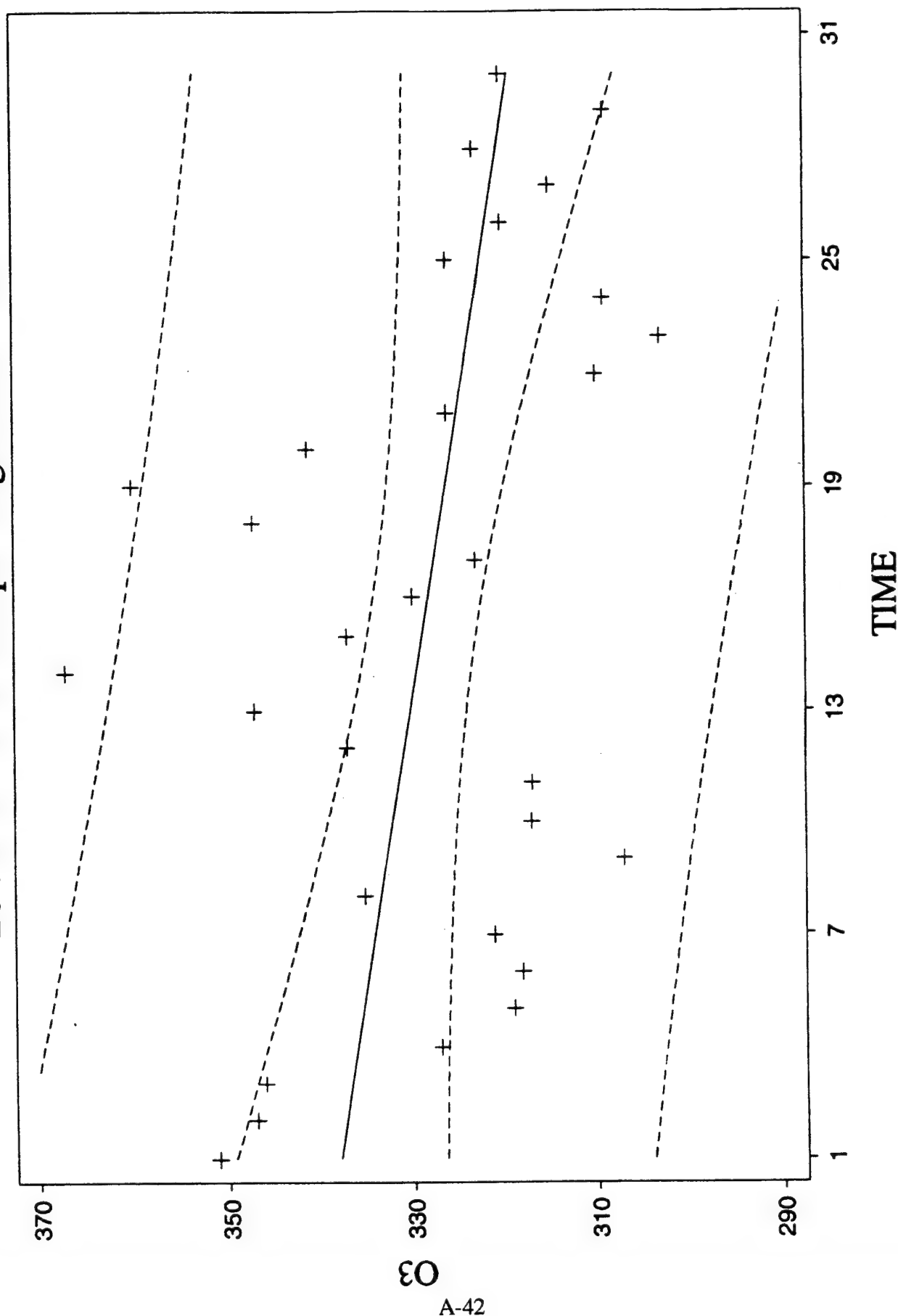PREDICTED/FITTED VALUES OF O3

LOWER PREDICTED BOUND	266.12	LOWER FITTED BOUND	296.24
PREDICTED VALUE	312.90	FITTED VALUE	312.90
UPPER PREDICTED BOUND	359.69	UPPER FITTED BOUND	329.57
SE (PREDICTED VALUE)	22.800	SE (FITTED VALUE)	8.1215

UNUSUALNESS (LEVERAGE)   0.1453
PERCENT COVERAGE   95.0
CORRESPONDING T   2.05

PREDICTOR VALUES: TIME = 30.000

20 Jan 83 WTR Simple Regression Plot

O3 = 338.54 - 0.6476 * TIME   95% conf and pred intervals

DESCRIPTIVE STATISTICS

VARIABLE	N	MEAN	SD	MINIMUM	MAXIMUM
O3	30	328.50	16.398	303.00	367.00

$$PI = 328.5 \pm 2.045 \cdot 16.398 \sqrt{1 + 1/30}$$

$$PI = (294.41,\ 362.59)$$

PREDICTED/FITTED VALUES OF O3

LOWER PREDICTED BOUND	284.24	LOWER FITTED BOUND	306.46
PREDICTED VALUE	318.46	FITTED VALUE	318.46
UPPER PREDICTED BOUND	352.69	UPPER FITTED BOUND	330.46
SE (PREDICTED VALUE)	16.708	SE (FITTED VALUE)	5.8592

UNUSUALNESS (LEVERAGE)   0.1402
PERCENT COVERAGE   95.0
CORRESPONDING T   2.05

PREDICTOR VALUES: TIME = 31.000

25 Jun 84 WTR Simple Regression Plot
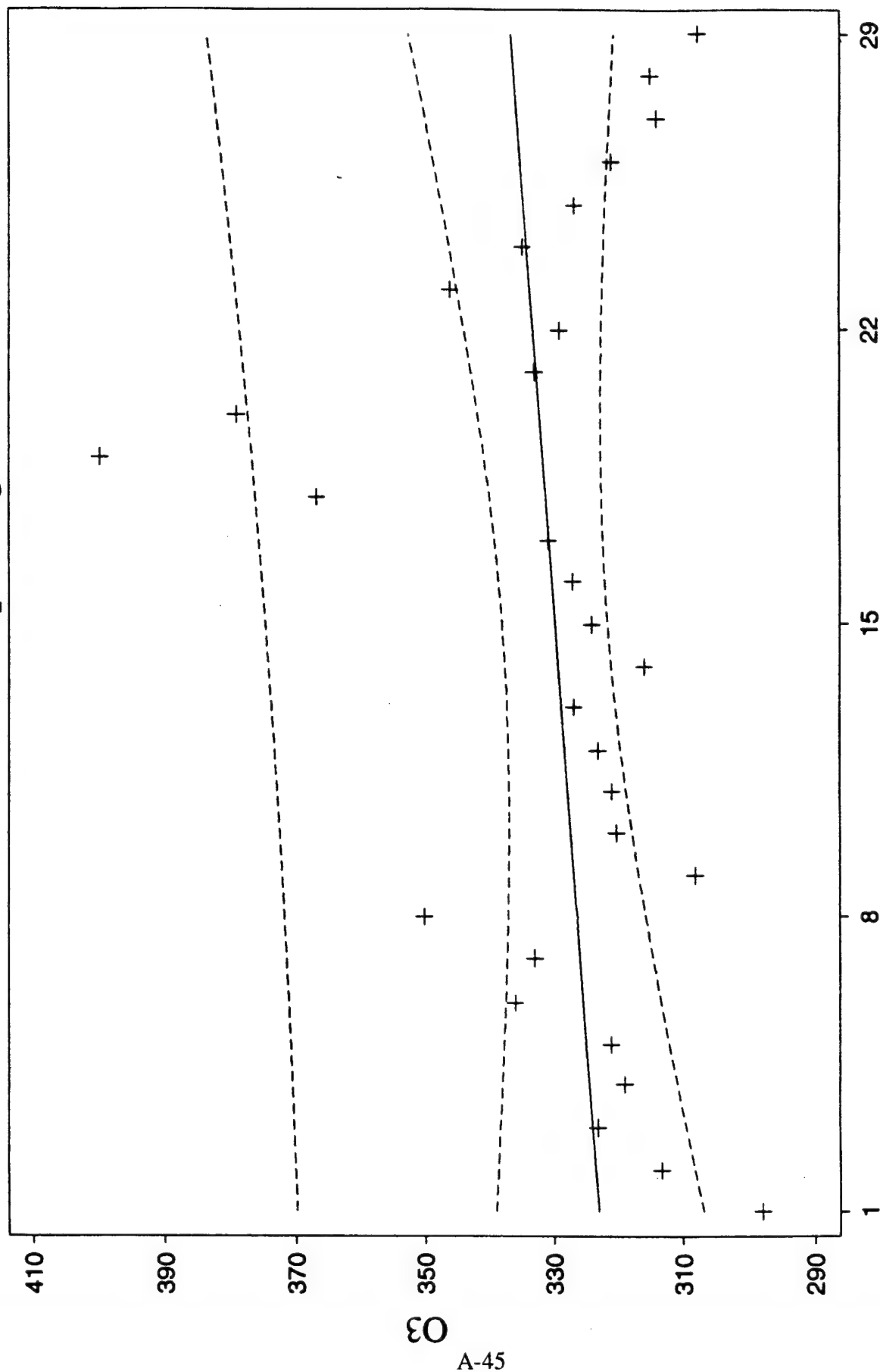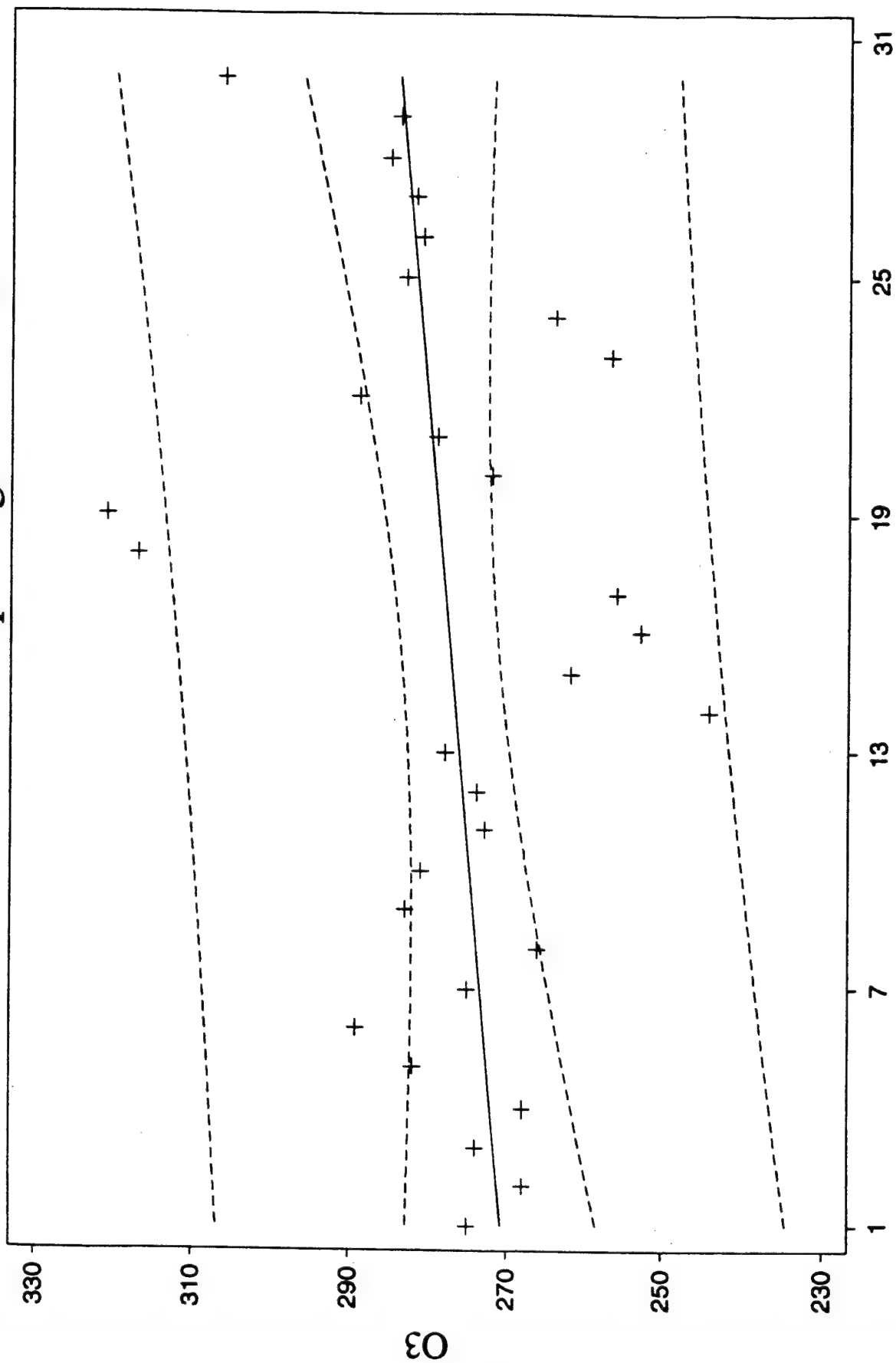
O3 = 322.40 + 0.4926 * TIME   95% conf and pred intervals

DESCRIPTIVE STATISTICS

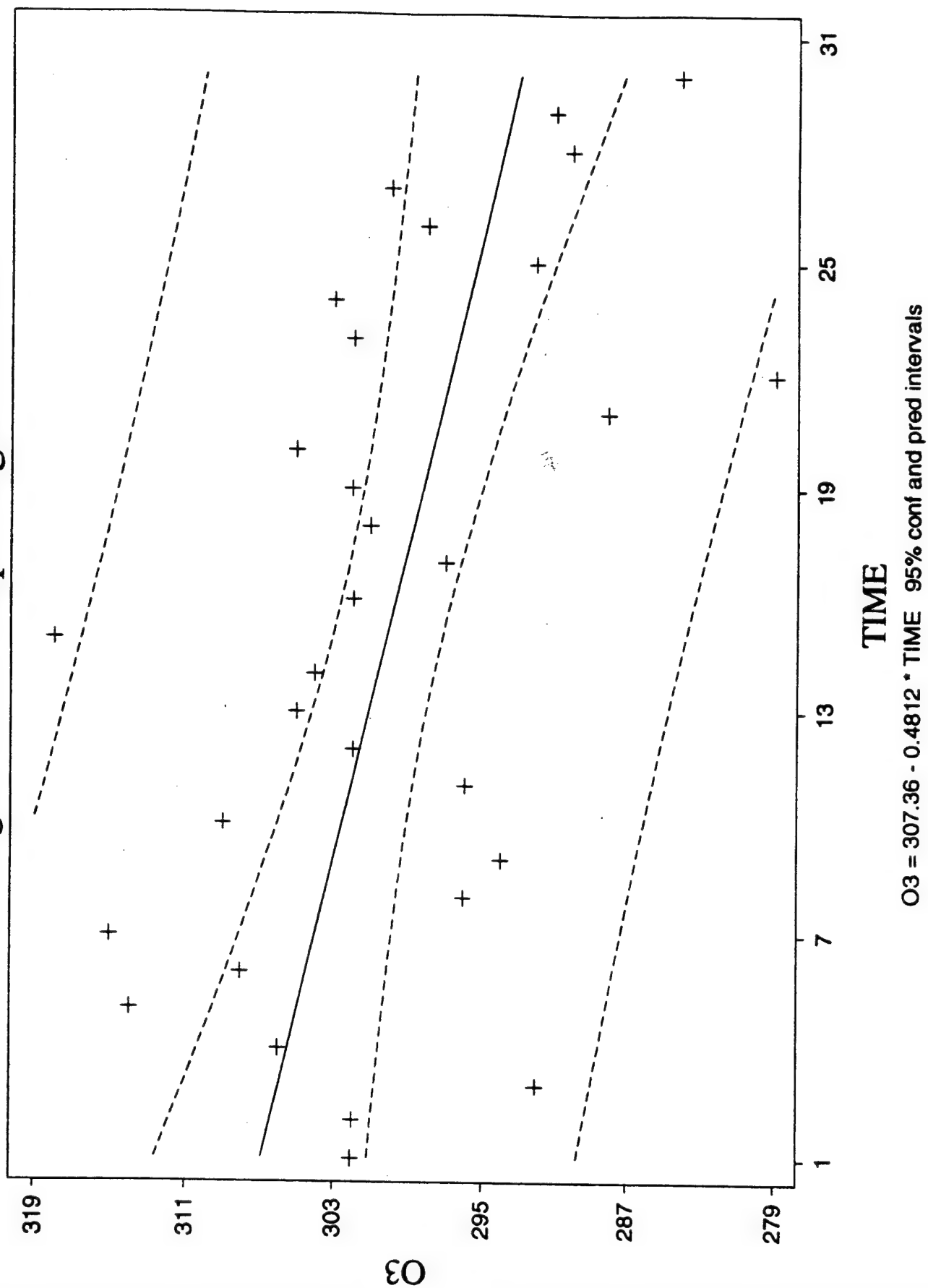| VARIABLE	N	MEAN	SD	MINIMUM	MAXIMUM
O3	29	329.79	21.538	298.00	400.00

$$PI = 329.79 \pm 2.048 \cdot 21.538 \sqrt{1 + 1/29}$$

$$PI = (284.93, 374.65)$$

4 Dec 84 WTR Simple Regression Plot

O3 = 270.23 + 0.4603 * TIME   95% conf and pred intervals

TIME

O3

28 Aug 85 WTR Simple Regression Plot

O3 = 307.36 - 0.4812 * TIME 95% conf and pred intervals

PREDICTED/FITTED VALUES OF O3

LOWER PREDICTED BOUND	275.22	LOWER FITTED BOUND	286.40
PREDICTED VALUE	292.44	FITTED VALUE	292.44
UPPER PREDICTED BOUND	309.67	UPPER FITTED BOUND	298.48
SE (PREDICTED VALUE)	8.4087	SE (FITTED VALUE)	2.9488

UNUSUALNESS (LEVERAGE)	0.1402
PERCENT COVERAGE	95.0
CORRESPONDING T	2.05

PREDICTOR VALUES: TIME = 31.000

APPENDIX B

VIEW DATA

CASE	DATE	O3
1	05/28/82	337.00
2	05/29/82	325.00
3	05/30/82	320.00
4	05/31/82	314.00
5	06/01/82	314.00
6	06/02/82	312.00
7	06/03/82	306.00
8	06/04/82	305.00
9	06/05/82	298.00
10	06/06/82	299.00
11	06/07/82	311.00
12	06/08/82	307.00
13	06/09/82	319.00
14	06/10/82	318.00
15	06/11/82	312.00
16	06/12/82	324.00
17	06/13/82	323.00
18	06/14/82	313.00
19	06/15/82	320.00
20	06/16/82	308.00
21	06/17/82	295.00
22	06/18/82	307.00
23	06/19/82	315.00
24	06/20/82	309.00
25	06/21/82	296.00
26	06/22/82	295.00
27	06/23/82	291.00
28	06/24/82	305.00
29	06/25/82	304.00
30	06/26/82	306.00

27 Jun 82 GD Simple Regression Plot

O3 = 319.71 - 0.6091 * TIME   95% conf and pred intervals

TIME

O3
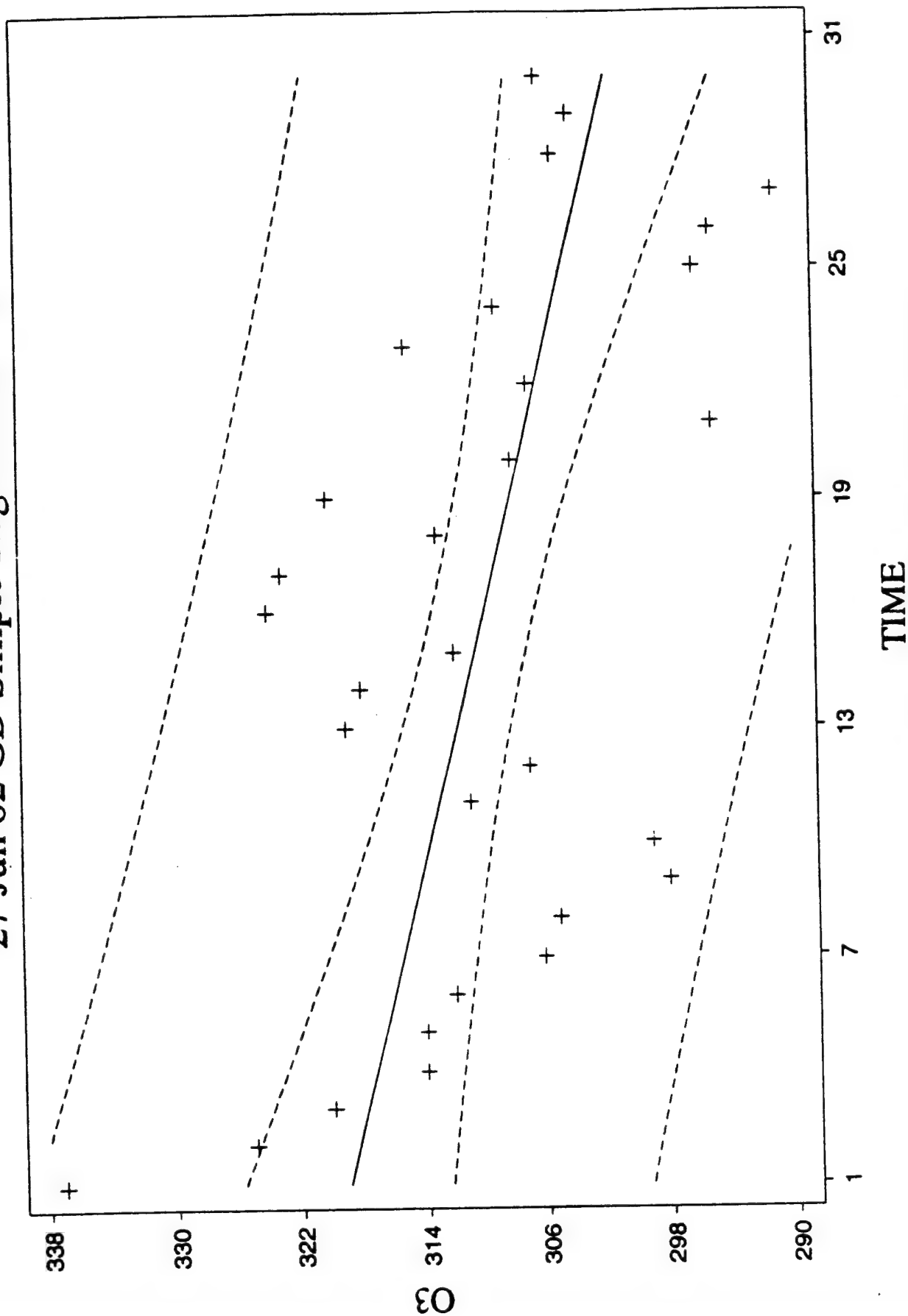
PREDICTED/FITTED VALUES OF O3

LOWER PREDICTED BOUND	280.93	LOWER FITTED BOUND	293.85
PREDICTED VALUE	300.83	FITTED VALUE	300.83
UPPER PREDICTED BOUND	320.72	UPPER FITTED BOUND	307.80
SE (PREDICTED VALUE)	9.7115	SE (FITTED VALUE)	3.4057

UNUSUALNESS (LEVERAGE)	0.1402
PERCENT COVERAGE	95.0
CORRESPONDING T	2.05

PREDICTOR VALUES: TIME = 31.000

03 Feb 84 GD Simple Regression Plot
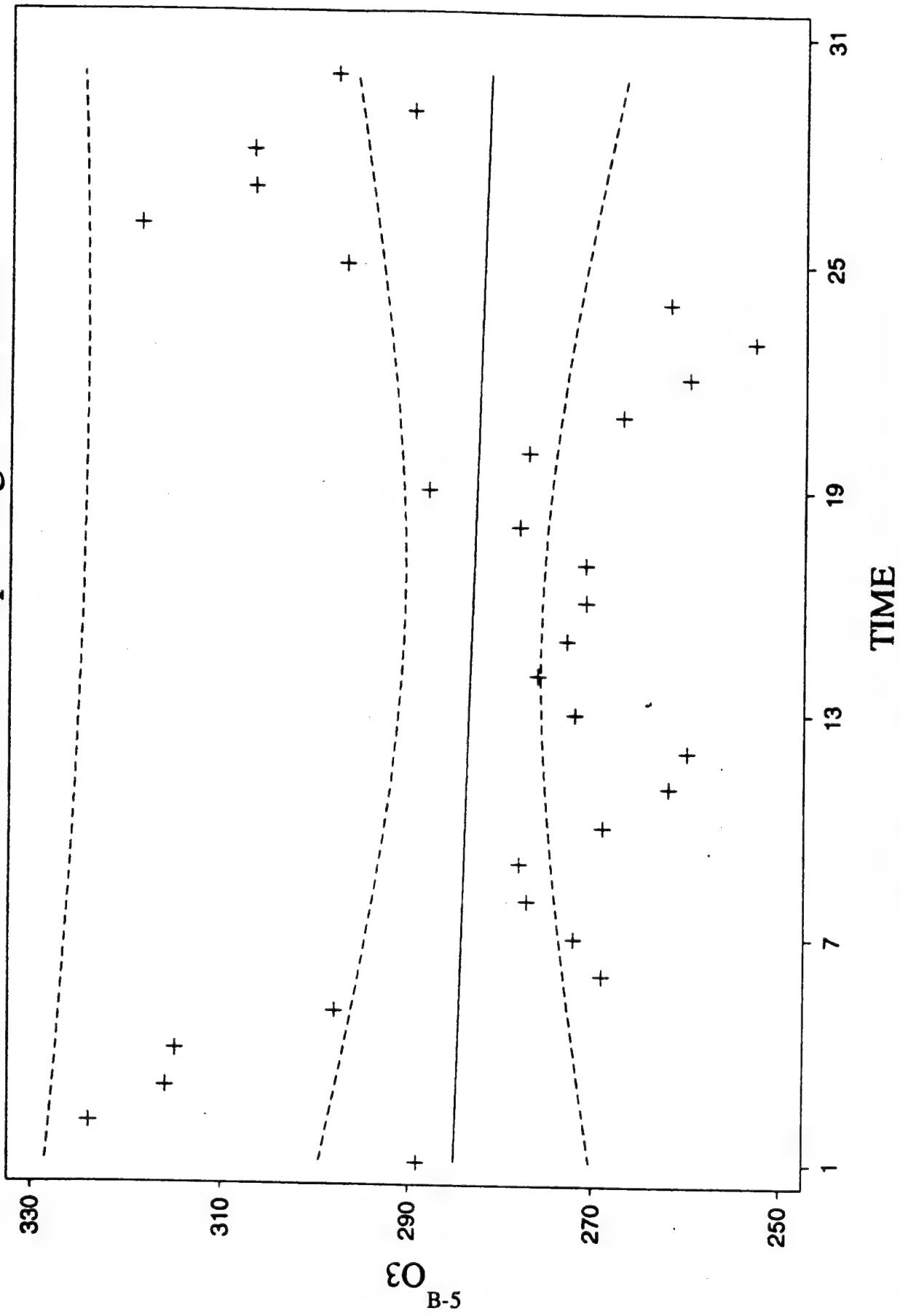
O3 = 285.01 - 0.1190 * TIME   95% conf and pred intervals
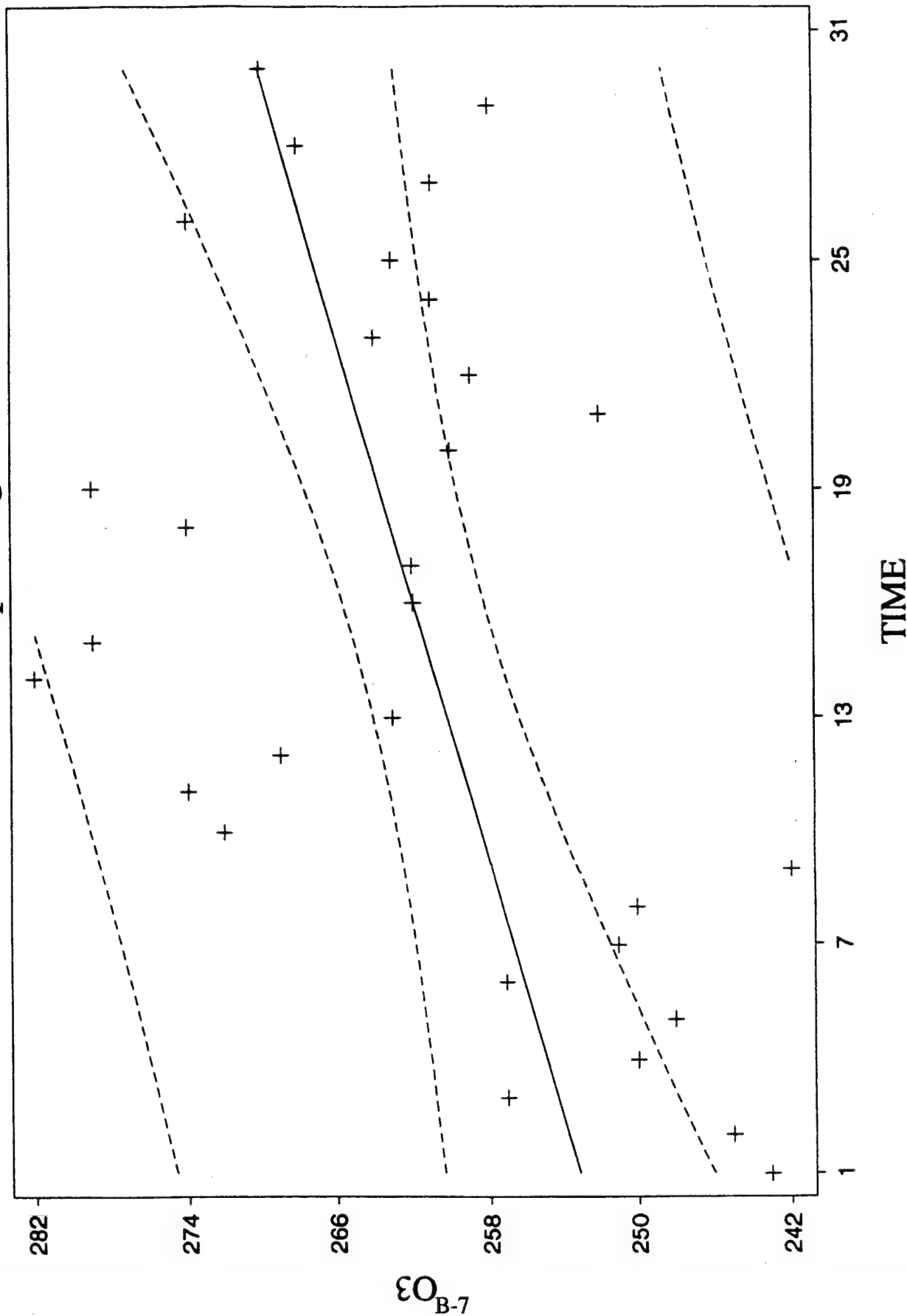
TIME

O3

B-5

DESCRIPTIVE STATISTICS

VARIABLE	N	MEAN	SD	MINIMUM	MAXIMUM
O3	30	283.17	19.728	253.00	324.00

$$PI = \bar{X} \pm t_{\alpha/2, n-1} \cdot S \sqrt{1 + 1/n} \qquad n = 30 \quad t_{.025, 29} = 2.045$$

$$PI = 283.17 \pm 2.045 \cdot 19.728 \sqrt{1 + 1/30}$$

$$PI = (242.16, 324.18)$$

12 Jan 86 GD Simple Regression Plot

TIME

$O3 = 252.58 + 0.5840 * TIME$ 95% conf and pred intervals

$O3_{B-7}$

PREDICTED/FITTED VALUES OF O3

LOWER PREDICTED BOUND	249.09	LOWER FITTED BOUND	263.11
PREDICTED VALUE	270.69	FITTED VALUE	270.69
UPPER PREDICTED BOUND	292.29	UPPER FITTED BOUND	278.26
SE (PREDICTED VALUE)	10.545	SE (FITTED VALUE)	3.6980

UNUSUALNESS (LEVERAGE)   0.1402
PERCENT COVERAGE   95.0
CORRESPONDING T   2.05

PREDICTOR VALUES: TIME = 31.000
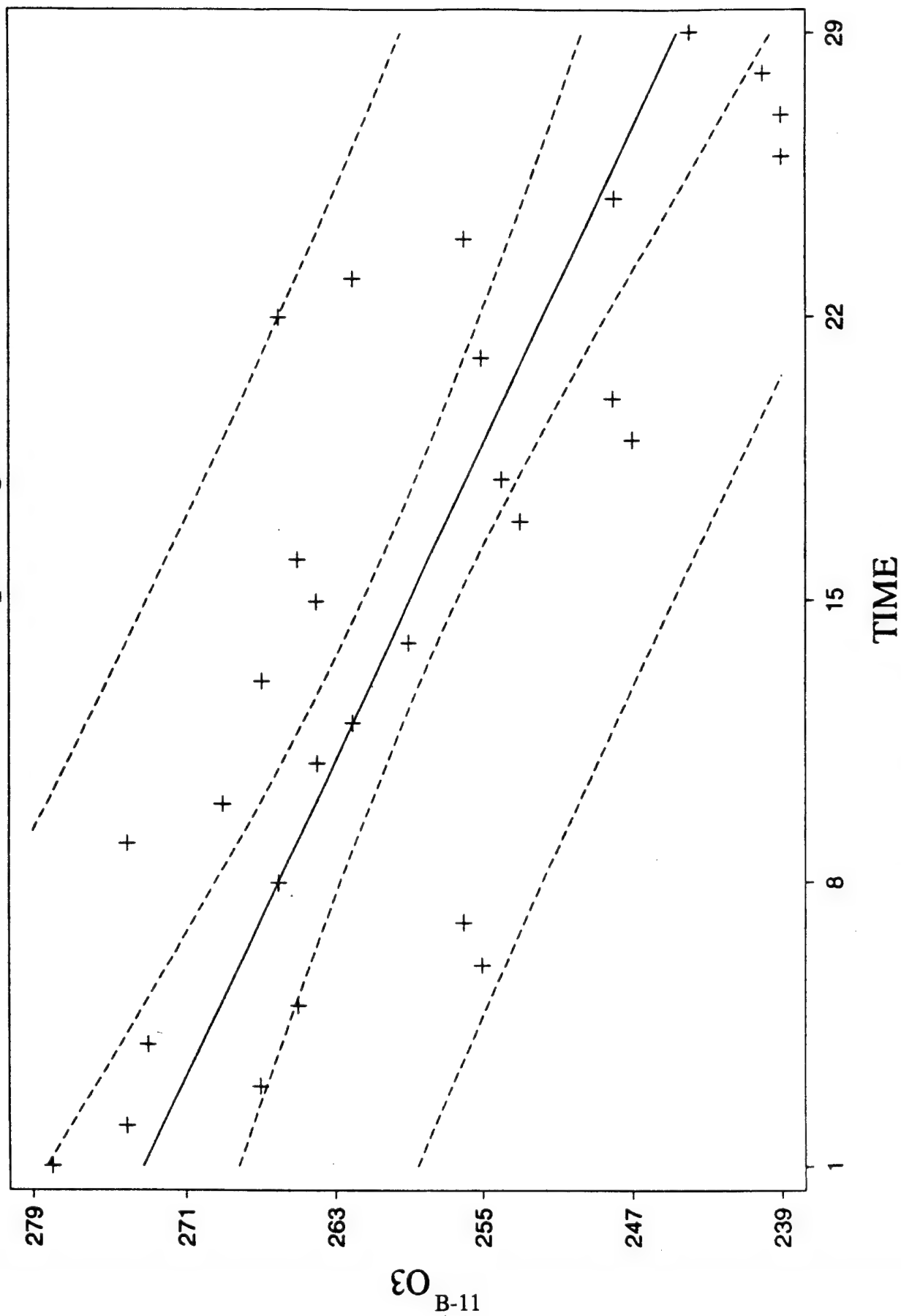
28 Jan 86 GD Simple Regression Plot

TIME

$O3 = 261.41 + 1.0641 \cdot TIME$ 95% conf and pred intervals

$O3_{B-9}$
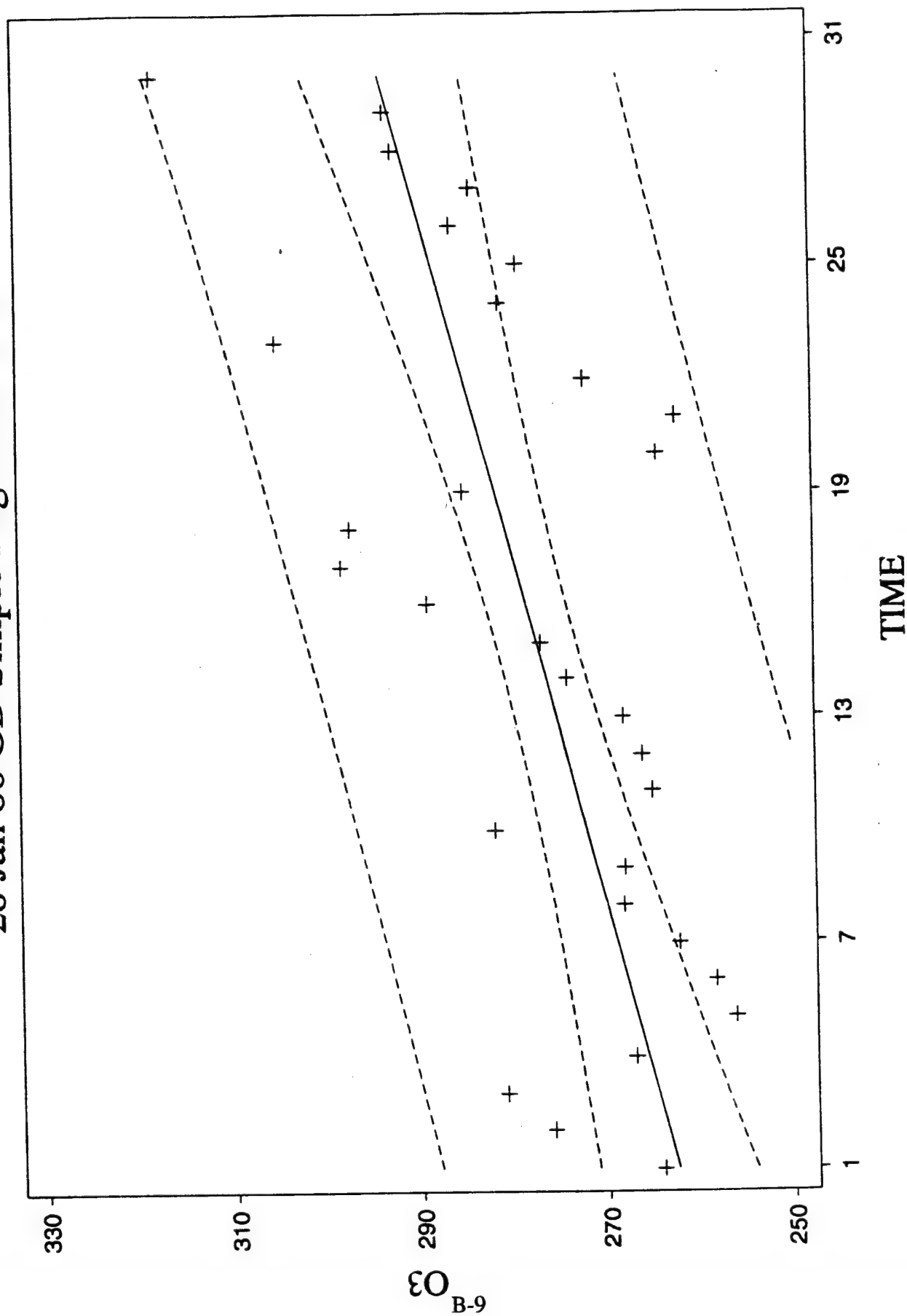
PREDICTED/FITTED VALUES OF O3

LOWER PREDICTED BOUND	268.74	LOWER FITTED BOUND	285.40
PREDICTED VALUE	294.39	FITTED VALUE	294.39
UPPER PREDICTED BOUND	320.04	UPPER FITTED BOUND	303.39
SE (PREDICTED VALUE)	12.521	SE (FITTED VALUE)	4.3911

UNUSUALNESS (LEVERAGE)	0.1402
PERCENT COVERAGE	95.0
CORRESPONDING T	2.05

PREDICTOR VALUES: TIME = 31.000

02 Dec 88 GD Simple Regression Plot

O3 = 274.26 - 1.0217 * TIME   95% conf and pred intervals

TIME

$O3_{B-11}$

PREDICTED/FITTED VALUES OF O3

LOWER PREDICTED BOUND	228.74	LOWER FITTED BOUND	238.31
PREDICTED VALUE	243.61	FITTED VALUE	243.61
UPPER PREDICTED BOUND	258.47	UPPER FITTED BOUND	248.90
SE (PREDICTED VALUE)	7.2435	SE (FITTED VALUE)	2.5802

UNUSUALNESS (LEVERAGE)   0.1453
PERCENT COVERAGE   95.0
CORRESPONDING T   2.05

PREDICTOR VALUES: TIME = 30.000

08 Aug 89 GD Simple Regression Plot
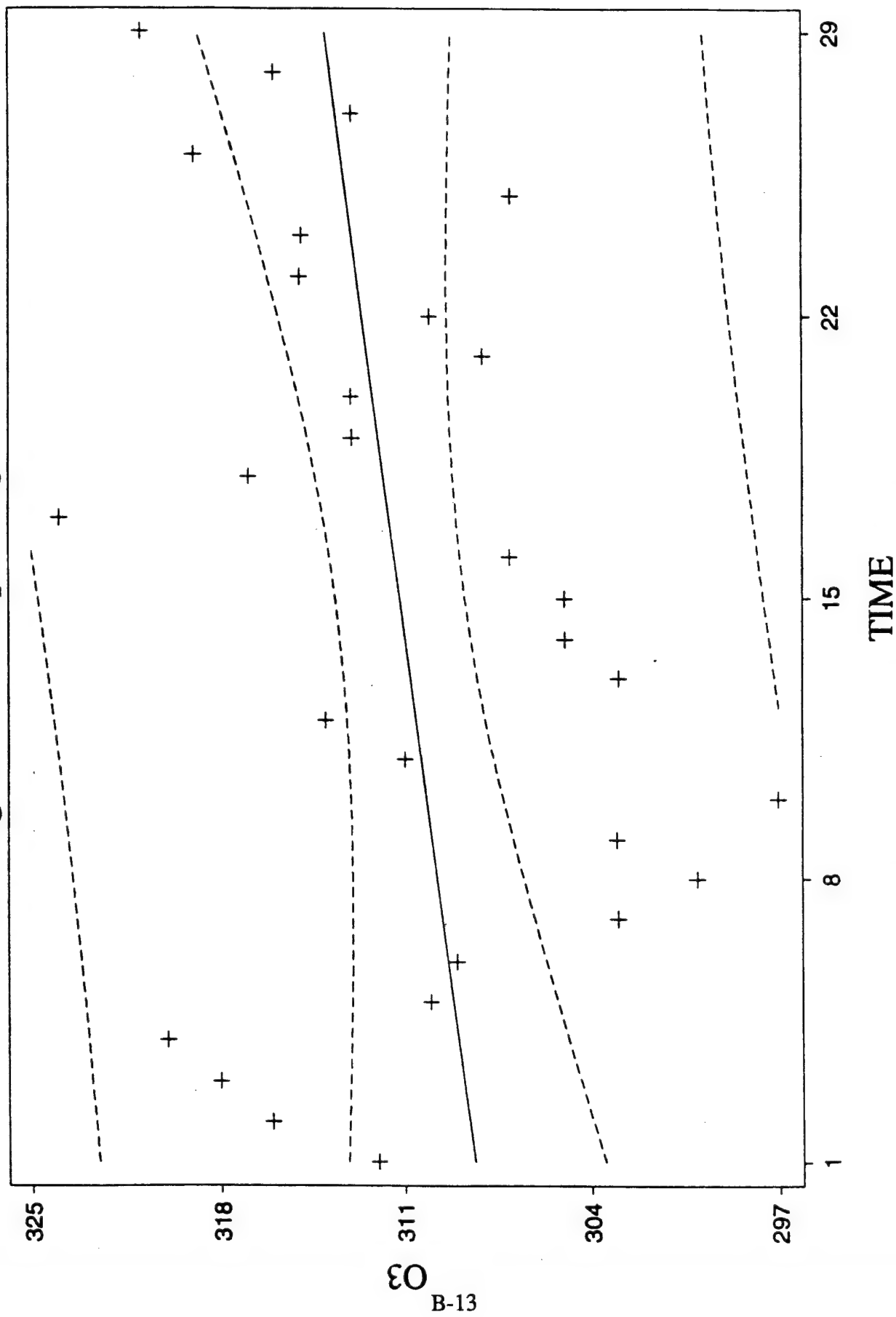
O3 = 308.10 + 0.2049 * TIME   95% conf and pred intervals

B-13

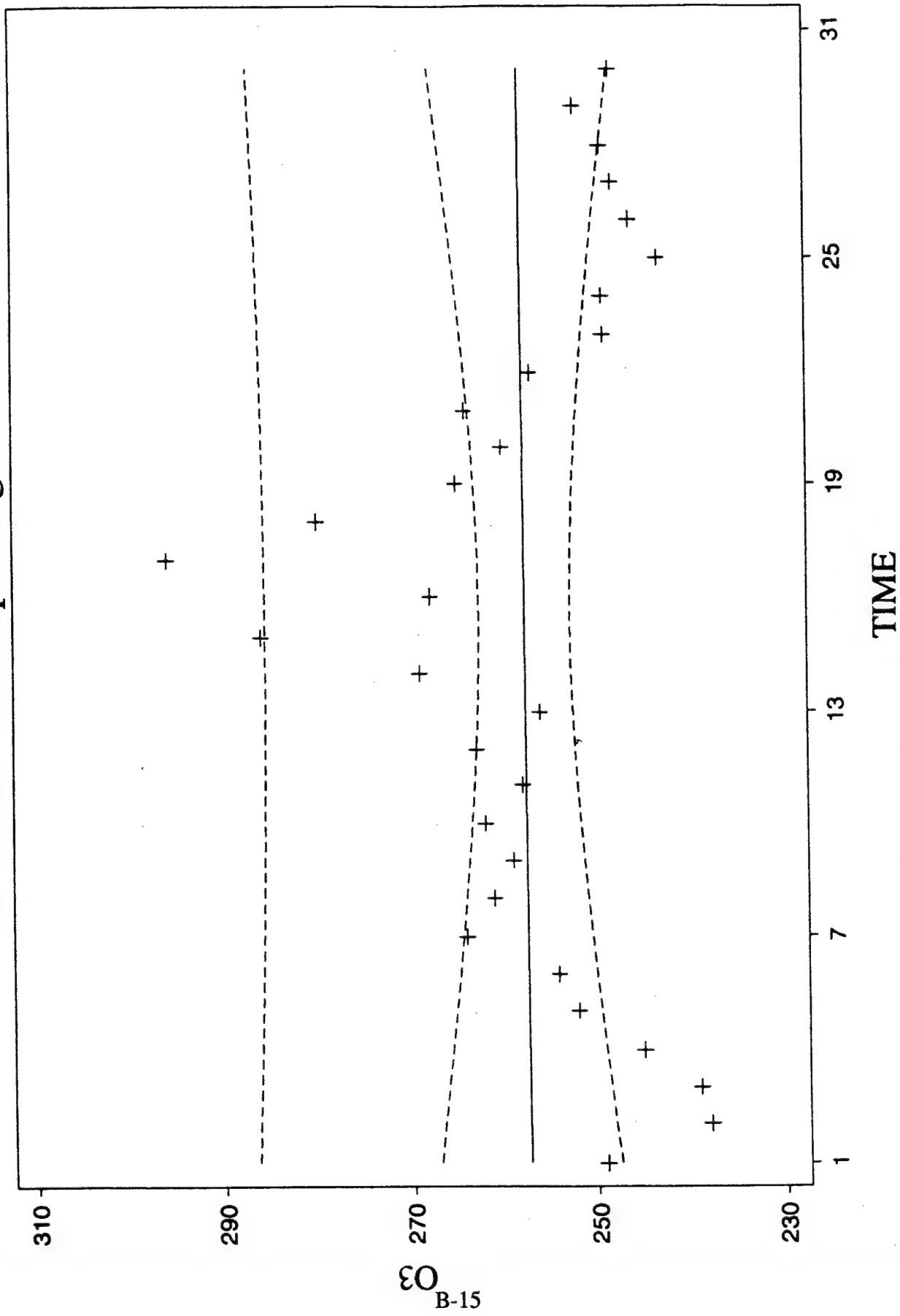DESCRIPTIVE STATISTICS

VARIABLE	N	MEAN	SD	MINIMUM	MAXIMUM
O3	29	311.17	6.6282	297.00	324.00

$$PI = 311.17 \pm 2.048 \cdot 6.6282 \sqrt{1 + 1/29}$$

$$PI = (297.36, 324.98)$$

09 Jan 90 GD Simple Regression Plot

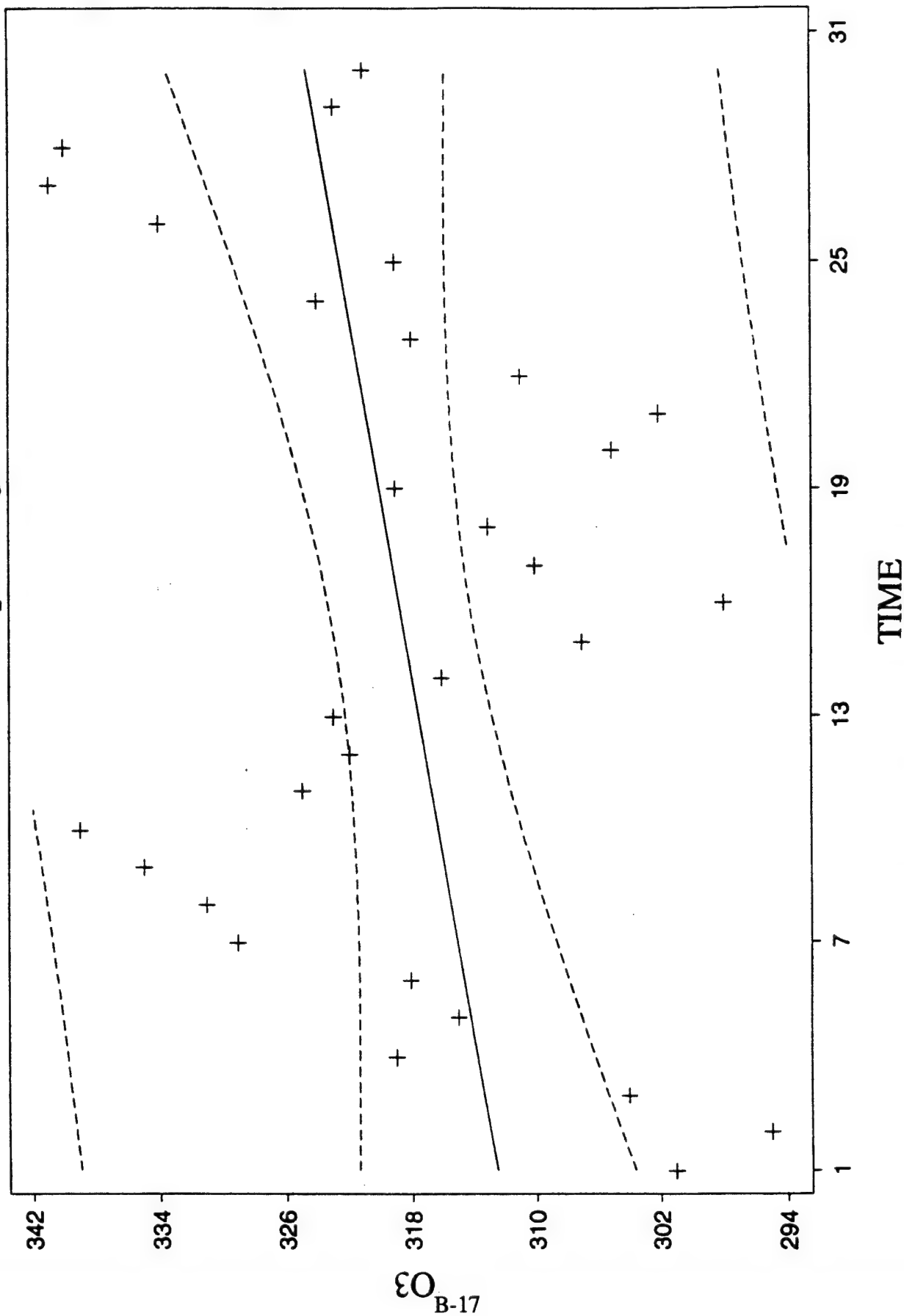O3 = 257.26 + 0.0242 * TIME   95% conf and pred intervals

TIME

O3

B-15

DESCRIPTIVE STATISTICS

VARIABLE	N	MEAN	SD	MINIMUM	MAXIMUM
O3	30	257.63	13.158	238.00	296.00

$$PI = 257.63 \pm 2.045 \cdot 13.158 \sqrt{1 + 1/30}$$

$$PI = (230.28, 284.98)$$
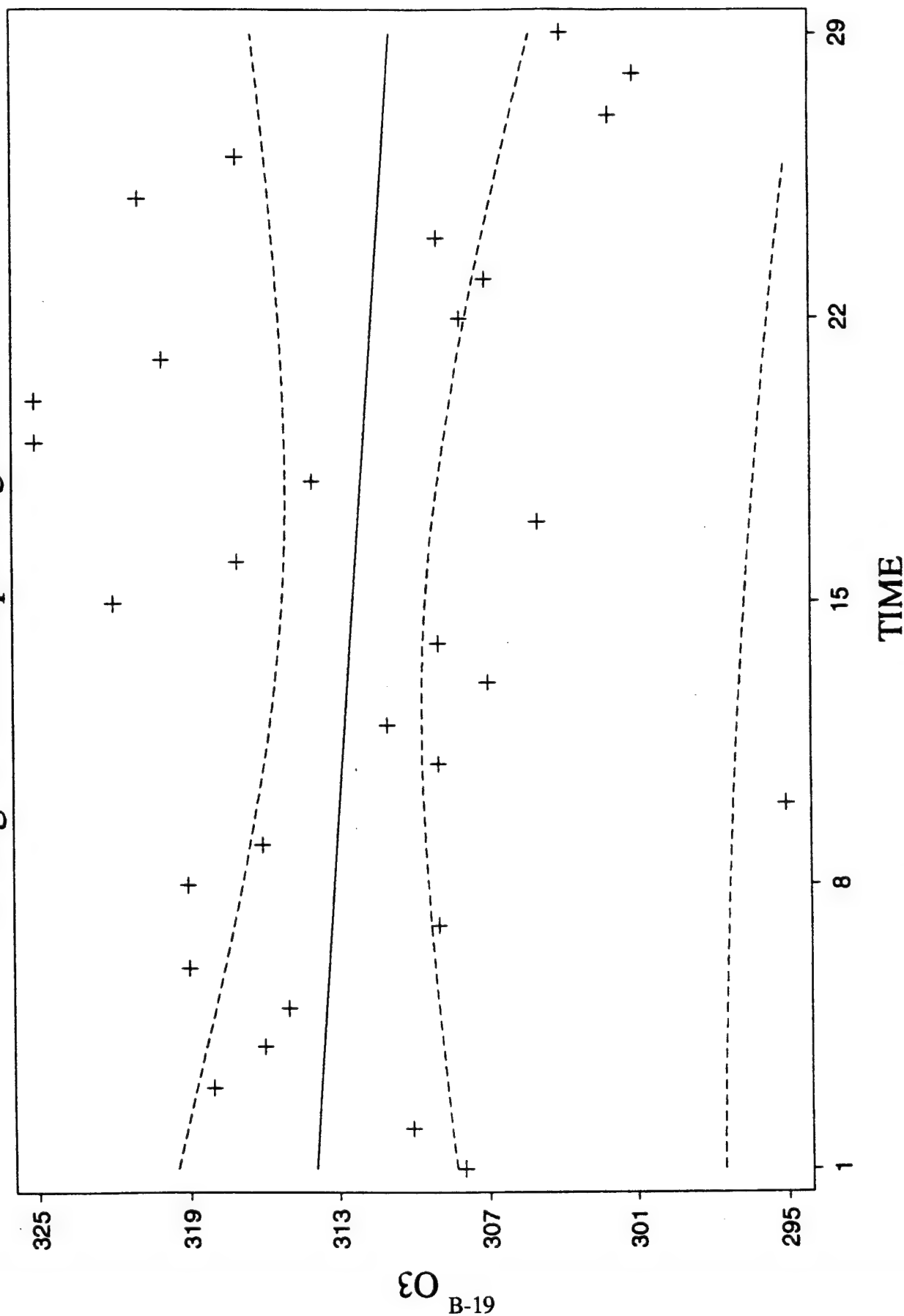
05 Jun 91 GD Simple Regression Plot

TIME

O3 = 312.07 + 0.4189 * TIME   95% conf and pred intervals

$O3_{B-17}$

DESCRIPTIVE STATISTICS

VARIABLE	N	MEAN	SD	MINIMUM	MAXIMUM
O3	30	318.57	12.530	295.00	341.00

$$PI = 318.57 \pm 2.045 \cdot 12.53 \sqrt{1 + 1/30}$$

$$PI = (292.52, 344.62)$$

02 Aug 91 GD Simple Regression Plot

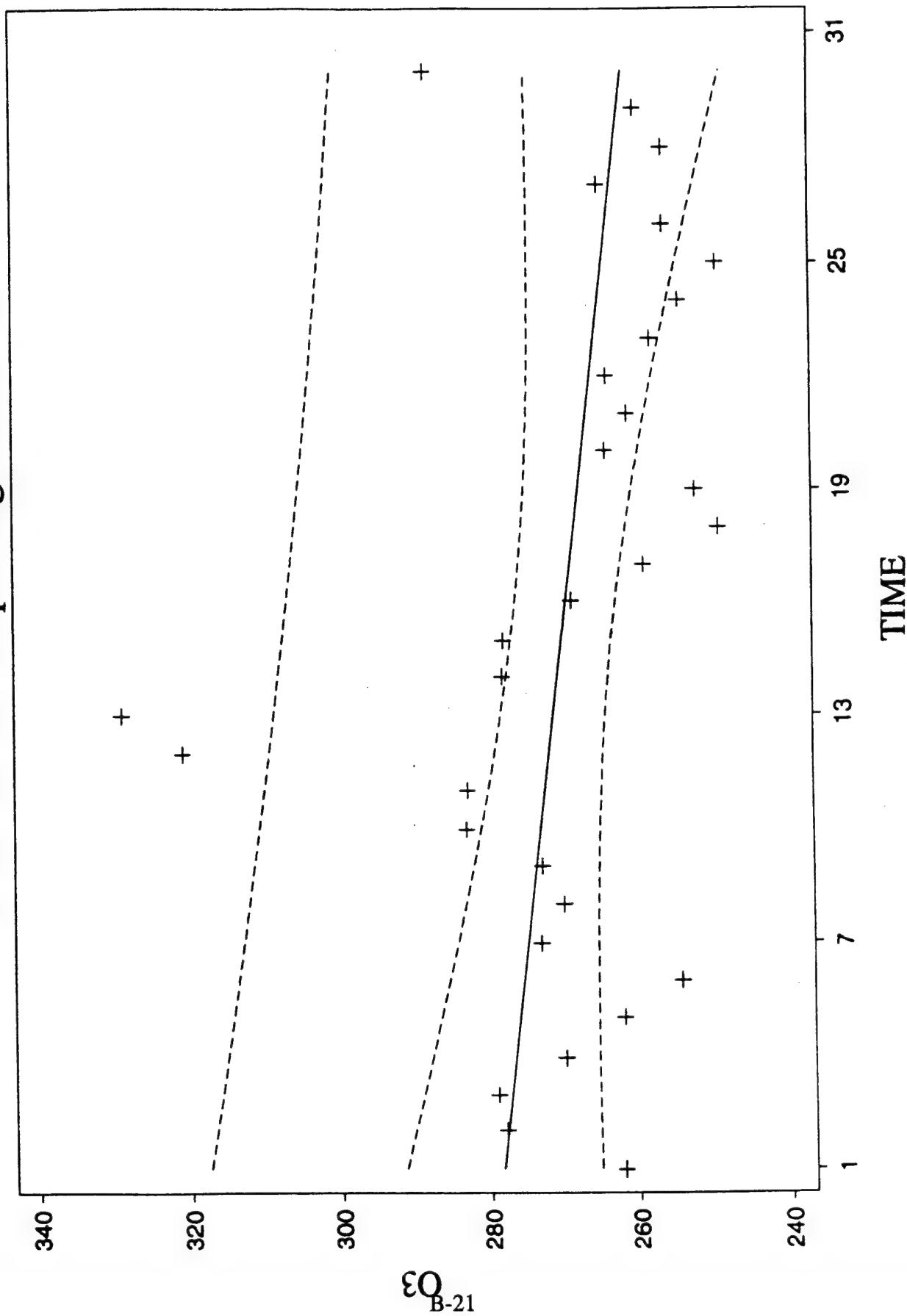O3 = 314.01 - 0.1113 * TIME   95% conf and pred intervals

TIME

O3

B-19

DESCRIPTIVE STATISTICS

VARIABLE	N	MEAN	SD	MINIMUM	MAXIMUM
O3	29	312.34	7.4512	295.00	325.00

$$PI = 312.34 \pm 2.048 \cdot 7.4512 \sqrt{1 + 1/29}$$

$$PI = (296.82, 327.86)$$
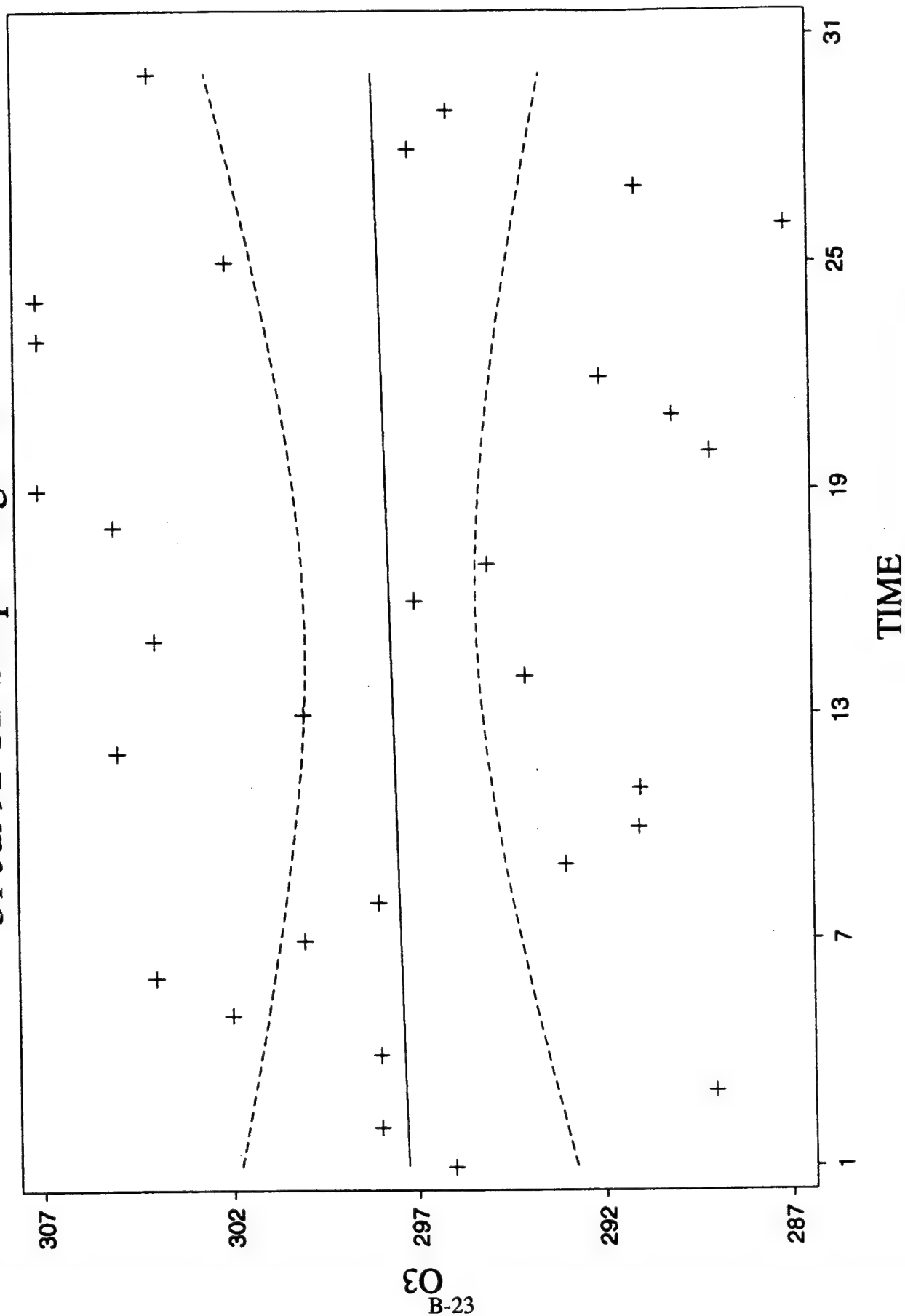
22 Jan 92 GD Simple Regression Plot

O3 = 278.95 - 0.5840 * TIME   95% conf and pred intervals

TIME

O3

B-21

DESCRIPTIVE STATISTICS

VARIABLE	N	MEAN	SD	MINIMUM	MAXIMUM
O3	30	269.90	18.399	249.00	329.00

$$PI = 269.9 \pm 2.045 \cdot 18.399 \sqrt{1 + 1/30}$$

$$PI = (231.65, 308.15)$$

31 Jul 92 GD Simple Regression Plot

TIME

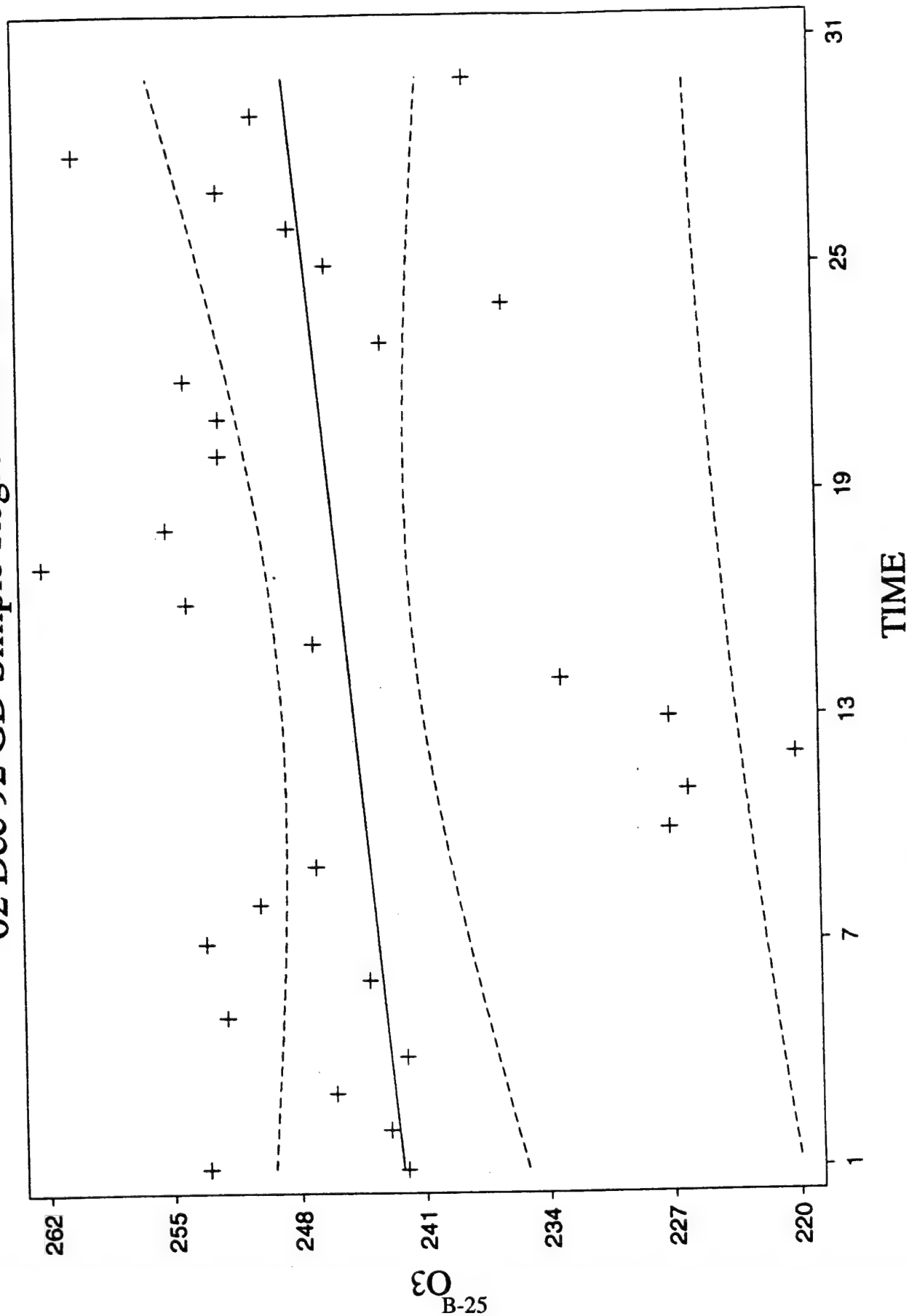O3 = 297.25 + 0.0247 * TIME   95% conf and pred intervals

O3

B-23

DESCRIPTIVE STATISTICS

VARIABLE	N	MEAN	SD	MINIMUM	MAXIMUM
O3	30	297.63	6.0883	287.00	307.00

$$PI = 297.63 \pm 2.045 \cdot 6.0883 \sqrt{1 + 1/30}$$

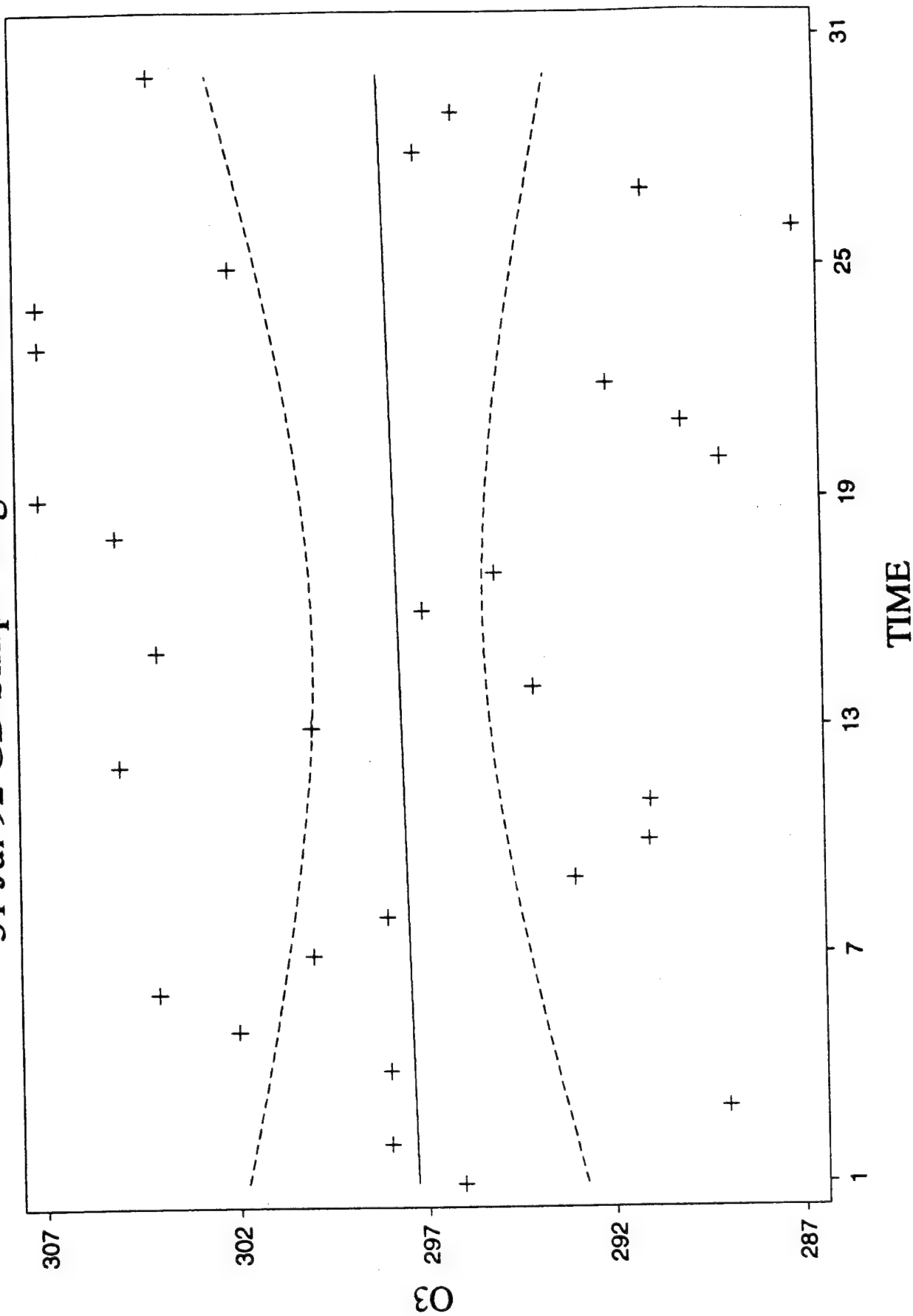$$PI = (284.97, 310.29)$$

02 Dec 92 GD Simple Regression Plot

$O3 = 242.09 + 0.2043 * TIME$ 95% conf and pred intervals

B-25

DESCRIPTIVE STATISTICS

VARIABLE	N	MEAN	SD	MINIMUM	MAXIMUM
O3	30	245.13	10.345	220.00	262.00

$$PI = 245.13 \pm 2.045 \cdot 10.345 \sqrt{1 + 1/30}$$

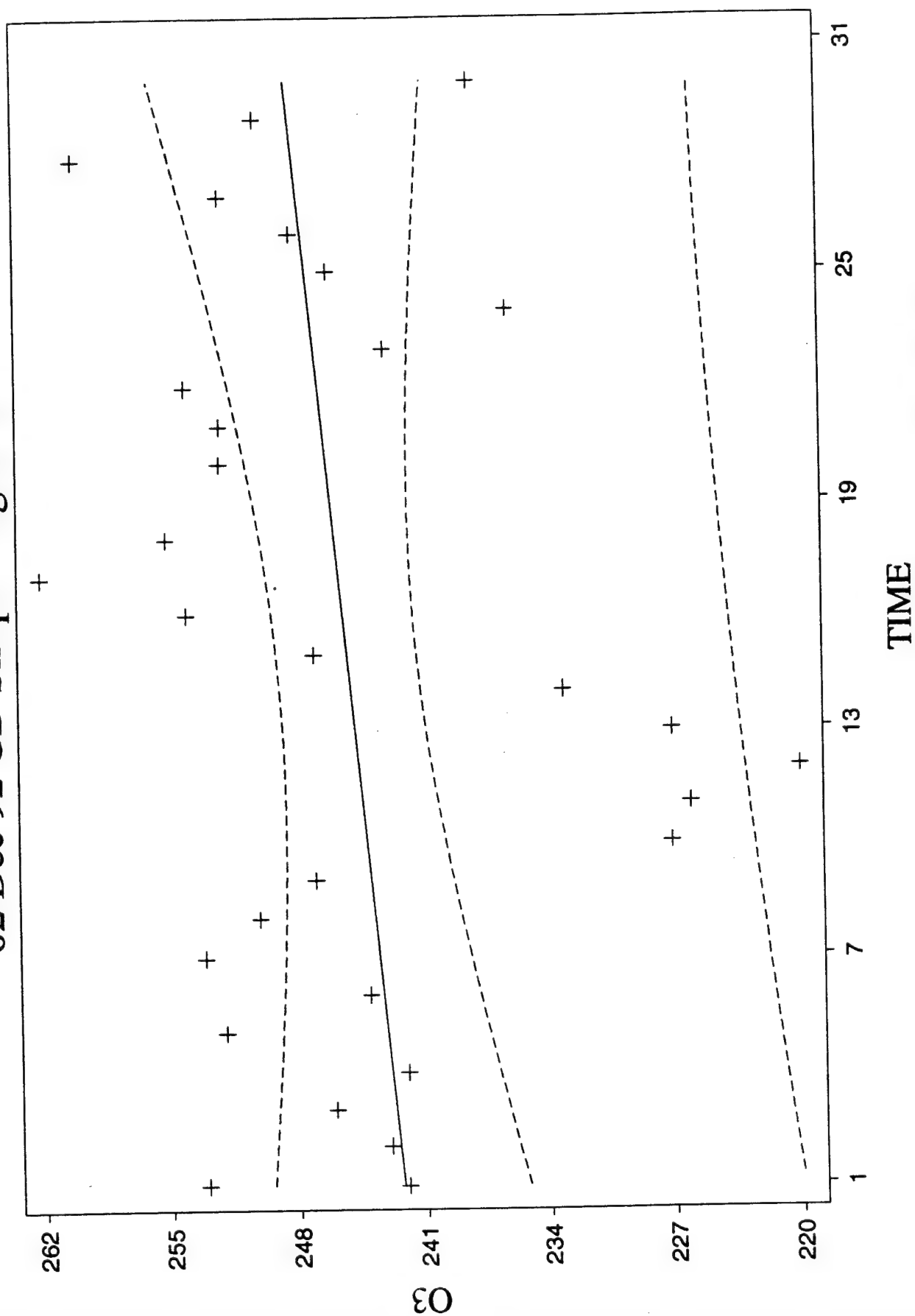$$PI = (223.62, 266.64)$$

31 Jul 92 GD Simple Regression Plot

TIME

O3 = 297.25 + 0.0247 * TIME   95% conf and pred intervals

O3

B-27

DESCRIPTIVE STATISTICS

VARIABLE	N	MEAN	SD	MINIMUM	MAXIMUM
O3	30	297.63	6.0883	287.00	307.00

$$PI = 297.63 \pm 2.045 \cdot 6.0883 \sqrt{1 + 1/30}$$

$$PI = (284.97, 310.29)$$

02 Dec 92 GD Simple Regression Plot

TIME
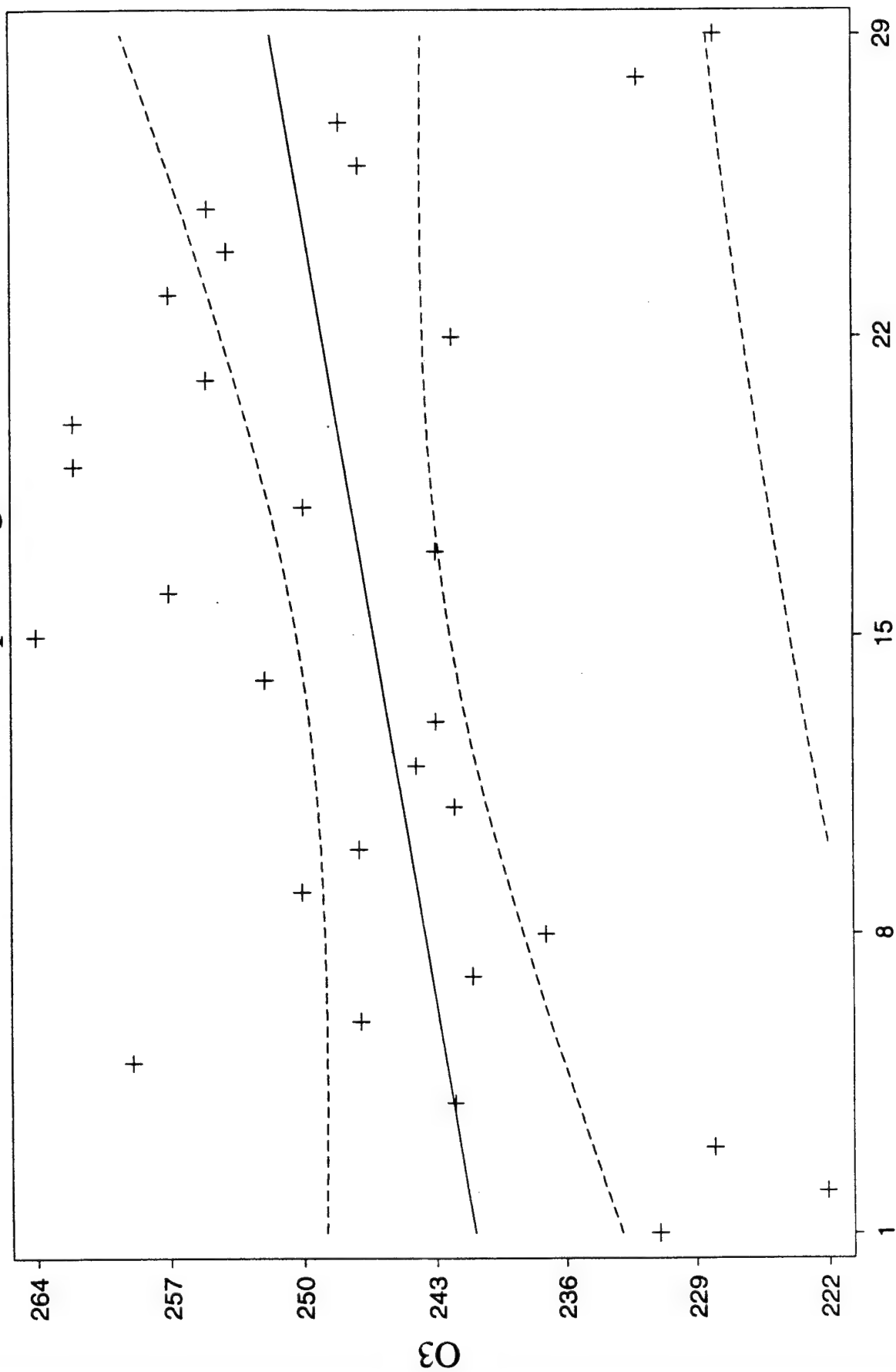
O3 = 242.09 + 0.2043 * TIME   95% conf and pred intervals

O3

DESCRIPTIVE STATISTICS

VARIABLE	N	MEAN	SD	MINIMUM	MAXIMUM
O3	30	245.13	10.345	220.00	262.00

$$PI = 245.13 \pm 2.045 \cdot 10.345 \sqrt{1 + 1/30}$$

$$PI = (223.62, 266.64)$$

13 Jan 93 GD Simple Regression Plot

O3 = 240.50 + 0.3828 * TIME   95% conf and pred intervals
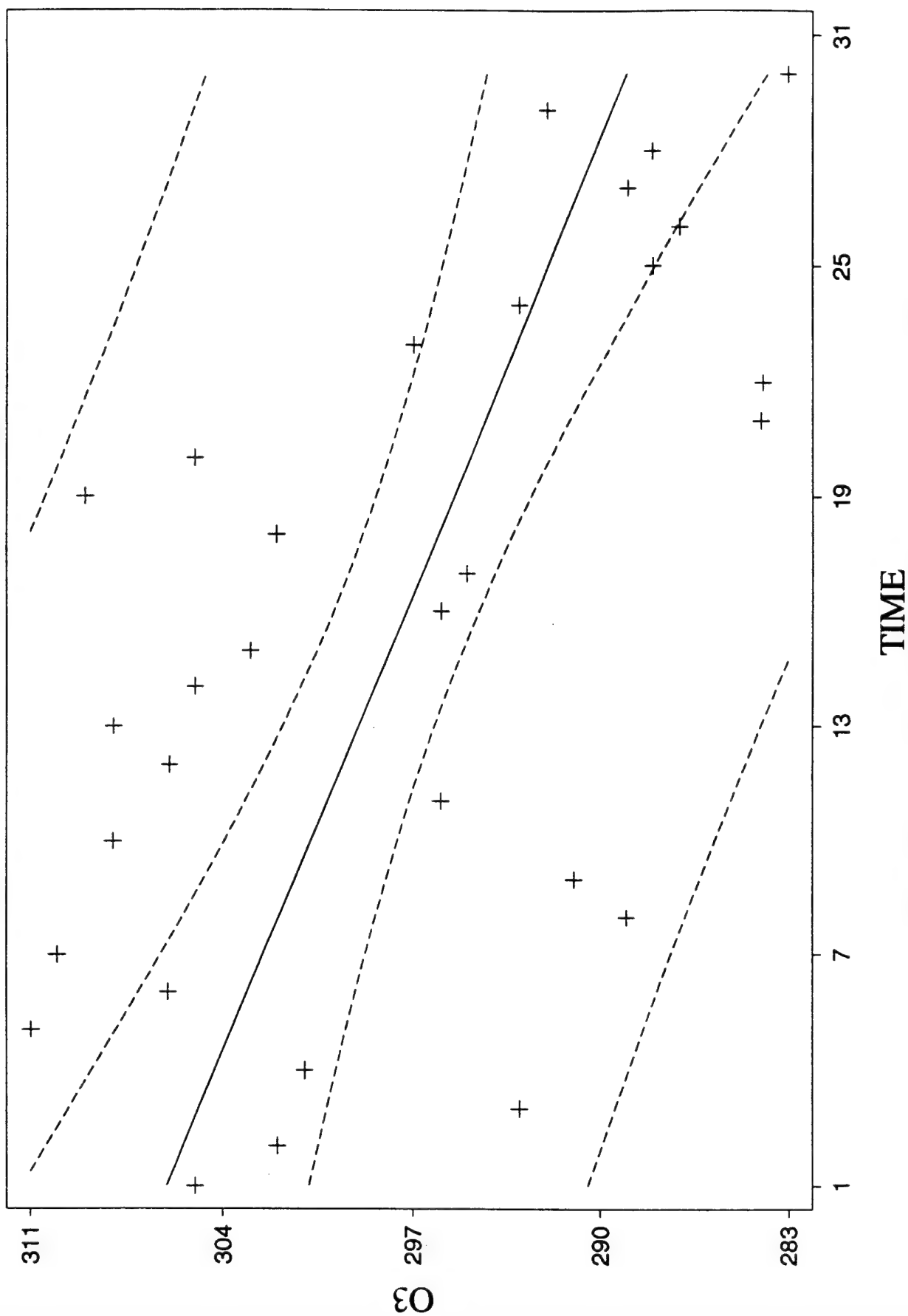
B-31

DESCRIPTIVE STATISTICS

VARIABLE	N	MEAN	SD	MINIMUM	MAXIMUM
O3	29	246.24	10.966	222.00	264.00

$$PI = 246.24 \pm 2.048 \cdot 10.966 \sqrt{1 + 1/29}$$

$$PI = (223.4, 269.08)$$

28 Aug 85 WTR GD Simple Regression Plot

O3 = 306.65 - 0.5882 * TIME   95% conf and pred intervals

TIME

O3

PREDICTED/FITTED VALUES OF O3

LOWER PREDICTED BOUND	272.71	LOWER FITTED BOUND	282.91
PREDICTED VALUE	288.42	FITTED VALUE	288.42
UPPER PREDICTED BOUND	304.12	UPPER FITTED BOUND	293.92
SE (PREDICTED VALUE)	7.6679	SE (FITTED VALUE)	2.6891

UNUSUALNESS (LEVERAGE)	0.1402
PERCENT COVERAGE	95.0
CORRESPONDING T	2.05

PREDICTOR VALUES: TIME = 31.000

VITA

Captain Brian K. George is from Lakewood, California. He graduated from Arizona State University in 1988 with a Bachelor of Science degree in Mechanical Engineering. After graduation, Captain George was assigned to the 6595th Aerospace Test Group at Vandenberg AFB, California.

During his tour at Vandenberg AFB, Captain George worked as the Air Force's lead engineer on the Titan II and Titan IV rocket propellant systems, ground systems, air frames, and liquid rocket engines. He also becasme the Group's lead environmental engineer, responsible for hazardous waste management and disposal as well as all air emissions permitting required for the space launch complex.

In June of 1993, Captain George was assigned to the 93rd Civil Engineering Squadron at Castle AFB, California, where he assummed control of the base's air pollution program. Captain George was also selected as the Engineering Flight Chief at Castle, where he was involved in the design and implementation of several base-closure environmental remediation and restoration projects. In May of 1995, Captain George was selected to attend the Air Force Institute of Technology.

In June of 1995, Captain George entered the Air Force Institute of Technology at Wright-Patterson AFB, Ohio. After completion of the required course work and this thesis, he graduated in December of 1996 with a Master of Science in Engineering and Environmental Management degree. He was subsequently assigned to the AFIT School of Civil Engineering and Services as an instructor.

REPORT DOCUMENTATION PAGE

1. AGENCY USE ONLY *(Leave blank)*	2. REPORT DATE December 1996	3. REPORT TYPE AND DATES COVERED Master's Thesis

4. TITLE AND SUBTITLE

Local Effects of Solid Rocket Motor Exhaust on Stratospheric Ozone Concentrations

5. FUNDING NUMBERS

6. AUTHOR(S)

Brian K. George, Capt, USAF

7. PERFORMING ORGANIZATION NAME(S) AND ADDRESS(ES)

Air Force Institute of Technology (AFIT)
Wright Patterson AFB, OH 45433-6583

8. PERFORMING ORGANIZATION REPORT NUMBER

AFIT/GEE/ENV/96D-04

9. SPONSORING / MONITORING AGENCY NAME(S) AND ADDRESS(ES)

10. SPONSORING / MONITORING AGENCY REPORT NUMBER

11. SUPPLEMENTARY NOTES

12a. DISTRIBUTION / AVAILABILITY STATEMENT

Approved for public release; distribution unlimited

12b. DISTRIBUTION CODE

13. ABSTRACT *(Maximum 200 words)*

Solid Rocket Motors (SRMs) power the initial flight of the Space Shuttle and Titan IV rocket. During those first two minutes after liftoff, the exhaust plumes from these motors emit large quantities of chlorine compounds and alumina particles into the atmosphere. For years scientists have argued that such a large chlorine input, injected directly into the stratosphere, would photochemically react with the surrounding air to cause significant ozone depletion. To answer the question of whether SRM exhaust causes a significant ozone depletion, Version 7 data from the Total Ozone Mapping Spectrometer (TOMS) instrument was analyzed for the 30 days prior to a launch to determine any trends and natural ozone variability, and a linear regression analysis was run to calculate a 95% Prediction Interval for the expected ozone range on the day of launch. Of the 23 Overpass data sets and 14 Field of View data sets analyzed, all of the TOMS post-launch total column ozone measurements were found to lie either within or higher than the 95% Prediction Interval range. This analysis indicated no significant reductions in the total column ozone process following a space shuttle or Titan rocket launch, either from Cape Canaveral AFS or Vandenberg AFB.

14. SUBJECT TERMS
solid rocket motor, stratosphere, ozone, depletion, satellite, TOMS, column ozone, chlorine, Space Shuttle, Titan IV, rocket, launch, space, statistical analysis, Cape Canaveral AFS, Vandenberg AFB

15. NUMBER OF PAGES
152

16. PRICE CODE

17. SECURITY CLASSIFICATION OF REPORT Unclassified	18. SECURITY CLASSIFICATION OF THIS PAGE Unclassified	19. SECURITY CLASSIFICATION OF ABSTRACT Unclassified	20. LIMITATION OF ABSTRACT UL

GENERAL INSTRUCTIONS FOR COMPLETING SF 298

The Report Documentation Page (RDP) is used in announcing and cataloging reports. It is important that this information be consistent with the rest of the report, particularly the cover and title page. Instructions for filling in each block of the form follow. It is important to *stay within the lines* to meet *optical scanning requirements*.

Block 1. Agency Use Only *(Leave blank)*.

Block 2. Report Date. Full publication date including day, month, and year, if available (e.g. 1 Jan 88). Must cite at least the year.

Block 3. Type of Report and Dates Covered. State whether report is interim, final, etc. If applicable, enter inclusive report dates (e.g. 10 Jun 87 - 30 Jun 88).

Block 4. Title and Subtitle. A title is taken from the part of the report that provides the most meaningful and complete information. When a report is prepared in more than one volume, repeat the primary title, add volume number, and include subtitle for the specific volume. On classified documents enter the title classification in parentheses.

Block 5. Funding Numbers. To include contract and grant numbers; may include program element number(s), project number(s), task number(s), and work unit number(s). Use the following labels:

C	-	Contract	PR	-	Project
G	-	Grant	TA	-	Task
PE	-	Program Element	WU	-	Work Unit Accession No.

Block 6. Author(s). Name(s) of person(s) responsible for writing the report, performing the research, or credited with the content of the report. If editor or compiler, this should follow the name(s).

Block 7. Performing Organization Name(s) and Address(es). Self-explanatory.

Block 8. Performing Organization Report Number. Enter the unique alphanumeric report number(s) assigned by the organization performing the report.

Block 9. Sponsoring/Monitoring Agency Name(s) and Address(es). Self-explanatory.

Block 10. Sponsoring/Monitoring Agency Report Number. *(If known)*

Block 11. Supplementary Notes. Enter information not included elsewhere such as: Prepared in cooperation with...; Trans. of...; To be published in.... When a report is revised, include a statement whether the new report supersedes or supplements the older report.

Block 12a. Distribution/Availability Statement. Denotes public availability or limitations. Cite any availability to the public. Enter additional limitations or special markings in all capitals (e.g. NOFORN, REL, ITAR).

DOD - See DoDD 5230.24, "Distribution Statements on Technical Documents."
DOE - See authorities.
NASA - See Handbook NHB 2200.2.
NTIS - Leave blank.

Block 12b. Distribution Code.

DOD - Leave blank.
DOE - Enter DOE distribution categories from the Standard Distribution for Unclassified Scientific and Technical Reports.
NASA - Leave blank.
NTIS - Leave blank.

Block 13. Abstract. Include a brief *(Maximum 200 words)* factual summary of the most significant information contained in the report.

Block 14. Subject Terms. Keywords or phrases identifying major subjects in the report.

Block 15. Number of Pages. Enter the total number of pages.

Block 16. Price Code. Enter appropriate price code *(NTIS only)*.

Blocks 17. - 19. Security Classifications. Self-explanatory. Enter U.S. Security Classification in accordance with U.S. Security Regulations (i.e., UNCLASSIFIED). If form contains classified information, stamp classification on the top and bottom of the page.

Block 20. Limitation of Abstract. This block must be completed to assign a limitation to the abstract. Enter either UL (unlimited) or SAR (same as report). An entry in this block is necessary if the abstract is to be limited. If blank, the abstract is assumed to be unlimited.